DOE/ET/20283-2

APPLICATION OF STATISTICAL TECHNIQUES TO WIND CHARACTERISTICS AT POTENTIAL WIND ENERGY CONVERSION SITES

Final Report for the Period October 1, 1978—September 30, 1979

By
Ross B. Corotis

May 1980

Work Performed Under Contract No. AS06-76ET20283

Department of Civil Engineering
Northwestern University
Evanston, Illinois

U.S. Department of Energy

Solar Energy

DISCLAIMER

DISCLAIMER

Available from the National Technical Information Service, U. S. Department of Commerce, Springfield, Virginia 22161.

Price: Printed Copy A09
Microfiche A01

DOE/ET/20283-2
Distribution Category UC-60

APPLICATION OF STATISTICAL TECHNIQUES TO WIND CHARACTERISTICS AT POTENTIAL WIND ENERGY CONVERSION SITES

Ross B. Corotis
Department of Civil Engineering
Northwestern University
Evanston, Illinois 60201

May 1980

PREPARED FOR THE U.S. DEPARTMENT OF ENERGY
OFFICE OF SOLAR POWER APPLICATIONS
FEDERAL WIND ENERGY PROGRAM

DOE CONTRACT No. DE-AS06-76ET20283

THIS PAGE

WAS INTENTIONALLY

LEFT BLANK

ACKNOWLEDGMENTS

Coordination and technical guidance for this project has come from Charles E. Elderkin, Larry L. Wendell, and David S. Renne of Pacific Northwest Laboratory.

The research team at Northwestern University for this period has consisted primarily of Karen C. Chou, Harish G. Rao and the author. Additional contributions have come from Fernando Cheng, Michael E. Harris, Lynn M. Kistler, Edwin C. Rossow, Mark W. Wales, and Lingyah Wu.

EXECUTIVE SUMMARY

In this report a number of new statistical techniques and mathematical models are developed to analyze wind data collected at a potential wind energy conversion site. These procedures are applications and extensions of models developed in prior studies (Corotis, 1976; 1977; 1979), which are available from the National Technical Information Service. Data to develop and verify the models have come principally from the National Climatic Center (NCC) hourly data tapes from about three dozen sites in the continental United States. A companion handbook has been developed to describe basic application of the methods. The Rayleigh distribution is often used for the probability of hourly wind speed. Inherent in the derivation of the Rayleigh are the assumptions that the horizontal vector components of wind speed are zero-mean, identically distributed, independent, normal random variables. Herein, the assumptions of independence and equal variance are relaxed and the resulting wind speed distribution is derived in summation form. A parameter sensitivity analysis indicates that for practical purposes the resulting distribution is well modelled by the Rayleigh.

Two separate 24-hour records consisting of continuous data were made at a site in northeastern Illinois. These records were digitized with one 20-second average every twenty seconds. These records were then used to study the sensitivity of derived statistics as a function of various averaging times and sampling rates. The mean and variance of wind speed were seen to be relatively insensitive to sampling

variations of practical interest. A distinct increase in the autocorrelation function for a given lag time as a function of increasing averaging time was observed, as well as an increase in the wind speed persistence (run duration) with decreasing sampling rate.

A simple approximate procedure was derived for the time series simulation of hourly wind speed at a site. The procedure was based on the Weibull distribution for wind speed and used conditional parameters updated each hour as a function of the wind speed simulated for the previous hour and the value of the autocorrelation function for a one-hour lag. The model is an exact procedure for a normally-distributed random variable. The implicit assumption that the autocorrelation function was a decaying exponential is found to be satisfied with actual site data. A related procedure is developed for the time series simulation of total hourly power generated by a regional array of wind turbines. Here the normal assumption can be substantiated, but an equivalent linear wind turbine operating characteristic curve is required. Autocorrelation as well as spatial correlation was included in the approach. The simulated results for three different regions and six different wind turbines (ranging from 45 kW to 2.5 MW) were compared with observed data and with a different simulation model. The means and variances of power were seen to agree well with the actual observed data. Histograms of array power from the simulated model agreed reasonably well with the observed data, except for some disagreement in the extreme ranges. Array power autocorrelation from the simulation and observed data matched very well in form, although there

were some quantitative discrepancies at longer lag times (fortunately, the agreement was very good at the important initial few hours of lag). Mean run durations also compared very favorably between the simulation and the observed data, although there were substantial differences in isolated cases.

Bayesian statistics were applied for the wind speed probability density function. Sampling uncertainty due to finite duration of site data collection was reflected through a gamma prior distribution for the site mean wind speed. Inherent uncertainty was included with a Rayleigh distribution. The resulting Bayesian distribution must be tested further, but it appears that sampling uncertainty is strongly dominated by inherent variability for a year or more of field data.

Additional NCC data generally confirm the applicability of previously derived procedures and lead to new regression curves for calibration of the wind persistence model.

ABSTRACT

The distribution for the magnitude of the vector sum of two orthogonal horizontal wind velocity components is often modelled by the Rayleigh, which is derived assuming that the components are independent, identically distributed, zero-mean, Gaussian random variables; the probability density function for a more realistic case where the two components are correlated and not equal in variance is derived. It is found that the derived distribution is adequately modelled by the Rayleigh distribution. A 24-hour record of 20-second average wind speed was collected to assess the effect of sampling rate and averaging time on computed wind speed means and variances, autocorrelation, and run duration. Definite effects on autocorrelation and run duration due to averaging time and sampling rate, respectively, are observed. An approximate procedure is developed to simulate the time sequence of wind speed at a single site; the procedure uses a Weibull distribution with conditional parameters updated each hour as a function of the previously simulated value and the autocorrelation. A Gaussian distribution is used to simulate the hourly power from a regional array of wind turbines; results of the simulated model (ARASIM) developed here are compared with another approximate and actual results. Both simulation models appear to give good approximation to the actual data.

A Bayesian analysis of wind speed leads to a new distribution that combines the inherent variability in the wind with uncertainty due to finite sampling duration.

Data obtained from the National Climatic Center for a number

of relatively windy sites confirm the suitability and limitations of models developed in previous reports. Refined regression curves are derived to calibrate the run duration model.

TABLE OF CONTENTS

TABLE OF CONTENTS (continued)

LIST OF TABLES

LIST OF TABLES (continued)

LIST OF FIGURES

LIST OF FIGURES (continued)

LIST OF FIGURES (continued)

LIST OF FIGURES (continued)

NOTATION

$E[\ ]$	Expectation of quantity in brackets.
$Var[\ ]$	Variance of quantity in brackets.
$f_X(x)$	Probability density function of X.
$F_X(x)$	Cumulative density function of X.
σ	Standard deviation
σ^2	Variance
m	Mean (expected value)
$Cov[\ ]$	Covariance of quantity in brackets.
exp	Exponential (the base of the natural logarithms).
v	Magnitude of the horizontal vector of wind velocity, referred to as the wind speed.
v_i	Velocity at which the wind turbine first produces usable power, referred to as the cut-in speed.
v_r	Velocity at which the wind turbine reaches its design capacity, referred to as the rated speed.
v_o	Velocity at which the WECS must be feathered in order to preserve the structural integrity of the device, referred to as the cut-out speed.

CHAPTER 1

INTRODUCTION

This report is the fourth comprehensive document resulting from research at Northwestern University on the development of mathematical models that can be used to assess the potential for wind energy conversion from short-term site wind records (Corotis, 1976; 1977; 1979). Described herein is the development of a number of new statistical techniques and mathematical models, as well as the testing of previous procedures with additional data from the National Climatic Center (NCC) and two short, continuously sampled records. A companion document, entitled Handbook for the Application of Statistical Techniques to Wind Characteristics at Potential Wind Energy Conversion Sites, explains in straightforward form the techniques for utilizing the procedures derived and verified in this and the prior reports.

In Chapter 2, the probability density function is derived for the wind speed with horizontal vector components that are orthogonal and unequally distributed. Then, the effect of correlated components is considered and the probability density function is rederived.

In Chapter 3, the effect of averaging time and sampling rate is studied from a 24-hour record of 20-second-average wind speed collected from an anemometer located on a tower atop the Northwestern Technological Institute in Evanston, Illinois. The results are then compared with the analysis of Won (1979).

Two approximate simulation models are developed in Chapter 4. The

first model provides the simulation of an hourly time-series of wind speed at a single site. The second model simulates a sequence of hourly power from a regional array of wind turbines. The array power results are compared with observed data (obtained from the National Climatic Center) and another simulation model developed by Cliff, Justus and Elderkin (1978).

In Chapter 5 the concept of Bayesian statistics is reviewed and then the concept applied for the wind speed probability density function. Inherent variability in the wind is reflected by using a Rayleigh distribution. A posterior distribution for the mean wind speed is based on a gamma prior. A Bayesian distribution of wind speed is then derived that reflects the combined uncertainty of the basic wind and a finite field data collection period.

NCC hourly data tapes from a number of relatively windy sites are analyzed in Chapter 6 in order to verify the applicability of previously developed models (notably the Rayleigh probability distribution for wind speed, the interannual variability and the power-exponential probability distribution for run duration). New regression curves are derived to determine the parameter for the power-exponential run duration probability distribution.

Finally, some conclusions and recommendations are presented in Chapter 7.

The material contained in this report is intended to assist in the assessment of potential wind energy conversion sites. The analyses contained herein and the material from the three prior reports provide

the theoretical framework upon which the companion Handbook is based. While the Handbook may be used by itself, these supporting documents provide useful explanatory information.

CHAPTER 2

MEAN WIND SPEED WITH UNEQUAL VARIANCE

2.1 REVIEW OF THE RAYLEIGH DISTRIBUTION

The Rayleigh distribution is often used to model hourly wind speed (Cliff, 1977; Doran et al, 1977). The speed is implicitly assumed to be the vector sum of two orthogonal, horizontal, independent, identically-distributed, zero-mean, Gaussian wind components, denoted X and Y. This chapter investigates a relaxation of certain assumptions inherent in the Rayleigh distribution. A more general distribution is sought that can be simply calibrated in term of basic wind data such as hourly speed and direction or speed in two orthogonal directions. The Rayleigh probability density function (pdf) of vector speed V is given by

$$f_V(v) = \frac{\pi}{2}\frac{v}{m^2}\exp\left[-\frac{\pi}{4}(v/m)^2\right] \tag{2.1}$$

in which

$$m = E[V] = \sqrt{\frac{\pi}{2}}\,\sigma \tag{2.2}$$

where σ is the standard deviation of one component. The variance of the vector speed is given by

$$\mathrm{Var}[V] = \left[\frac{4}{\pi} - 1\right] E^2[V] = \left[\frac{4-\pi}{2}\right]\sigma^2 \tag{2.3}$$

and the cumulative density function (cdf) of the vector V is given by

$$F_V(v) = 1 - \exp\left[-\frac{\pi}{4}(v/m)^2\right] \tag{2.4}$$

2.2 EFFECT OF UNEQUAL COMPONENT VARIANCES

Consider now the somewhat more realistic case in which the variances of the two components are not equal (i.e., $\sigma_x^2 \neq \sigma_y^2$). For simplicity of computation, let $R = X^2$, $S = Y^2$, and $U = V^2$. Then

$$V = \sqrt{U} = \sqrt{X^2 + Y^2} = \sqrt{R + S} \tag{2.5}$$

Since X and Y are zero-mean Gaussian variates, their pdf's are

$$f_X(x) = \frac{1}{\sigma_x\sqrt{2\pi}} \exp\left[-x^2/2\sigma_x^2\right] \tag{2.6}$$

$$f_Y(y) = \frac{1}{\sigma_y\sqrt{2\pi}} \exp\left[-y^2/2\sigma_y^2\right] \tag{2.7}$$

The cumulative distribution function (cdf) of R may be found from the cdf of X as follows:

$$F_R(r) = P\left[R \leq r\right] = P\left[-\sqrt{r} \leq X \leq \sqrt{r}\right]$$

$$= 2F_X(\sqrt{r}) - 1 \tag{2.8}$$

from which the pdf of R is found:

$$f_R(r) = \frac{dF_R(r)}{dr} = \frac{d}{dx}\left[2F_X(\sqrt{r}) - 1\right]\frac{dx}{dr}$$

$$= 2 f_X(\sqrt{r})/2\sqrt{r}$$

$$= \frac{1}{\sigma_x\sqrt{2\pi r}}\left\{\exp\left[-r/2\sigma_x^2\right]\right\} \tag{2.9}$$

Similarly, the pdf of S is

$$f_S(s) = \frac{1}{\sigma_y\sqrt{2\pi s}} \left\{ \exp\left[- s/2\sigma_y^2\right] \right\} \tag{2.10}$$

Since U = R + S, the pdf of U is found from the convolution integral

$$f_U(u) = \int_0^u f_R(r)\, f_S(u-r)\, dr$$

$$= \frac{1}{2\pi\sigma_x\sigma_y} \int_0^u \frac{1}{\sqrt{r}\,\sqrt{u-r}} \exp\left[\frac{-r}{2\sigma_x^2} - \frac{(u-r)}{2\sigma_y^2} \right] dr$$

$$= \frac{1}{2\pi\sigma_x\sigma_y} \int_0^u \frac{1}{\sqrt{ur-r^2}} \exp\left[- \frac{1}{2} \left(\frac{r}{\sigma_x^2} + \frac{u}{\sigma_y^2} - \frac{r}{\sigma_y^2} \right) \right] dr \tag{2.11}$$

$$= \frac{1}{2\pi\sigma_x\sigma_y} \exp\left[- u/2\sigma_y^2\right] \int_0^u \frac{1}{\sqrt{ur-r^2}} \exp\left[- \frac{1}{2} \left(\frac{\sigma_y^2-\sigma_x^2}{\sigma_x^2\sigma_y^2} \right) r \right] dr$$

For ease of notation, let the following substitution be made:

$$A = \frac{1}{2\pi\sigma_x\sigma_y} \exp\left[- u/2\sigma_y^2\right] \tag{2.12}$$

$$B = \frac{\sigma_x^2-\sigma_y^2}{2\sigma_x^2\sigma_y^2} \tag{2.13}$$

Then

$$f_U(u) = A \int_0^u \frac{1}{\sqrt{ur-r^2}} \exp\left[Br\right] dr \tag{2.14}$$

Let the exponent now be expanded in an infinite power series. For simplicity, only the first three terms in the series will be shown:

$$f_U(u) = A \int_0^u \frac{1}{\sqrt{ur-r^2}} \left[1 + Br + \frac{B^2r^2}{2} + ...\right] dr \tag{2.15}$$

Standard integration may now be used for each term in the series, leading to

$$f_U(u) = A\left\{\sin^{-1}\left(\frac{r-u/2}{u/2}\right) + B\left[-\sqrt{ur-r^2} + \frac{u}{2}\sin^{-1}\left(\frac{r-u/2}{u/2}\right)\right]\right.$$
$$+ \frac{B^2}{2}\left[-\frac{r}{2}\sqrt{ur-r^2} - \frac{3u}{4}\sqrt{ur-r^2} + \frac{3u^2}{8}\sin^{-1}\left(\frac{r-u/2}{u/2}\right)\right]$$
$$\left. + \ldots\ldots\right\}\Bigg|_0^u \qquad (2.16)$$

Evaluating at the limits leads to

$$f_U(u) = A\left\{\pi + B\left[\frac{u}{2}\pi\right] + \frac{B^2}{2}\left[\frac{3u^2}{8}\pi\right] + \ldots.\right\}$$
$$= A\pi\sum_{n=0}^{\infty}\left[\frac{(2n)!\,(Bu)^n}{2^{2n}\,(n!)^3}\right] \qquad (2.17)$$

Since $V = \sqrt{U}$, the rule of monotonic derived distributions can be used to find the pdf of V,

$$f_V(v) = \frac{du}{dv} f_U(v^2)$$
$$= 2v\, f_U(v^2)$$
$$= 2\,v\,A\,\pi\sum_{n=0}^{\infty}\left[\frac{(2n)!\,(Bu)^n}{2^{2n}\,(n!)^3}\right] \qquad (2.18)$$

Substituting for A and B in terms of the original parameters leads to

$$f_V(v) = \frac{v}{\sigma_x\sigma_y}\exp\left[-v^2/2\sigma_y^2\right]\sum_{n=0}^{\infty}\frac{(2n)!\,v^{2n}}{2^{2n}\,(n!)^3}\left[\frac{\sigma_x^2-\sigma_y^2}{2\sigma_x^2\sigma_y^2}\right]^n \qquad (2.19)$$

The mean speed can be obtained as follows:

$$m_V = \int_0^\infty v\, f_V(v)\, dv$$

$$= \frac{\sigma_y^2}{\sigma_x} \sqrt{\frac{\pi}{2}} \sum_{n=0}^{\infty} \frac{1\cdot 3\cdot 5 \ldots (2n+1)\ (2n)!}{2^{2n}\ (n!)^3} \left[\frac{\sigma_x^2 - \sigma_y^2}{2\sigma_x^2} \right]^n \qquad (2.20)$$

Similarly, the variance is given by

$$\sigma_V^2 = \int_0^\infty v^2\, f_V(v)\, dv - (m_V)^2 \qquad (2.21)$$

where

$$\int_0^\infty v^2\, f_V(v)\, dv = \frac{\sigma_y^2}{\sigma_x} \sum_{n=0}^{\infty} \frac{(2n)!\ (n+1)}{2^{2n-1}\ (n!)^2} \left[\frac{\sigma_x^2 - \sigma_y^2}{\sigma_x^2} \right]^n \qquad (2.22)$$

Equations (2.20) and (2.21) can be approximated by rectangular integration as follows:

$$m_V \simeq \sum_{i=0}^{\infty} v_i\, f_V(v_i)\, \Delta v \qquad (2.23)$$

and

$$\sigma_V^2 \simeq \sum_{i=0}^{\infty} v_i^2\, f_V(v_i)\, \Delta v - \left[\sum_{i=0}^{\infty} v_i\, f_V(v_i)\, \Delta v \right]^2 \qquad (2.24)$$

When $\sigma_x = \sigma_y$ (B = 0), Eq. (2.19) reduces to the Rayleigh distribution, and Equations (2.20) and (2.21) reduce to Equations (2.2) and (2.3), respectively.

In order to assess the significance of the unequal variance probability distribution, Eq. (2.19) has been evaluated numerically for different values of σ_x and σ_y. For illustration purposes, one variance

was evaluated from Eq. (2.2) for m equal to 4 m/s, 6 m/s and 8 m/s (8.9, 13.4 and 17.9 mph) while the other variance was allowed to vary from 0.5 to 4.0 times the reference variance. Some selected results are presented in Figures 2.1 - 2.9.

In each of the figures, the derived probability density function (Eq. (2.19)) is shown, along with the Rayleigh distribution with the same mean. The mean was evalulated from Eq. (2.23) with an increment of 0.1 m/s. The reference variance was based on an original mean speed of 4 m/s, 6 m/s and 8 m/s (8.9, 13.4, 17.9 mph).

As can be seen from the nine figures, the derived distribution is well modeled by Rayleigh, even for the relatively wide range of variance ratios that was considered. The slight shift to the right by the Rayleigh suggests that the Rayleigh may fit better with the mode of observed data than with the mean (except in the extreme upper tail region). The mode can be found by setting the first derivative of Eq. (2.1) equal to zero, which leads to

$$\text{mode} = m\sqrt{\frac{2}{\pi}} \tag{2.25}$$

It is interesting to note that a given ratio of variances X and Y and the inverse ratio yield the same probability function. This can easily be verified by letting $\sigma_y^2 = \sigma^2$ in Eq. (2.2) Let σ_y be constant and vary σ_x, defining

$$K = \frac{\sigma_x}{\sigma_y} = \frac{\sigma_x}{\sigma} \tag{2.26}$$

Then Eq. (2.19) can be written as

$$f_V(v) = \frac{v}{K\sigma^2} \exp\left[-v^2/2\sigma^2\right] \sum_{n=0}^{\infty} \frac{(2n)!\, v^{2n}}{2^{2n}\,(n!)^3} \left[\frac{K^2 - 1}{2K^2\sigma^2}\right]^n \tag{2.27}$$

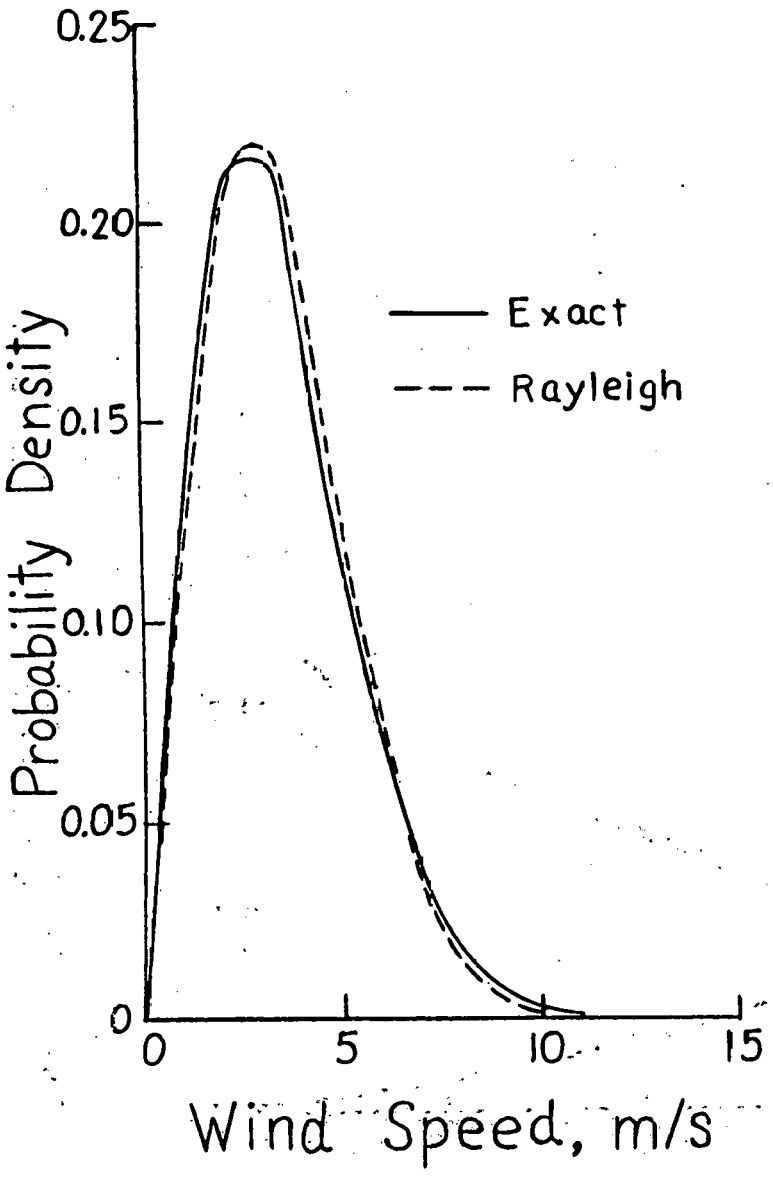

FIGURE 2.1 Exact and Fitted Rayleigh Probability Distribution for Variance Ratio of 0.5, Initial Mean Wind Speed of 4 m/s.

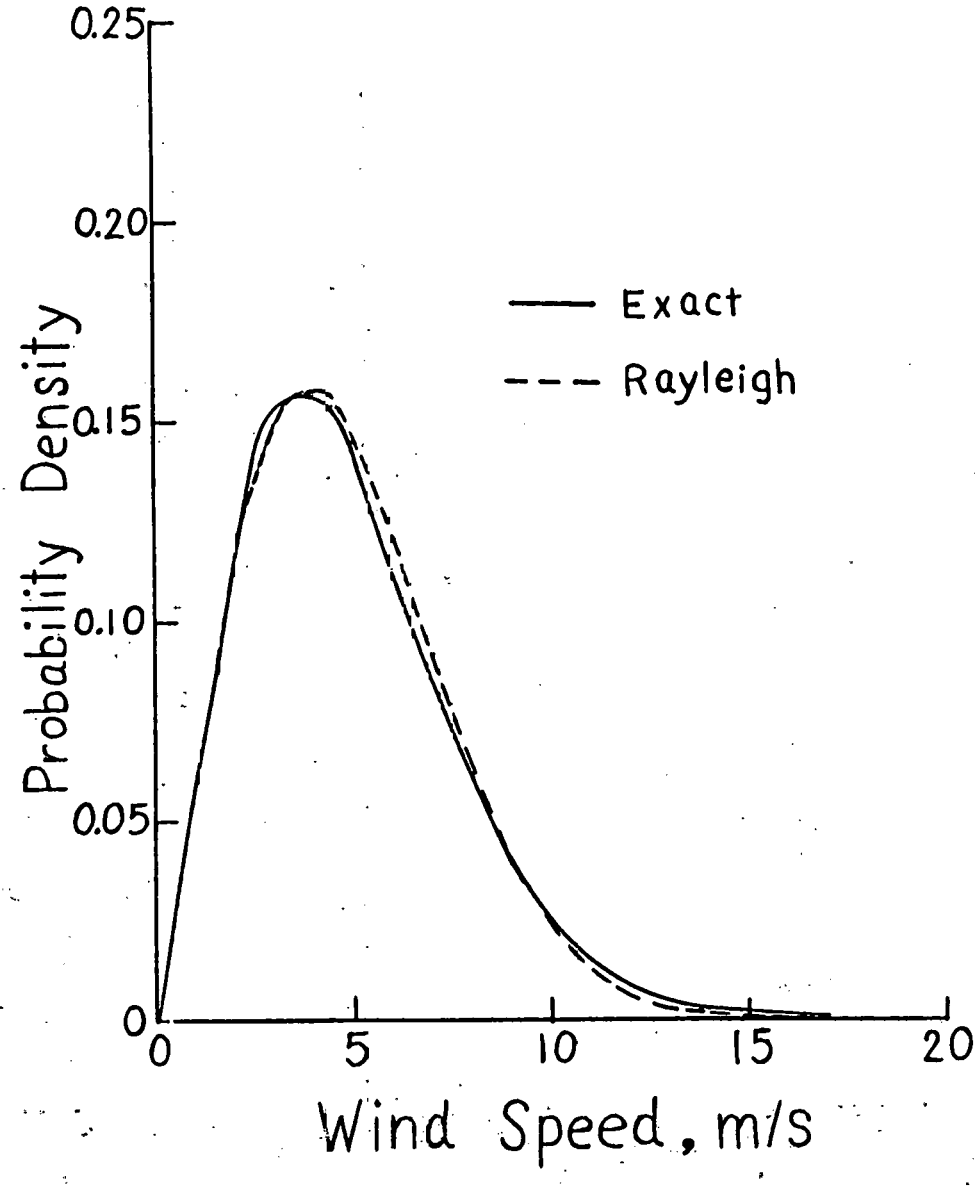

FIGURE 2.2 Exact and Fitted Rayleigh Probability Distribution for Variance Ratio of 2.0, Initial Mean Wind Speed of 4 m/s.

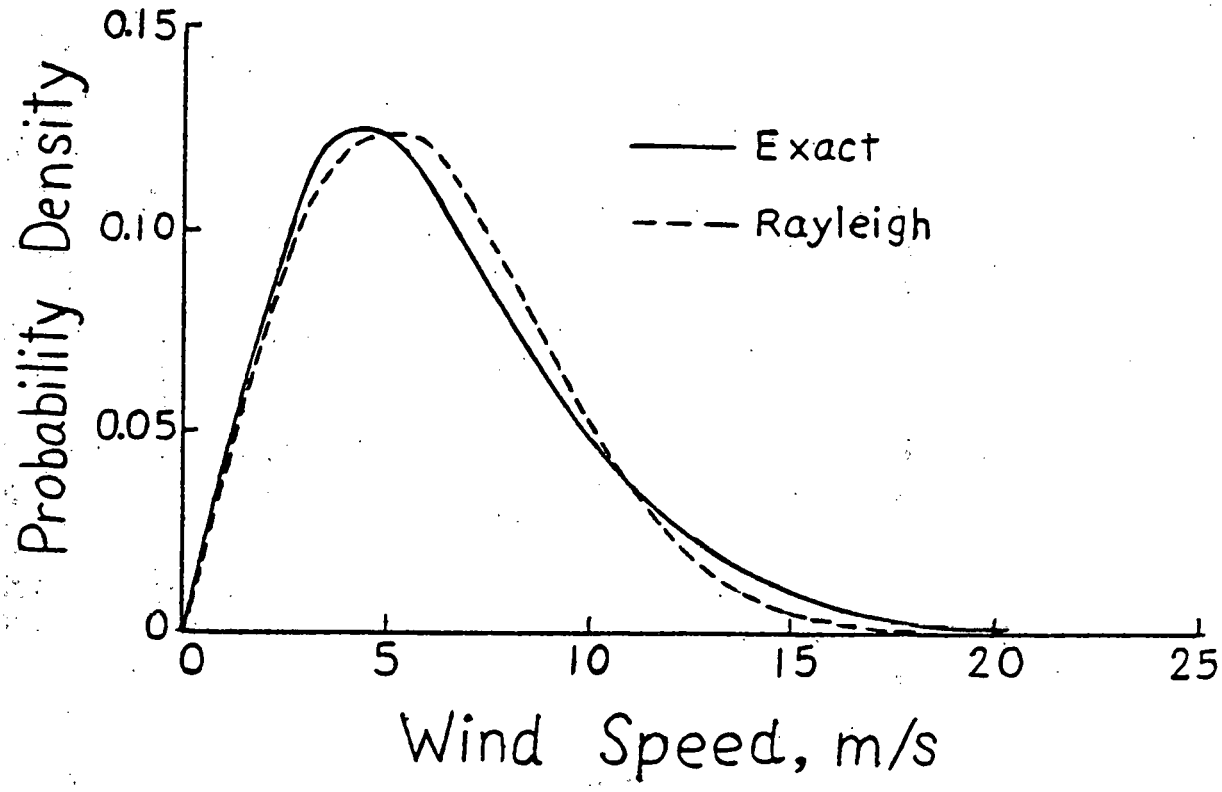

FIGURE 2.3 Exact and Fitted Rayleigh Probability Distribution for Variance Ratio of 4.0, Initial Mean Wind Speed of 4 m/s (8.9 mph).

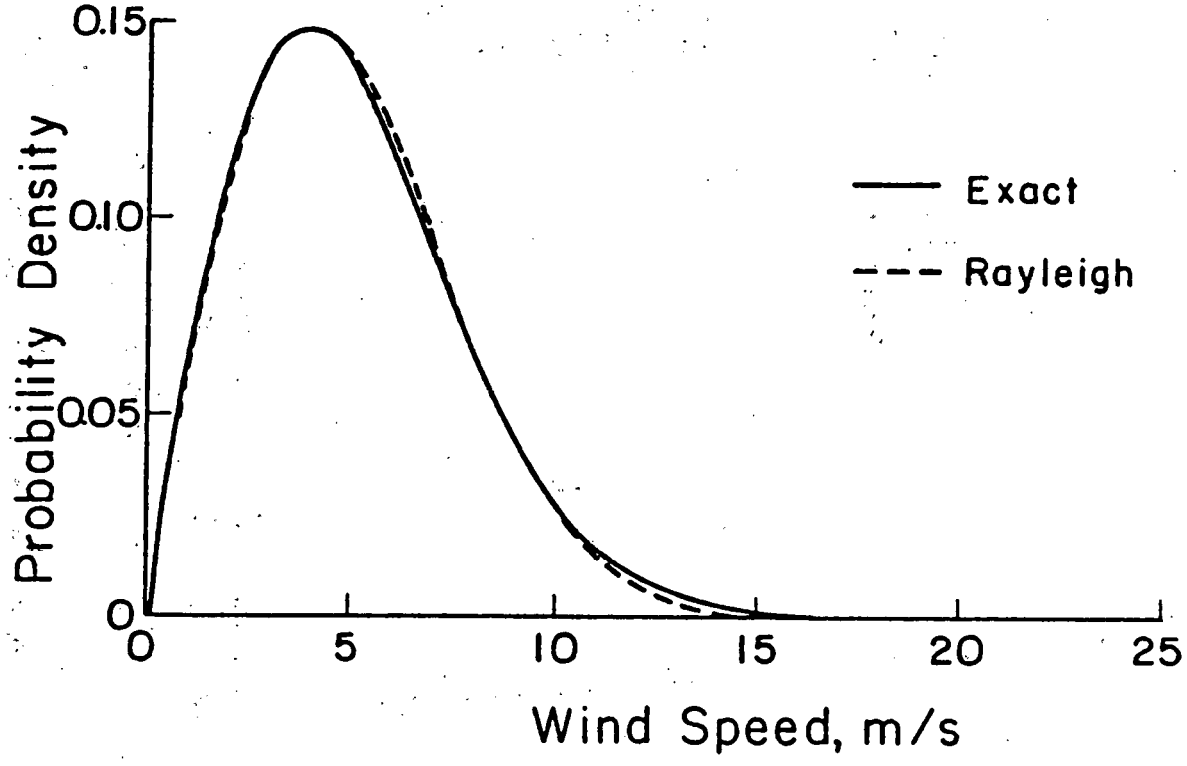

Figure 2.4 Exact and Fitted Rayleigh Probability Distribution for Variance Ratio of 0.5, Initial Mean Wind Speed of 6 m/s (13.4 mph).

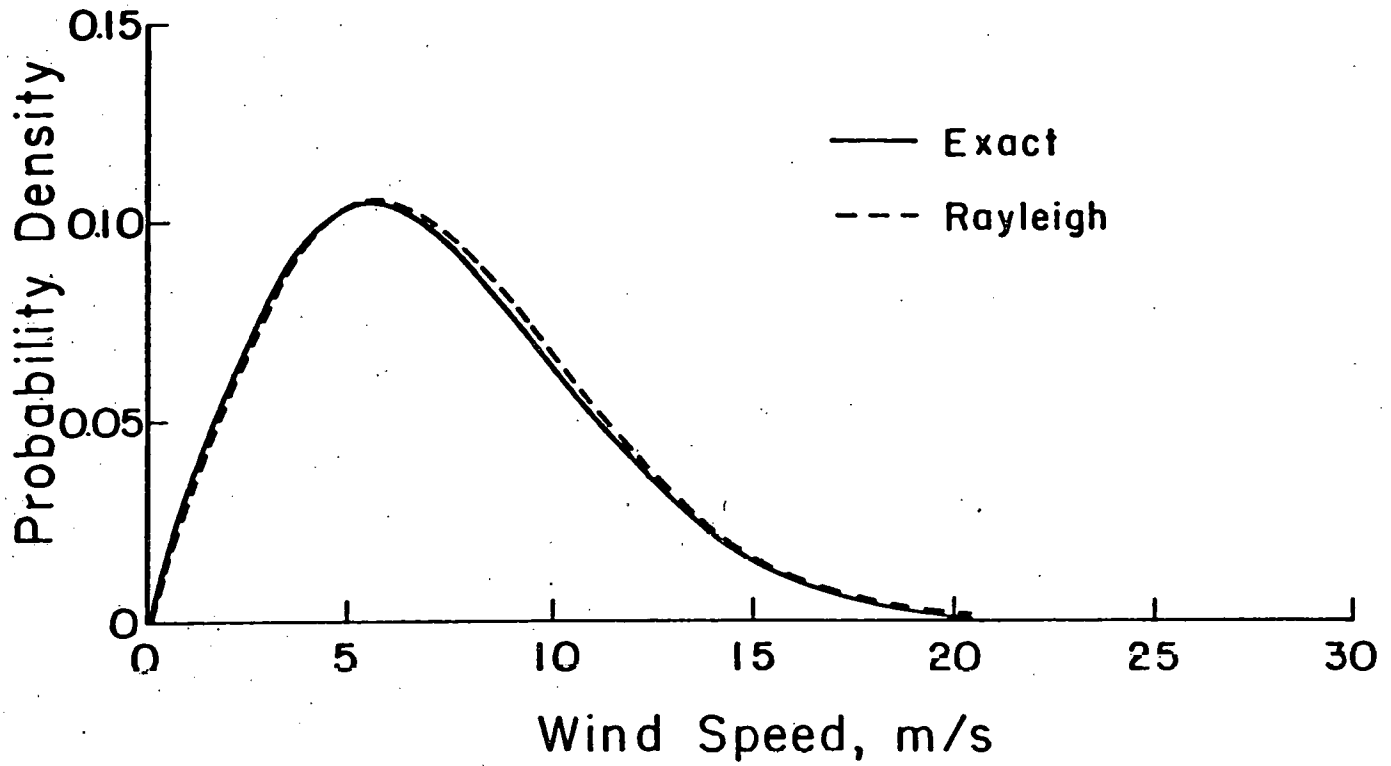

FIGURE 2.5 Exact and Fitted Rayleigh Probability Distribution for Variance Ratio of 2.0, Initial Mean Wind Speed of 6 m/s.

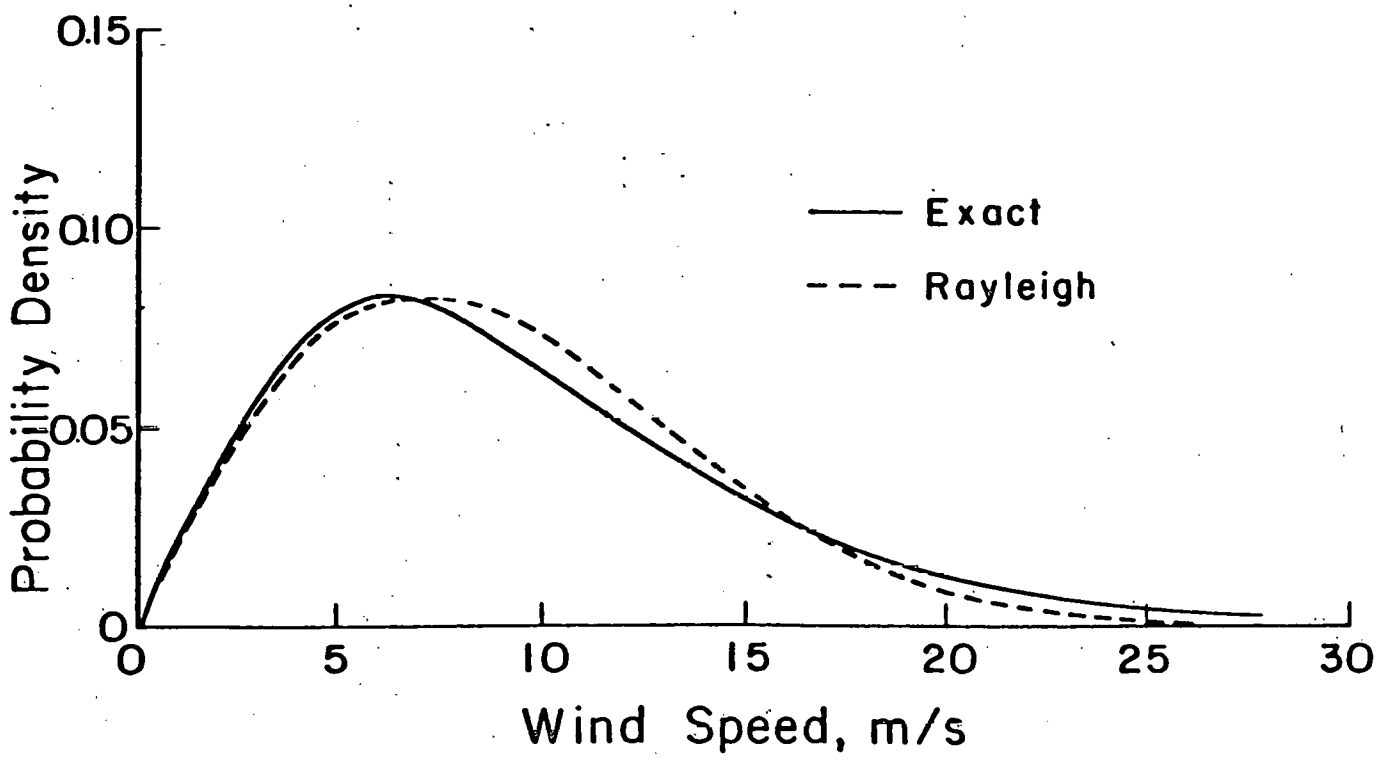

FIGURE 2.6 Exact and Fitted Rayleigh Probability Distribution for Variance Ratio of 4.0, Initial Mean Wind Speed of 6 m/s.

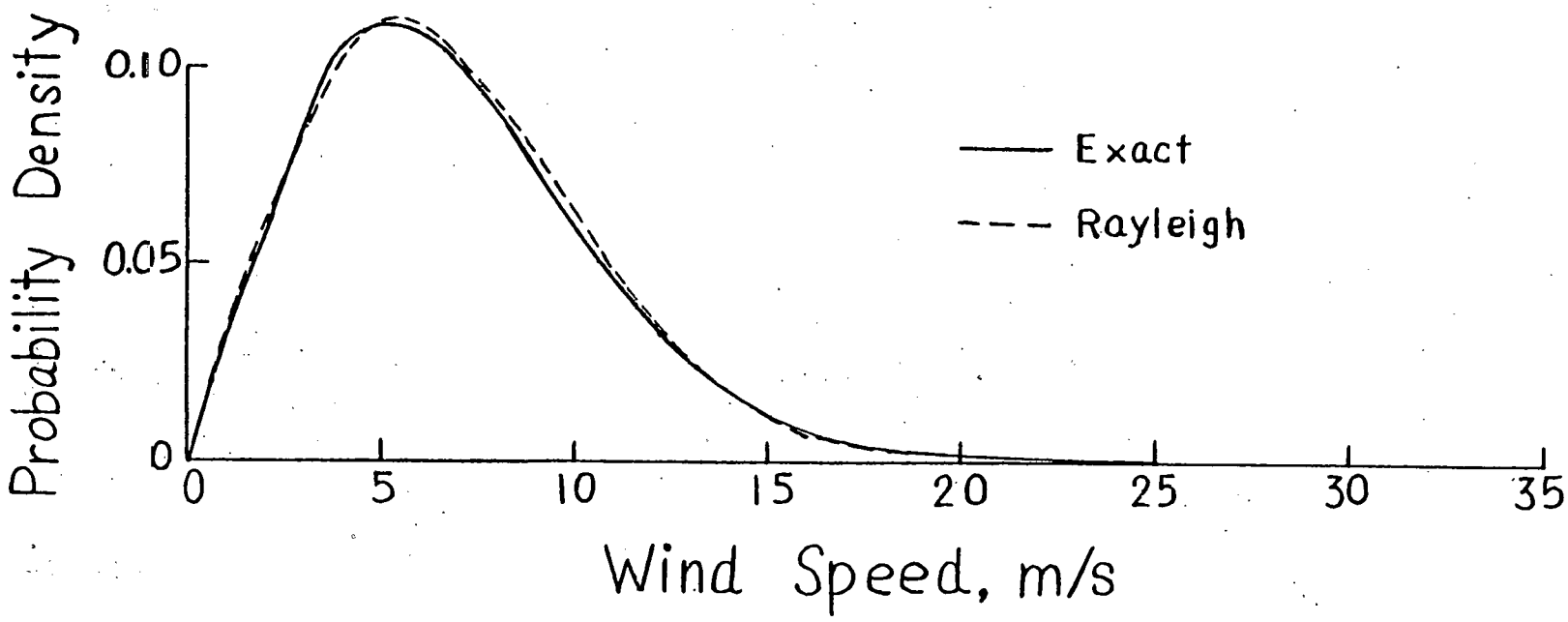

FIGURE 2.7 Exact and Fitted Rayleigh Probability Distribution for Variance Ratio of 0.5, Initial Mean Wind Speed of 8 m/s (17.9 mph).

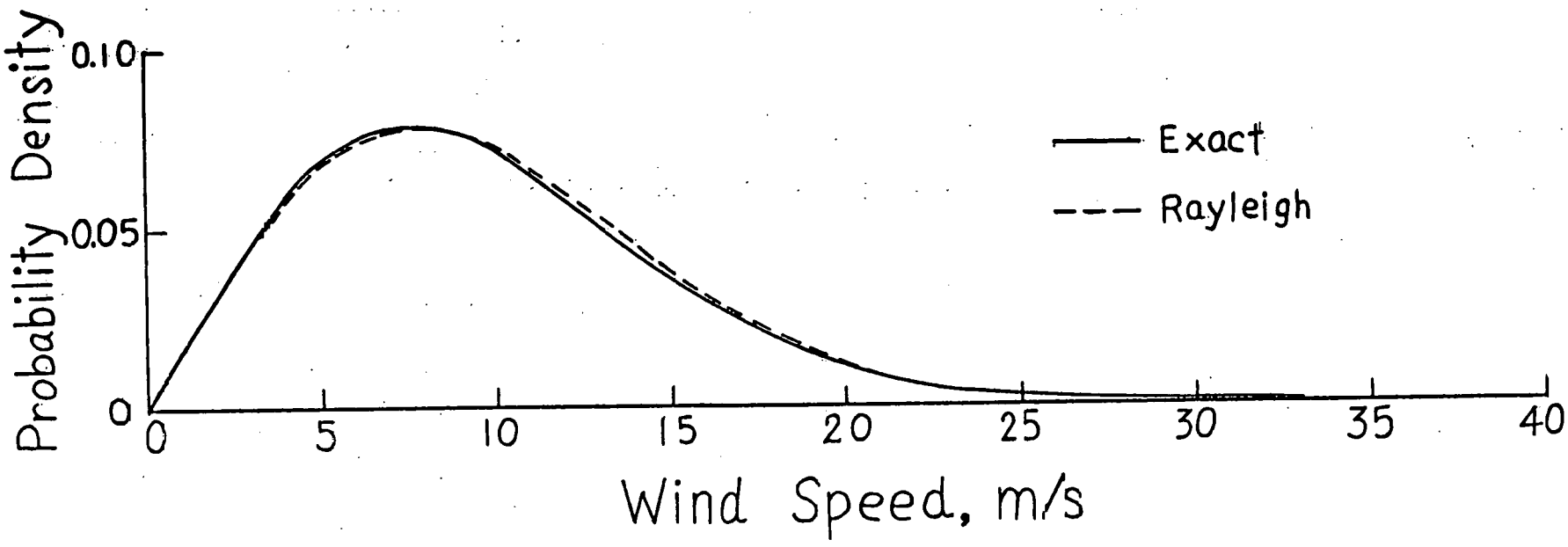

FIGURE 2.8 Exact and Fitted Rayleigh Probability Distribution for Variance Ratio of 2.0, Initial Mean Wind Speed of 8 m/s (17.9 mph).

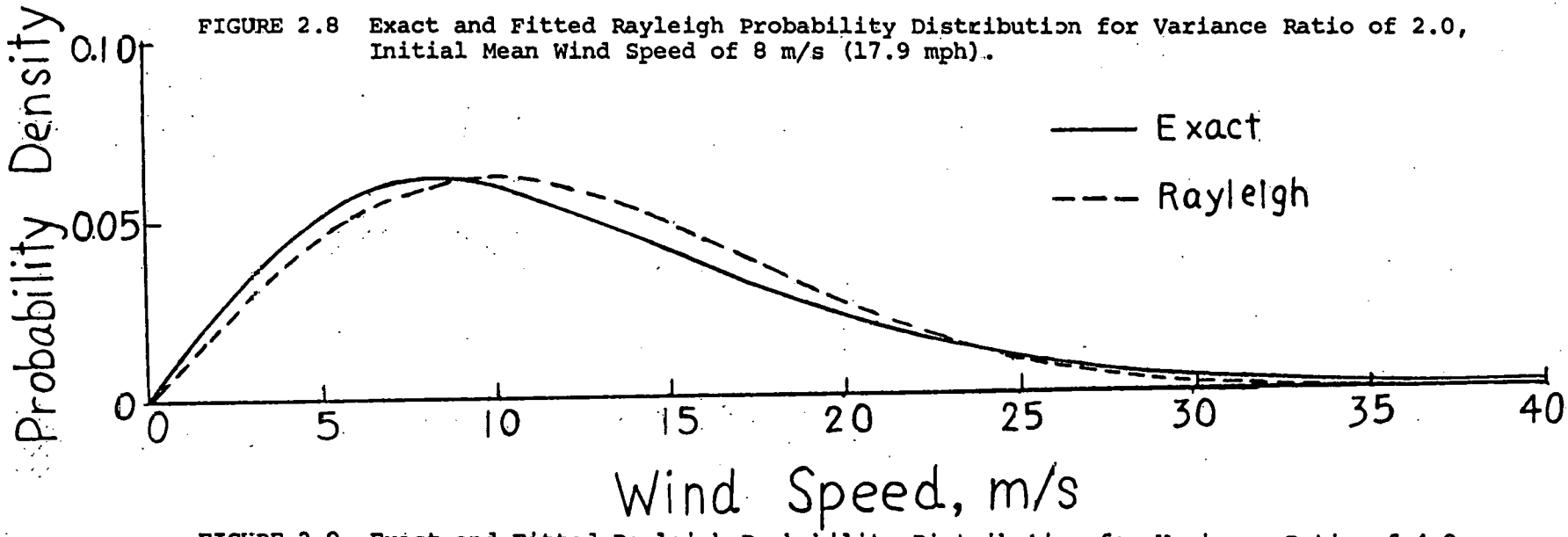

FIGURE 2.9 Exact and Fitted Rayleigh Probability Distribution for Variance Ratio of 4.9, Initial Mean Wind Speed of 8 m/s (17.9 mph).

Now, let

$$k = \frac{\sigma}{\sigma_x} \tag{2.28}$$

$$f_V(v) = \frac{v}{\sigma^2/k} \exp\left[-v^2/2\sigma^2\right] \sum_{n=0}^{\infty} \frac{(2n)!\, v^{2n}}{2^{2n}\,(n!)^3} \left[\frac{1/k^2 - 1}{2\sigma^2/k^2}\right]^n \tag{2.29}$$

Since k is the inverse of K, Eqs. (2.27) and (2.29) are equivalent.

It is of interest to note that for a given ratio of variances of X and Y, the simulated mean speed and the standard deviation vary linearly with the Rayleigh mean wind speed, m. This can be shown by substituting Eq. (2.26) into Eqs. (2.20 - 2.22) and letting

$$C = \sqrt{\frac{\pi}{2}}\, \frac{1\cdot 3\cdot 5 \ldots (2n+1)\ (2n)!}{2^{2n}\,(n!)^3} \tag{2.30}$$

$$\overline{C} = \frac{(2n)!\ (n+1)}{2^{2n-1}\,(n!)^2} \tag{2.31}$$

Then Eq. (2.20) becomes

$$m_V = \sigma \sum_{n=0}^{\infty} \frac{C}{K}\left[\frac{K^2-1}{2K^2}\right]^n \tag{2.32}$$

and Eq. (2.21) becomes

$$\sigma_V^2 = \sigma^2 \left\{ \sum_{n=0}^{\infty} \frac{\overline{C}}{K}\left[\frac{K^2-1}{K^2}\right]^n - \left[\sum_{n=0}^{\infty} \frac{C}{K}\left[\frac{K^2-1}{2K^2}\right]^n\right]^2 \right\} \tag{2.33}$$

Thus, for a given variance ratio, the derived mean and standard deviation are directly proportional to σ, and hence to m by Eq. (2.2). This means that the coefficient of variation,

$$V_V = \sigma_V / m_V \tag{2.34}$$

is independent of the Rayleigh mean wind speed and varies only with the variance ratio. Table 2.1 provides some statistics based on various Rayleigh (referred to as initial) mean wind speeds and variance ratios.

One may notice from Figs. 2.1 - 2.9 that the standard deviation of wind speed increases with increasing variance ratio and initial mean wind speed. In Fig. 2.10 pdf's are shown for various variance ratios (ranging from 0.5 to 4.0) with the same initial mean wind speed of 6 m/s (13.4 mph). Figure 2.11 shows the pdf's for the combined effects of variance ratio and initial mean wind speed. When the wind speed standard deviation gives a broad $f_V(v)$, calculation of m_V and σ_V (Eqs. (2.23-2.24)) should include the probability density function for high values of wind speed. Then more terms are needed to compute the infinite summation in Eq. (2.19) in order to ensure that Eqs. (2.23-2.24) are reasonably good approximations for Eqs. (2.20) and (2.21).

2.3 EFFECT OF COMPONENT CORRELATION

Now consider a more general case in which the two horizontal wind components are correlated. These two components form an elliptical bivariate normal (zero-mean) distribution (Crutcher and Baer, 1962). The joint probability density function for components X and Y is

$$f_{XY}(x,y) = \frac{1}{2\pi\sigma_x\sigma_y\sqrt{1-\rho^2}} \exp\left\{\frac{-1}{2(1-\rho^2)}\left[\left(\frac{x}{\sigma_x}\right)^2 - 2\rho\frac{xy}{\sigma_x\sigma_y} + \left(\frac{y}{\sigma_y}\right)^2\right]\right\} \tag{2.35}$$

where ρ is the correlation between X and Y. Let α be defined as the angle between the X-Y axes and a new set of axes, X'-Y'. Then

$$X' = X\cos\alpha + Y\sin\alpha \tag{2.36}$$

TABLE 2.1 Input Variables and Derived Statistics for the Horizontal Wind Speed Vector for Various Initial Mean Speed

IMV[1] (m/s)	$R = \frac{\sigma_y}{\sigma_x}$	m_V[2] (m/s)	σ_V[3] (m/s)	Coefficient of Variation
4.0	0.7	3.427	1.854	.5410
4.0	0.8	3.611	1.914	.5301
4.0	0.9	3.803	1.994	.5244
4.0	1.0	4.000	2.091	.5227
4.0	1.1	4.202	2.202	.5241
4.0	1.2	4.409	2.327	.5277
4.0	1.4	4.833	2.605	.5390
4.0	1.5	5.049	2.755	.5457
4.0	2.0	6.125	3.532	.5766
6.0	0.7	5.140	2.780	.5410
6.0	0.8	5.417	2.872	.5301
6.0	0.9	5.704	2.991	.5244
6.0	1.0	6.000	3.136	.5227
6.0	1.1	6.304	3.304	.5241
6.0	1.2	6.614	3.490	.5277
6.0	1.4	7.250	3.980	.5390
6.0	1.5	7.571	4.129	.5457
6.0	2.0	9.252	5.385	.5766
8.0	0.7	6.853	3.707	.5410
8.0	0.8	7.222	3.829	.5301
8.0	0.9	7.605	3.988	.5244
8.0	1.0	8.000	4.182	.5227
8.0	1.1	8.405	4.405	.5241
8.0	1.2	8.818	4.653	.5277
8.0	1.4	9.666	5.210	.5390
8.0	1.5	10.099	5.510	.5457
8.0	2.0	12.249	7.062	.5766

[1] IMV = m_V when $\sigma_x = \sigma_y$

[2] Evaluated from Eq. (2.23)

[3] Evaluated from Eq. (2.24)

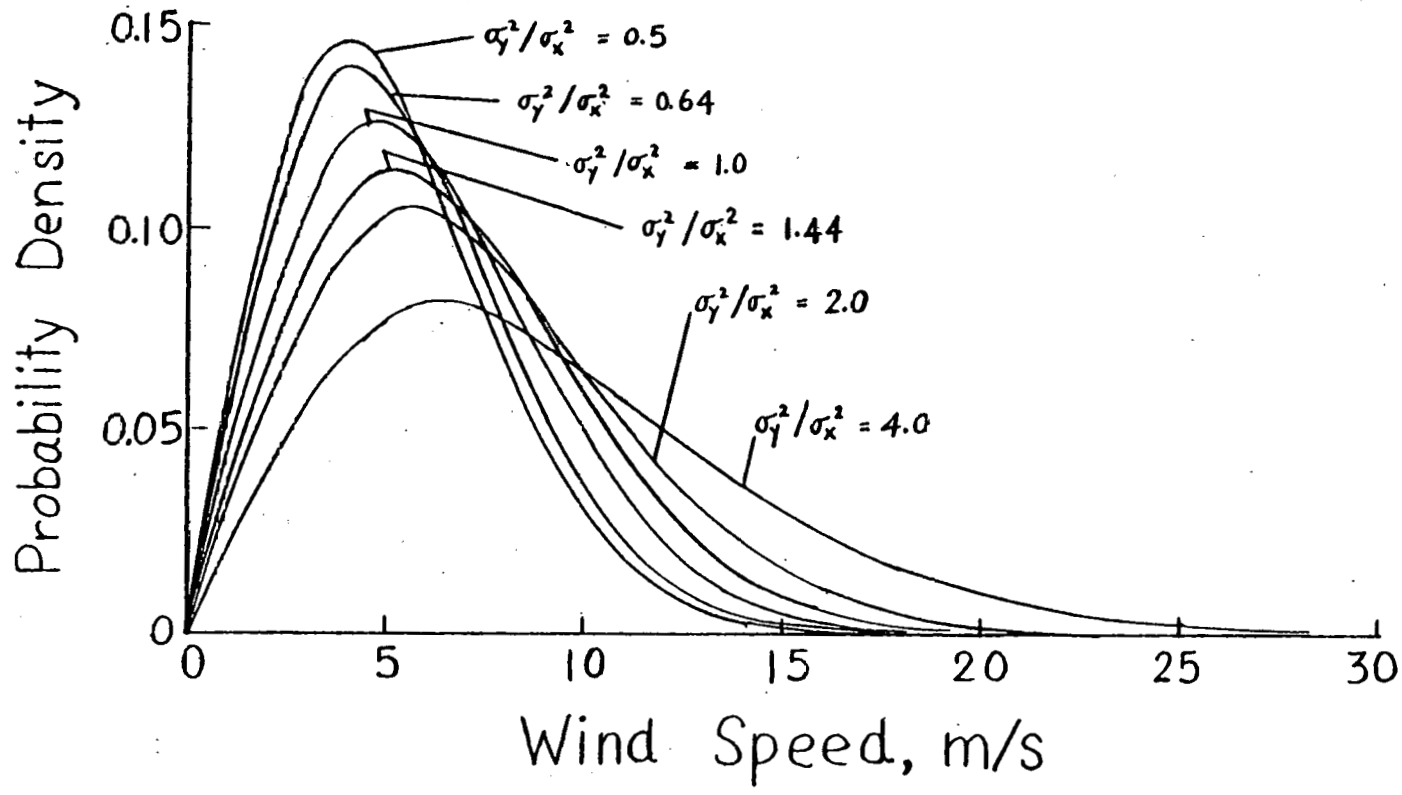

FIGURE 2.10 Probability Density Functions - with Initial Mean Wind Speed of 6 m/s (13.4 mph) and Various Variance Ratios.

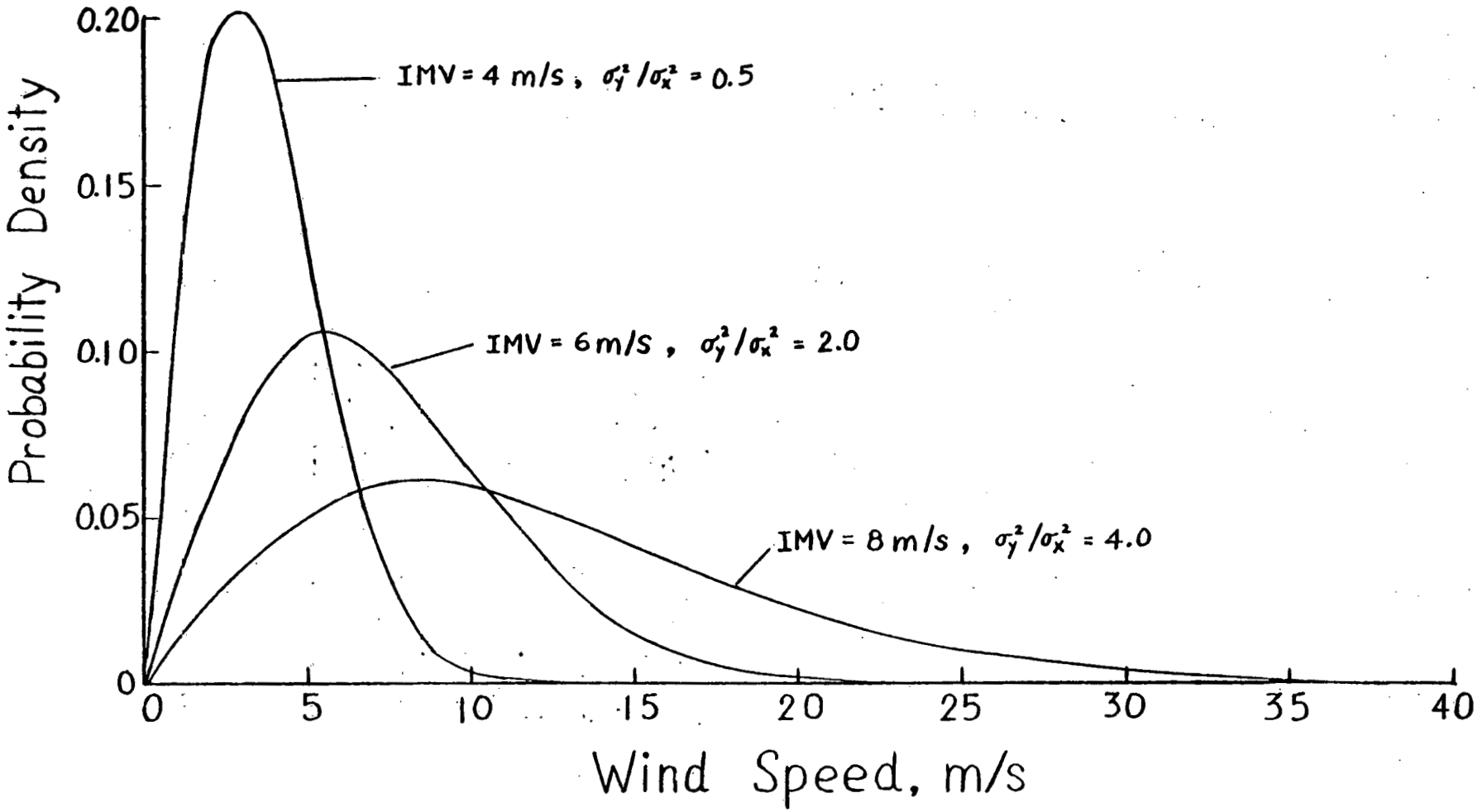

FIGURE 2.11 Probability Density Functions with Various Initial Mean Wind Speeds (IMV) and Variance Ratios

$$Y' = Y \cos \alpha - X \sin \alpha \tag{2.37}$$

The iso-probability contours of the joint probability function form ellipses of various orientations. By selecting α such that the major-minor axes of the ellipses coincide with the X'-Y' axes, components expressed in the new X'-Y' system are independent. It may be shown (Hald, 1952) that such an angle, α, is given by

$$\tan 2\alpha = \begin{cases} \dfrac{2\rho\, \sigma_x \sigma_y}{\sigma_x^2 - \sigma_y^2} & \sigma_x \neq \sigma_y \\ \dfrac{\pi}{4} & \sigma_x = \sigma_y \end{cases} \tag{2.38}$$

and the joint pdf for the X' and Y' components is

$$f_{X'Y'}(x', y') = \frac{1}{2\pi\, \sigma_{x'} \sigma_{y'}} \exp \left\{ -\frac{1}{2} \left[\left(\frac{x'}{\sigma_{x'}} \right)^2 + \left(\frac{Y'}{\sigma_{y'}} \right)^2 \right] \right\} \tag{2.39}$$

Since the components are independent, Eq. (2.39) can be factored into the marginal density functions

$$f_{X'}(x') = \frac{1}{\sigma_{x'} \sqrt{2\pi}} \exp \left[-\frac{1}{2} \left(\frac{x'}{\sigma_{x'}} \right)^2 \right] \tag{2.40}$$

and

$$f_{Y'}(y') = \frac{1}{\sigma_{y'} \sqrt{2\pi}} \exp \left[-\frac{1}{2} \left(\frac{Y'}{\sigma_{y'}} \right)^2 \right] \tag{2.41}$$

The independence of X' and Y', and the similarity of Equations (2.40) and (2.41) to Eqs. (2.6) and (2.7), respectively, imply that Eqs. (2.8 - 2.19) can be used with X' and Y' to derive the probability density function of the horizontal wind speed. It is necessary to

obtain $\sigma_{x'}$ and $\sigma_{y'}$ in terms of σ_x and σ_y and the correlation ρ. Comparing Eq. (2.39) with Eq. (2.35), leads to a system of two equations with two unknowns,

$$\sigma_{x'}\,\sigma_{y'} = \sigma_x \sigma_y \sqrt{1-\rho^2} \tag{2.42}$$

$$\sigma_{x'}^2 + \sigma_{y'}^2 = \sigma_x^2 + \sigma_y^2 \tag{2.43}$$

By solving Eqs. (2.42) and (2.43) simultaneously and letting

$$D = \sqrt{\sigma_x^2 + \sigma_y^2 + 2\sigma_x\sigma_y\sqrt{1-\rho^2}} \tag{2.44}$$

$$E = \sqrt{\sigma_x^2 + \sigma_y^2 - 2\sigma_x\sigma_y\sqrt{1-\rho^2}} \tag{2.45}$$

for ease of notation, one obtains

$$\sigma_{x'} = \begin{cases} \frac{1}{2}(D + E) & \rho > 0 \\ \frac{1}{2}(D - E) & \rho < 0 \end{cases} \tag{2.46}$$

$$\sigma_{y'} = D - \sigma_{x'} \tag{2.47}$$

Analogous to the procedure for the unequal variances with zero correlation, Eq. (2.19) for X' and Y' components was evaluated numerically for different values of variances of X and Y and correlation ρ. Again, one variance was held constant and evaluated from Eq. (2.2) for a vector mean wind speed equal to 6 m/s (13.4 mph) while the other variance was varied from 0.5 to 4 times the reference variance. Component correlation values of $\pm$ 0.5 and $\pm$ 0.2 were introduced for each variance ratio. Selected results are shown in Figures (2.12 - 2.19). As in the previous section, the derived

probability density function (Eq. (2.19)) is shown along with the Rayleigh for the same mean (computed from Eq. (2.23)). Although the Rayleigh does not fit the derived pdf for the correlated quite as well as the non-correlated components, it still gives a reasonable approximation.

There are two interesting features of the distribution of the wind vector that are worthy of note. One is that the density function is symmetric with respect to the sign of the correlation between the components. The other is that the derived mean, m_v, decreases with increasing correlation. The latter was observed from the results of Eq. (2.23) and can be seen in Table 2.2. The former can be verified as follows: When $\rho > 0$,

$$\frac{\sigma_{x'}}{\sigma_{y'}} = \frac{D + E}{D - E} \tag{2.48a}$$

and for $\rho < 0$,

$$\frac{\sigma_{x'}}{\sigma_{y'}} = \frac{D - E}{D + E} \tag{2.48b}$$

which is the inverse ratio of that for $\rho > 0$. Thus from Eqs. (2.26 - 2.29), the unequal variance with $\pm\rho$ have the same pdf.

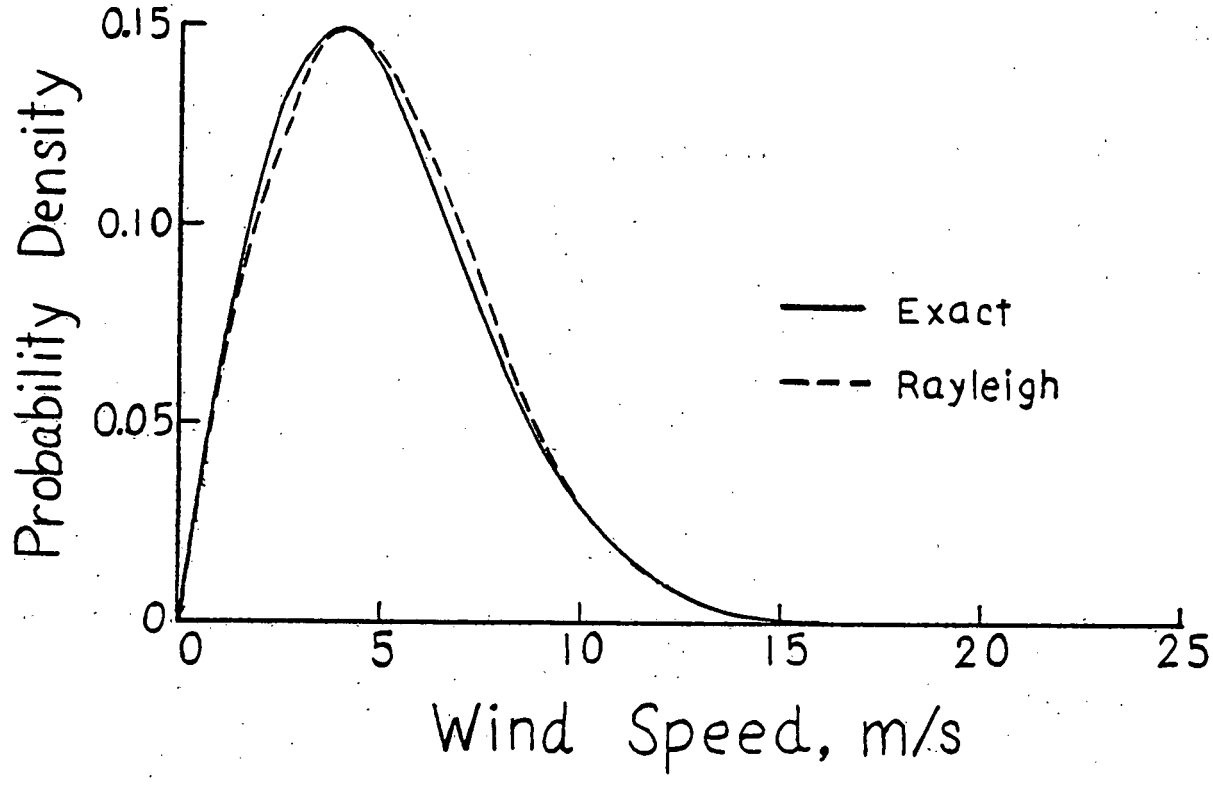

FIGURE 2.12 Exact and Fitted Rayleigh Probability Distribution for Variance Ratio of 0.5, $\rho = 0.2$.

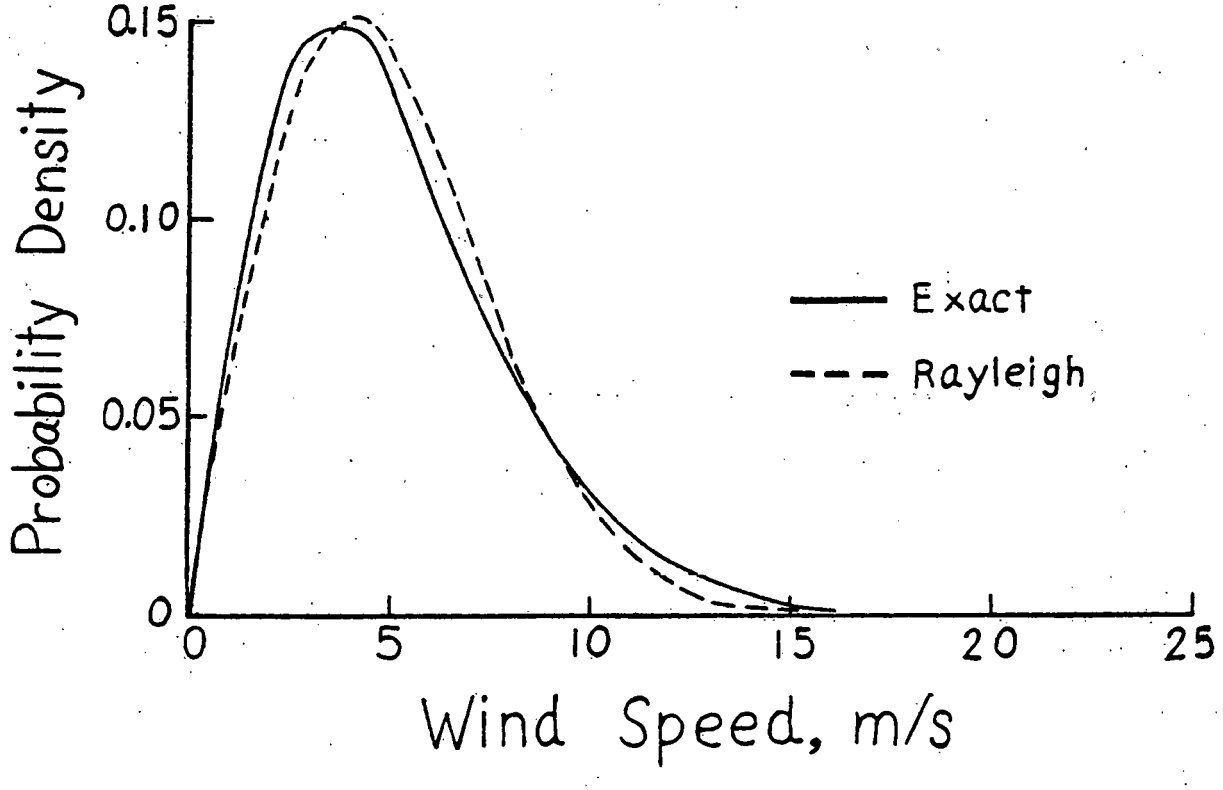

FIGURE 2.13 Exact and Fitted Rayleigh Probability Distribution for Variance Ratio of 0.5, $\rho = 0.5$.

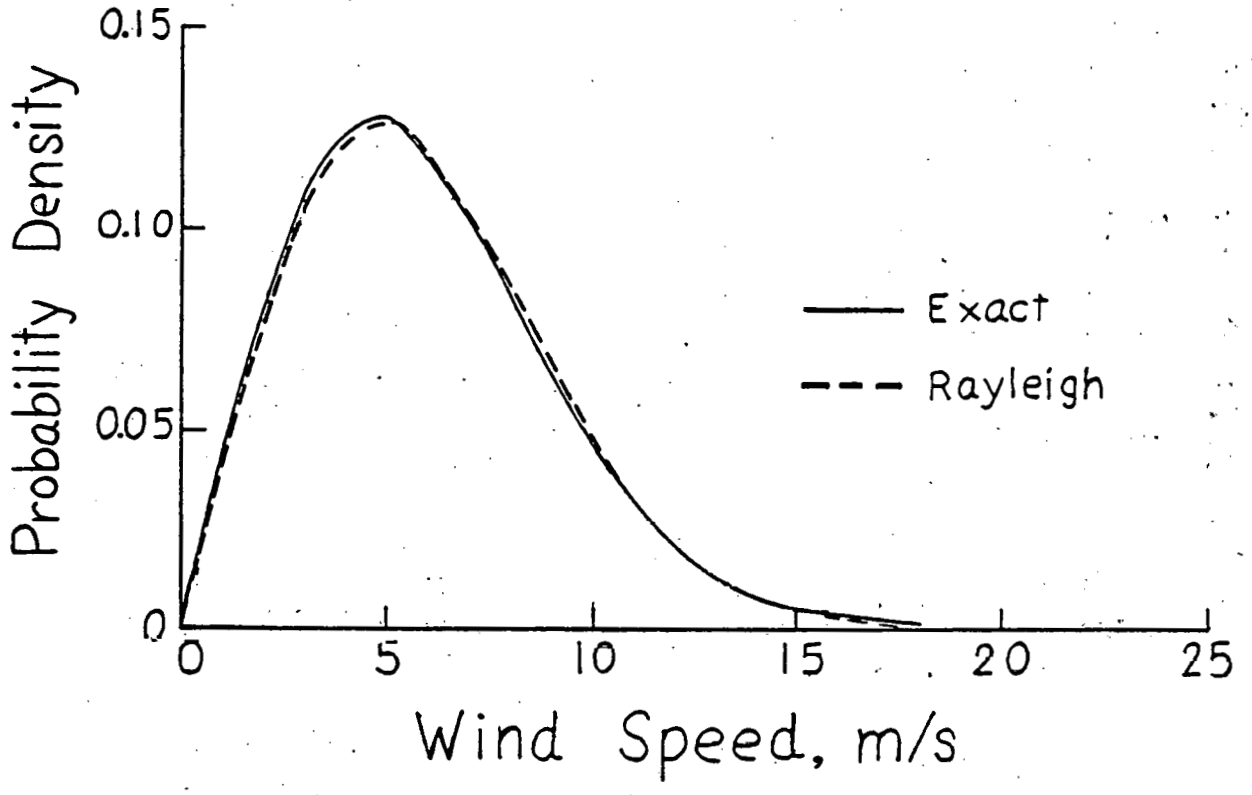

FIGURE 2.14 Exact and Fitted Rayleigh Probability Distribution for Variance Ratio of 1.0, $\rho = 0.2$.

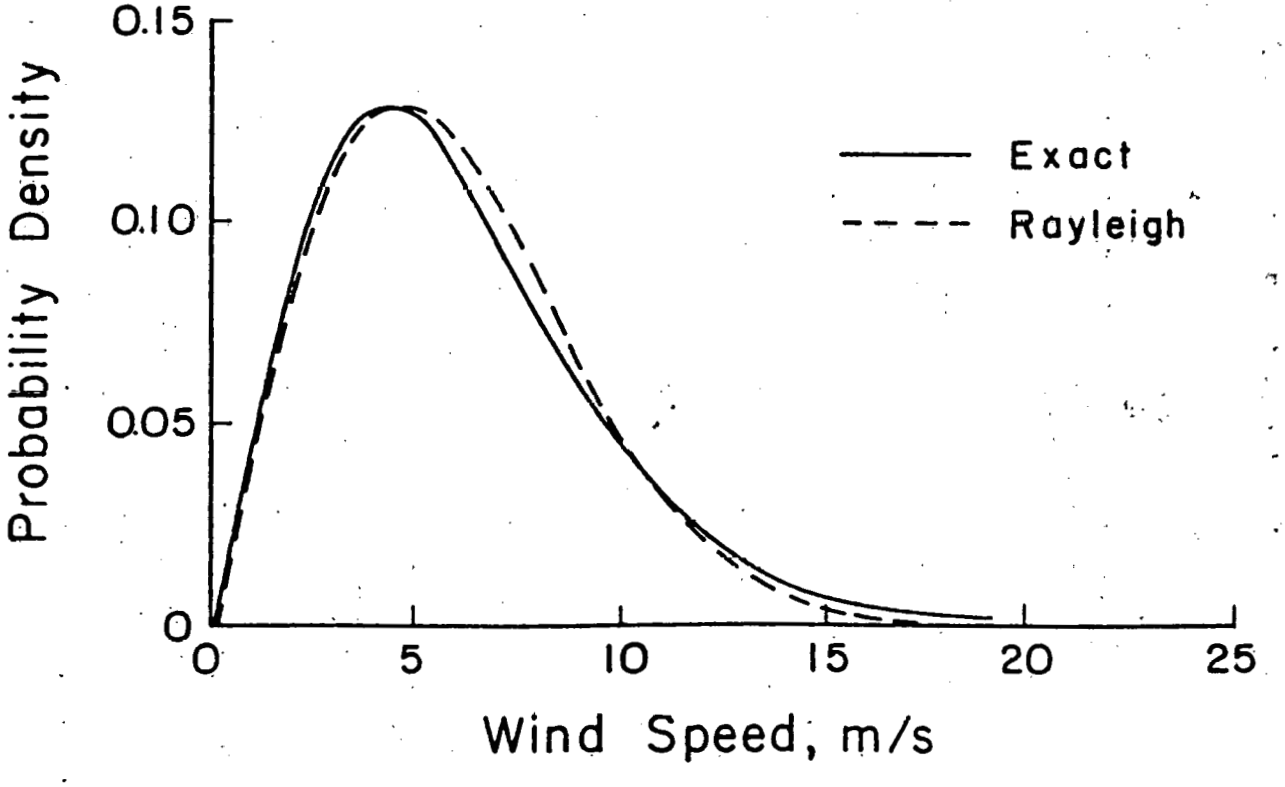

FIGURE 2.15 Exact and Fitted Rayleigh Probability Distribution for Variance Ratio of 1.0, $\rho = 0.5$.

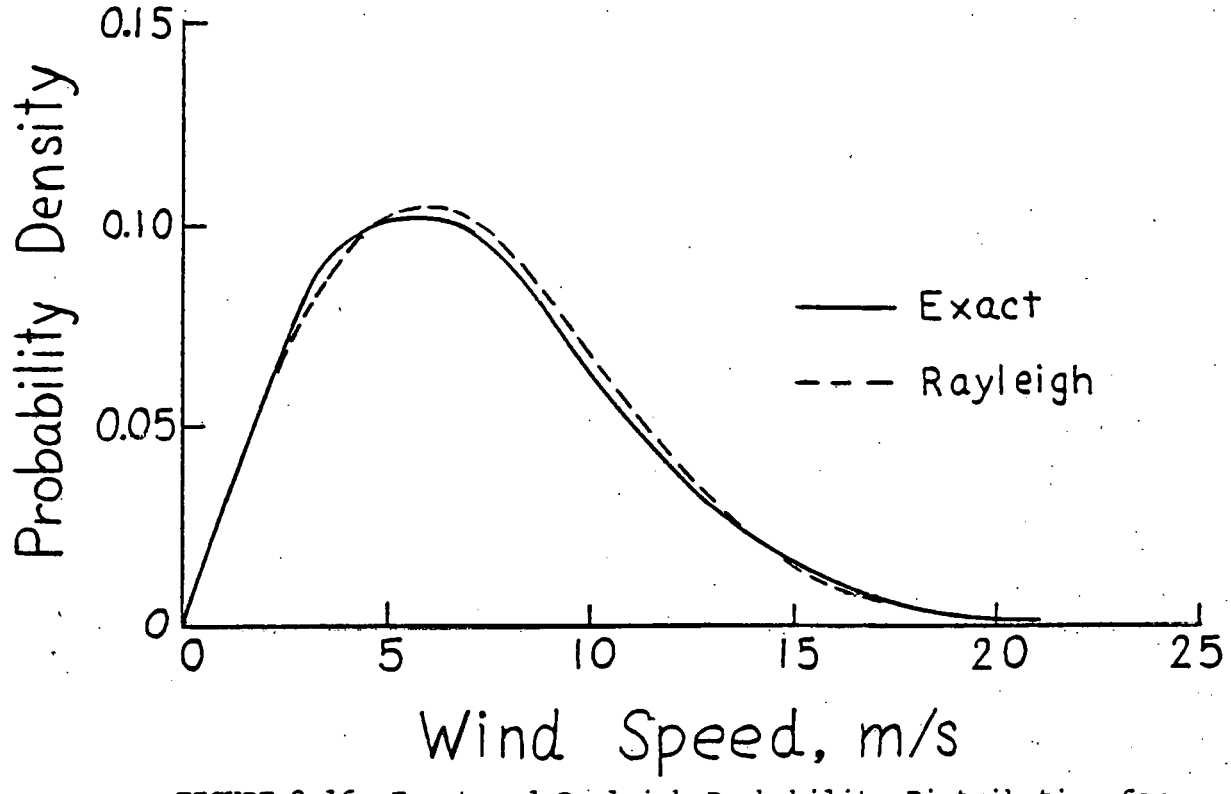

FIGURE 2.16 Exact and Rayleigh Probability Distribution for Variance Ratio of 2.0, $\rho = 0.2$.

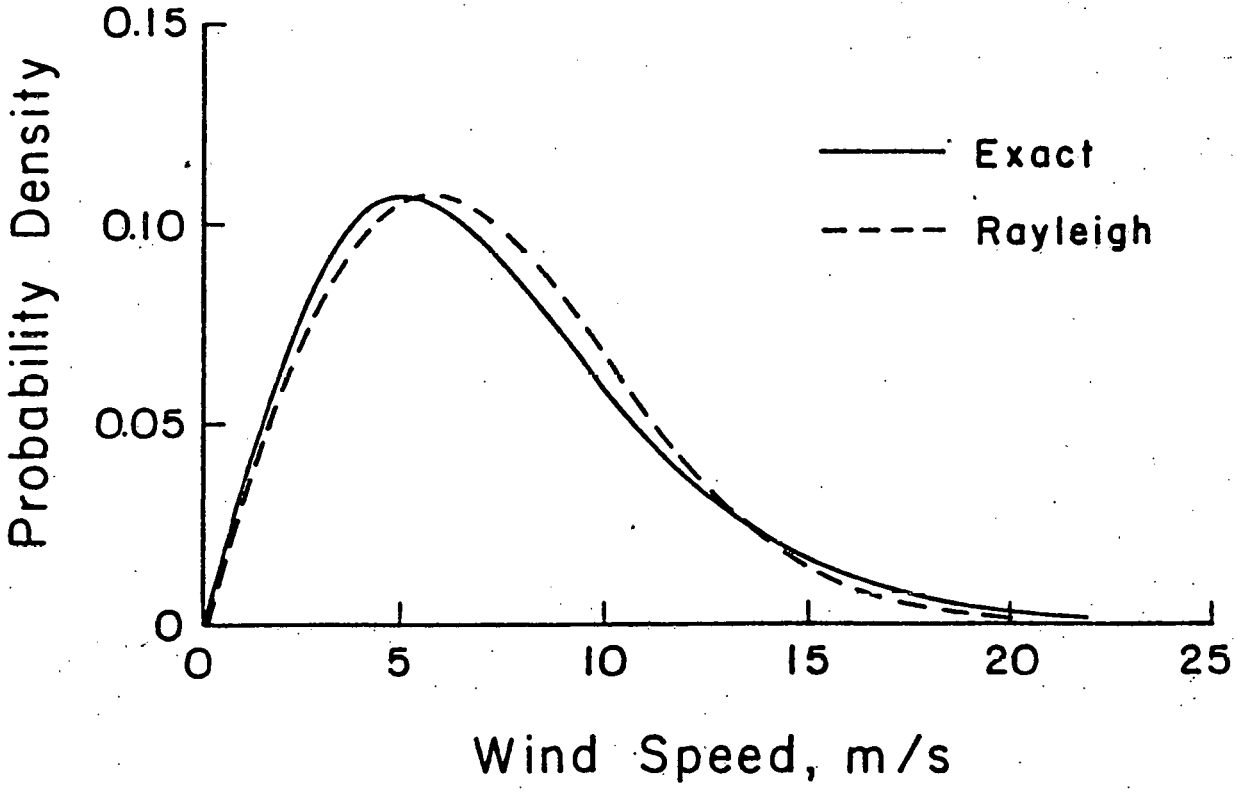

FIGURE 2.17 Exact and Rayleigh Probability Distribution for Variance Ratio of 2.0, $\rho = 0.5$.

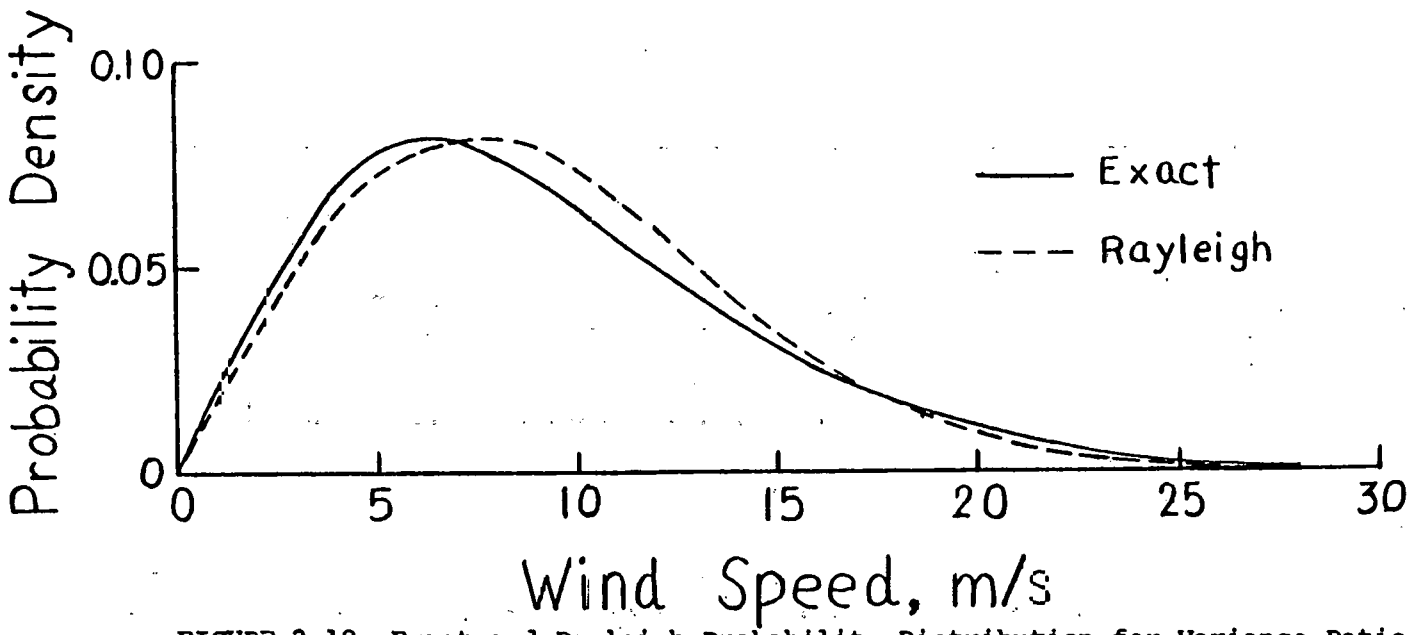

FIGURE 2.18 Exact and Rayleigh Probability Distribution for Variance Ratio of 4.0, $\rho = 0.2$.

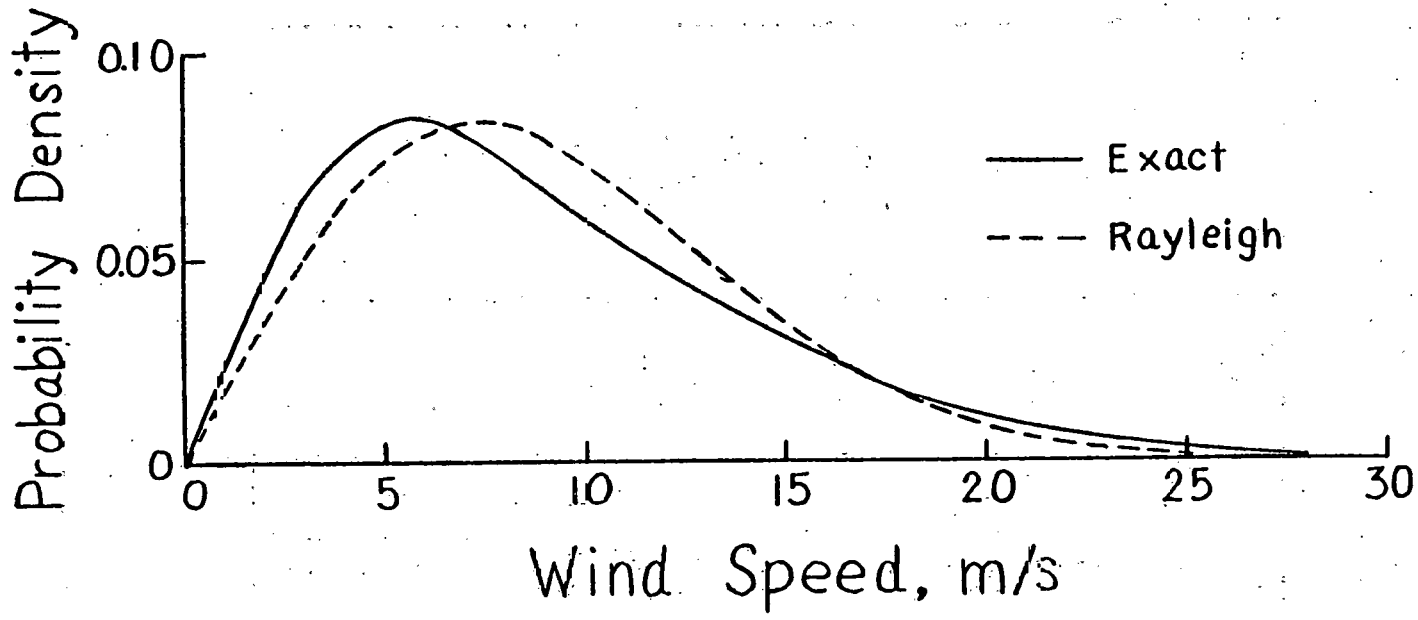

FIGURE 2.19 Exact and Rayleigh Probability Distribution for Variance Ratio of 4.0, $\rho = 0.5$.

TABLE 2.2 Input Variables and Derived Statistics for the Horizontal Wind Speed Vector for Initial Mean Speed m = 6 m/s

ρ	$R = \frac{\sigma_y}{\sigma_x}$	m_V [1]	σ_V [2]	Coefficient of Variation
-0.5	0.7	5.059	2.924	.5781
-0.2	0.7	5.128	2.803	.5466
0.0	0.7	5.140	2.780	.5410
0.2	0.7	5.128	2.803	.5466
0.5	0.7	5.059	2.924	.5781
-0.5	0.8	5.329	3.032	.5690
0.0	0.8	5.417	2.872	.5301
0.5	0.8	5.329	3.032	.5690
-0.5	1.0	5.900	3.321	.5628
-0.2	1.0	5.985	3.165	.5289
0.0	1.0	6.000	3.136	.5227
0.2	1.0	5.985	3.165	.5289
0.5	1.0	5.900	3.321	.5628
-0.5	1.2	6.505	3.688	.5670
0.0	1.2	6.614	3.490	.5277
0.5	1.2	6.505	3.688	.5670
-0.5	1.4	7.136	4.113	.5765
-0.2	1.4	7.233	3.940	.5448
0.0	1.4	7.250	3.908	.5391
0.2	1.4	7.233	3.940	.5448
0.5	1.4	7.136	4.113	.5765
-0.5	2.0	9.129	5.591	.6125
-0.2	2.0	9.232	5.415	.5867
0.0	2.0	9.252	5.385	.5820
0.2	2.0	9.232	5.415	.5867
0.5	2.0	9.129	5.591	.6125

[1] Evaluated from Eq. (2.23)

[2] Evaluated from Eq. (2.24)

CHAPTER 3

VARIATION DUE TO SAMPLING

To investigate the sensitivity of models based on National Weather Service data (which are one-minute averages sampled once an hour) to wind speed sampling rate and averaging time, a 24-hour record of wind speed (from 6:00 p.m. on 11 April 1979 to 6:00 p.m. on 12 April 1979), was selected from several days of continuous observation (during the week of 9 April 1979). With the assistance of Professor A. Kistler of the Northwestern University Mechanical Engineering Department, the data were collected from the same anemometer as in 1978 (Won, 1979).

The wind data were recorded on a strip chart attached to the output of a three-cup anemometer, which is located on a tower atop the Northwestern Technological Institute in Evanston, Illinois (shown in Appendix H) about 200 meters from Lake Michigan. The anemometer, which is 5.7 meters above the flat roof of the tower and 25.5 meters above ground level, is well above any nearby obstructions. The Anemometer, a Heathkit, was calibrated in the Northwestern University wind tunnel and was observed to have a response time on the order of one second. The wind data were digitized with one 20-second average every 20 seconds. The mean wind speed of the entire continuous record is 7.23 m/s.

Tables 3.1 - 3.2 present a statistical summary of the data for various averaging times and sampling rates. The within-hour variance is the variance among the readings within each hour (e.g., in Table 3.1 there are nine 20 second readings for an averaging time of 3 minutes). The readings in Table 3.2 are spaced uniformly throughout each hour (e.g., four readings

TABLE 3.1 Statistical Results for Various Averaging Times (Sampled Once an Hour) Using 1979 Data

AVERAGING TIME PER HOUR	MEAN (m/s)	VARIANCE (m/s)	TYP. WITHIN-HOUR VARIANCE $(m/s)^2$	BETWEEN-HOUR VARIANCE $(m/s)^2$	$v = \sigma/m$
20 seconds	6.89	8.38	0.00	8.38	0.420
1 minute	7.05	10.14	1.10	9.03	0.452
2 minutes	6.96	8.86	1.43	7.43	0.428
3 minutes	6.95	8.86	1.75	7.11	0.428
4 minutes	6.86	8.97	2.16	6.81	0.437
5 minutes	6.85	8.91	2.38	6.53	0.436
10 minutes	7.12	10.14	3.11	7.03	0.447
15 minutes	7.14	10.32	3.78	6.54	0.450
30 minutes	7.24	10.82	4.56	6.27	0.454
60 minutes	7.23	10.81	5.44	5.37	0.455

TABLE 3.2 Statistical Results for Various Sampling Rates (Using One-minute Average) Using 1979 Data

READINGS PER HOUR	MEAN (m/s)	VARIANCE (m/s)	TYP. WITHIN-HOUR VARIANCE $(m/s)^2$	BETWEEN-HOUR VARIANCE $(m/s)^2$	$v = \frac{\sigma}{m}$
1	7.05	10.14	0.00	9.03	0.457
2	7.13	8.26	1.80	6.46	0.403
4	7.33	8.79	2.87	5.92	0.404
6	7.26	9.49	3.56	5.93	0.424
12	7.26	9.68	4.11	5.57	0.429
60	7.23	9.41	4.04	5.37	0.424

per hour means one every 15 minutes). A trend of decreasing between-hour variance and increasing within-hour variance with increasing averaging time is observed in Table 3.1. The former trend clearly illustrates the decreasing variability associated with longer average data, while the latter shows that with sequential correlated data the variance among readings increases as the number of data increases (with sufficient data the variance becomes stationary). Similar effects are also observed for the sampling rate, as shown in Table 3.2. It can be seen that the between-hour variance is lower, for instance, with a one-minute average every 30 minutes than with a 2-minute average every 60 minutes (because of more independent data with the former). On the other hand, the within-hour variance is higher with the one-minute average every 30 minutes because of the increased independence.

Tables 3.3 - 3.4 summarize the data taken in 1978 and show similar effects of averaging time and sampling rate to the 1979 data. The 24-hour period was from noon on May 9, 1978, to noon on May 10, 1978. The mean wind speed of the entire continuous 1978 record was 3.89 m/s.

In order to assess the effect of sampling on the independence of readings, the autocorrelation functions were computed. Figures 3.1 and 3.2 show that there is a trend of increasing correlation with increasing averaging time, while the sampling rate shows no consistent effect on the correlation. The results found by Won for the 1978 data are shown in Figs. 3.3 - 3.4. The combined effects of the two years are shown in Figs. 3.5 - 3.6. It can be seen that, except for the apparently anomalous behavior of the one-minute average sampled

TABLE 3.3 Statistical Results for Various Averaging Times (Sampled Once an Hour) Using 1978 Data

AVERAGING TIME PER HOUR	MEAN (m/s)	VARIANCE $(m/s)^2$	TYP. WITHIN HOUR VARIANCE $(m/s)^2$	BETWEEN HOUR VARIANCE $(m/s)^2$	$V = \frac{\sigma}{m}$
20 seconds	3.99	5.28	0	5.28	0.576
1 minute	3.69	4.46	1.35	3.10	0.572
2 minutes	3.79	5.65	1.77	3.88	0.627
3 minutes	3.84	5.49	1.98	3.51	0.610
4 minutes	3.92	6.36	2.27	4.09	0.643
5 minutes	3.91	6.79	2.41	4.38	0.666
10 minutes	3.96	7.72	2.62	5.10	0.702
15 minutes	3.89	6.96	2.74	4.22	0.678
30 minutes	3.83	6.74	2.73	4.01	0.678
60 minutes	3.89	6.54	2.77	3.79	0.657

TABLE 3.4 Statistical Results for Various Sampling Rates (Using One-Minute Average) Using 1978 Data

READINGS PER HOUR	MEAN (m/s)	VARIANCE $(m/s)^2$	TYP. WITHIN HOUR VARIANCE $(m/s)^2$	BETWEEN HOUR VARIANCE $(m/s)^2$	$V = \frac{\sigma}{m}$
1	3.69	3.10	0.0	3.10	0.477
2	3.77	3.68	0.66	3.02	0.509
4	3.71	4.63	1.21	3.43	0.580
60	3.89	5.43	1.64	3.79	0.599

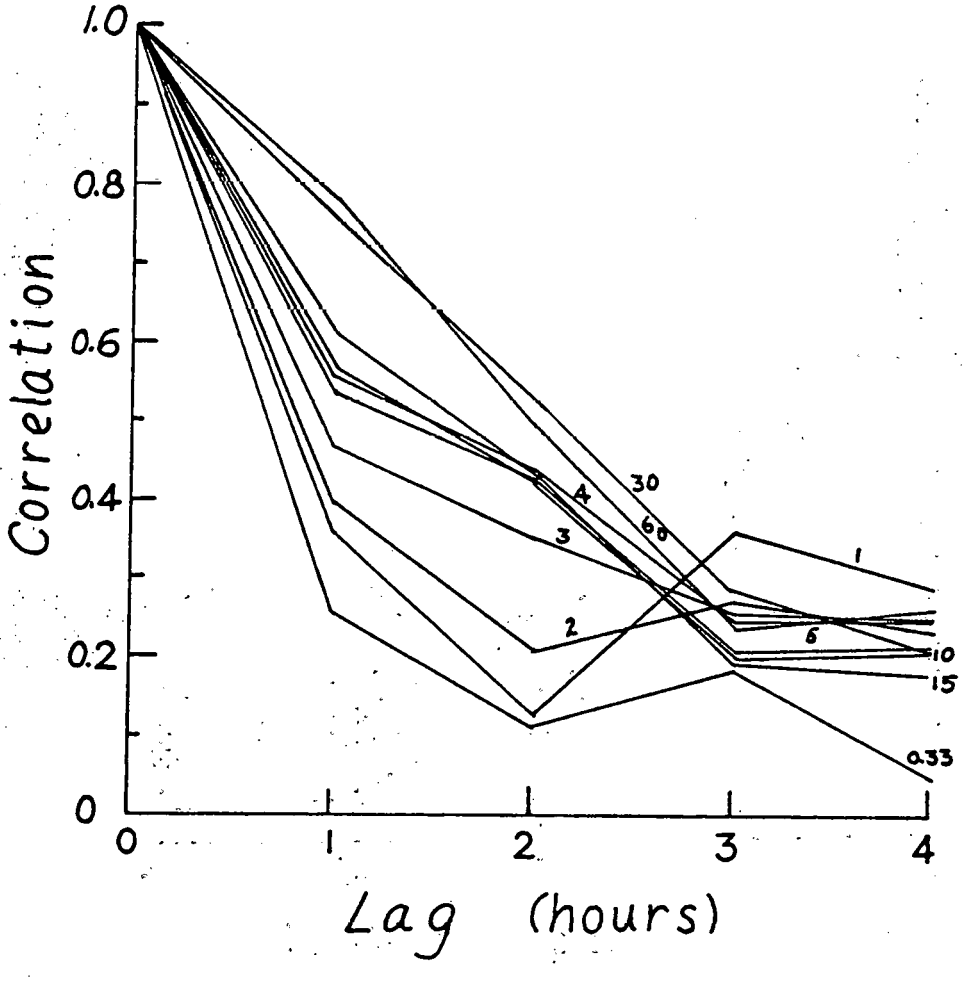

FIGURE 3.1 Effect of Averaging Time on Autocorrelation Function for Wind Speed Sampled Once an Hour, 1979 Data (number on curve is averaging time in minutes).

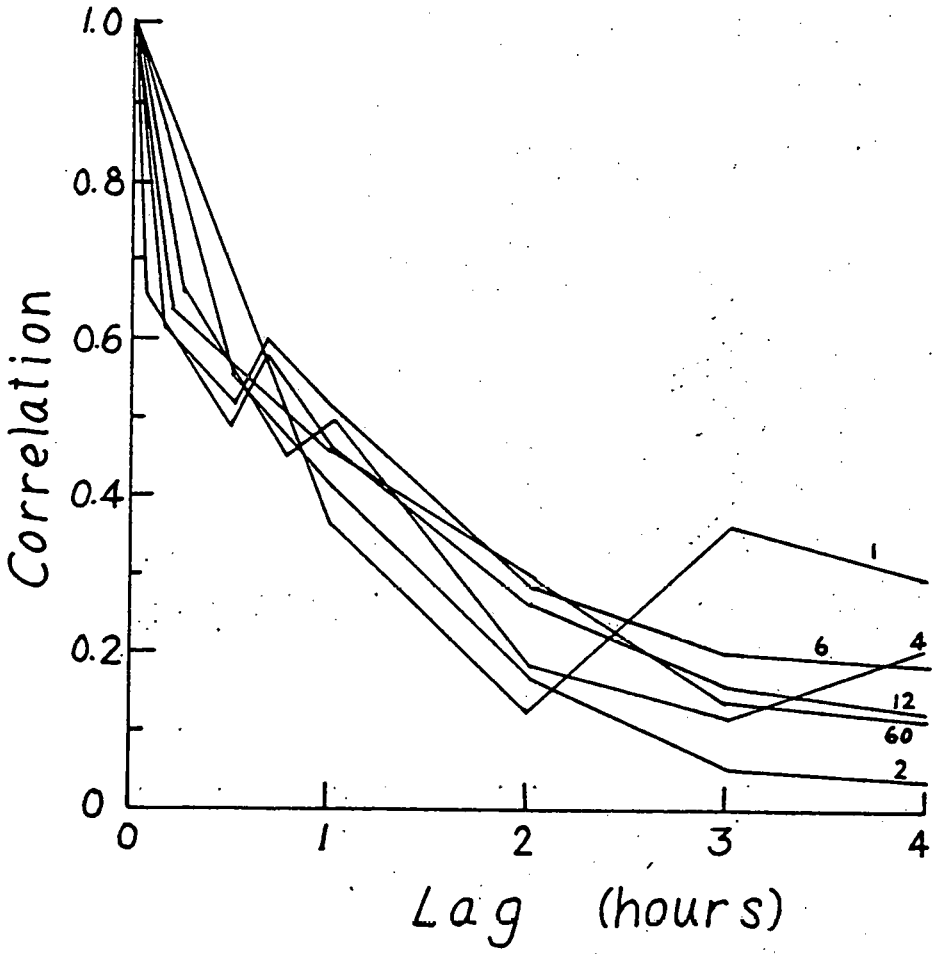

FIGURE 3.2 Effect of Sampling Rate on Autocorrelation Function for One Minute Average Wind Speed, 1979 Data (number on curve is samples per hour).

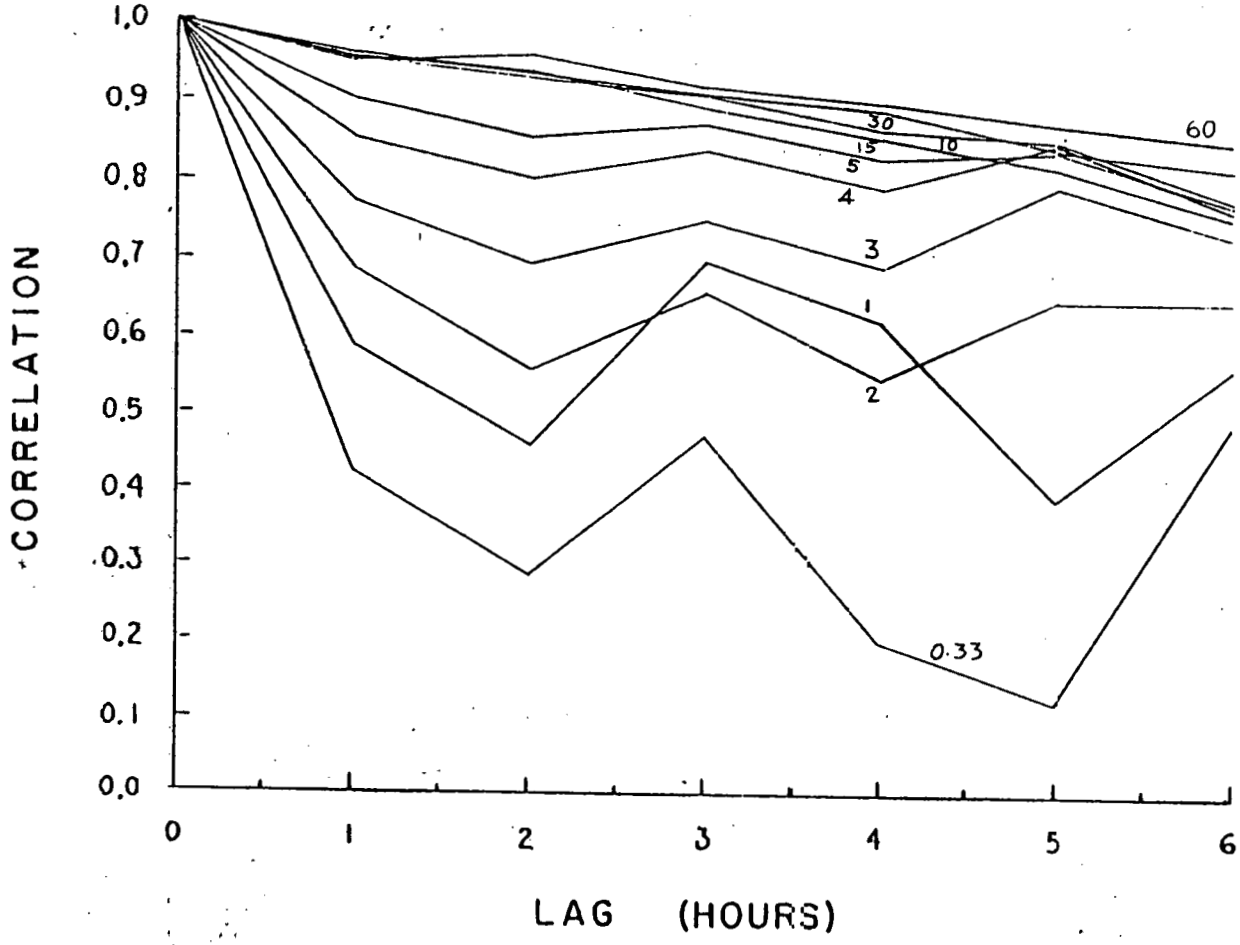

FIGURE 3.3 Effect of Averaging Time on Autocorrelation Function for Wind Speed Sampled Once an Hour, 1978 Data (number on curve is averaging time in minutes).

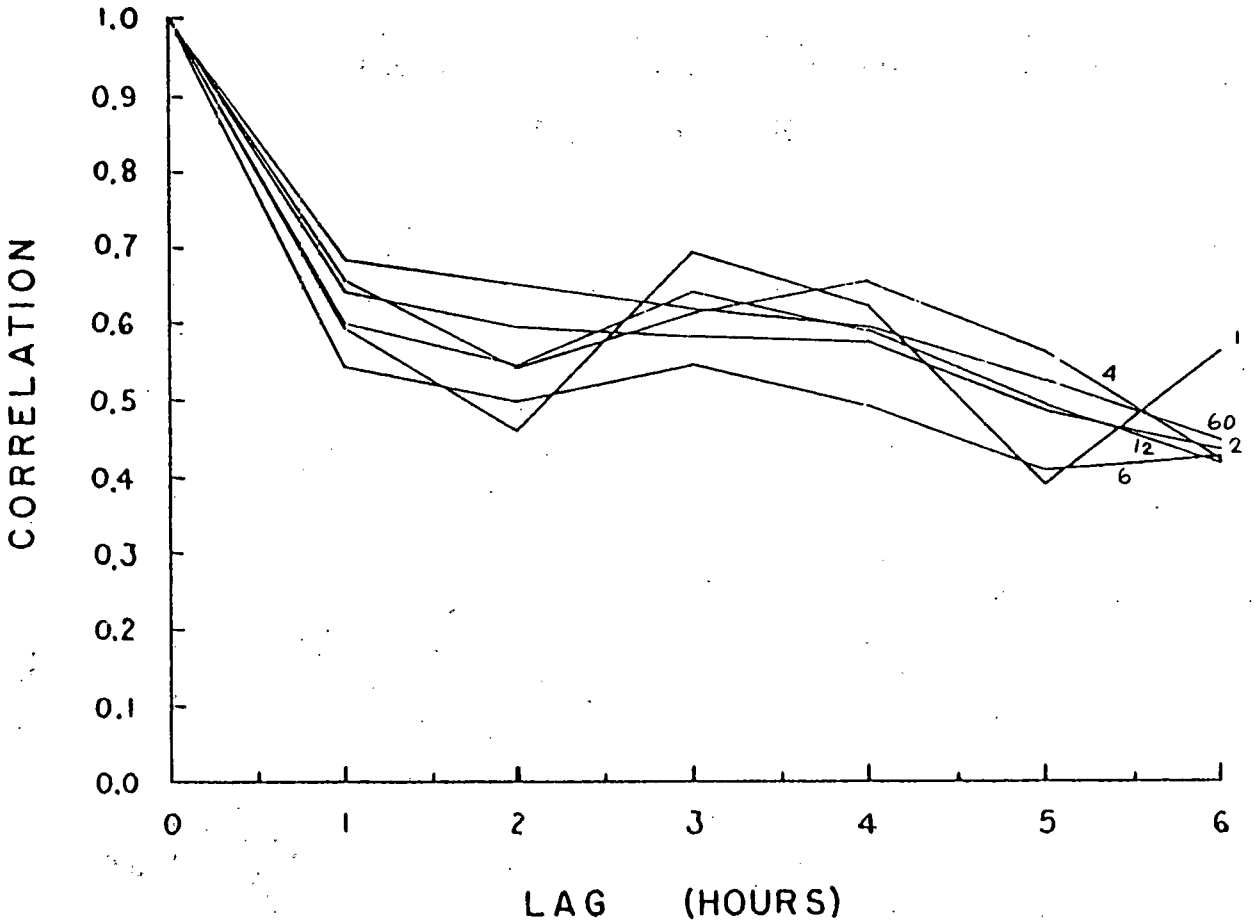

FIGURE 3.4 Effect of Sampling Rate on Autocorrelation Function for One Minute Average Wind Speed, 1978 Data (number on curve is samples per hour).

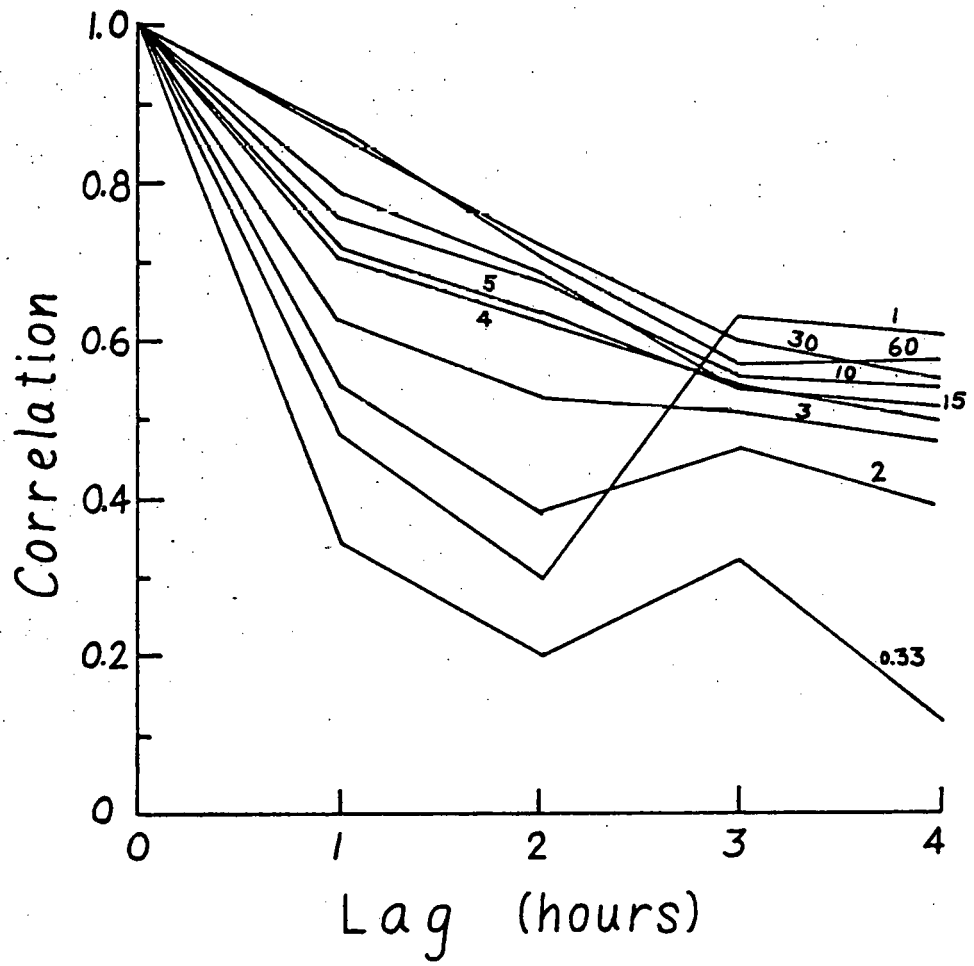

FIGURE 3.5 Effect of Averaging Time on Autocorrelation Function for Wind Speed Sampled Once an Hour, 1978 and 1979 Data (number on curve is averaging time in minutes).

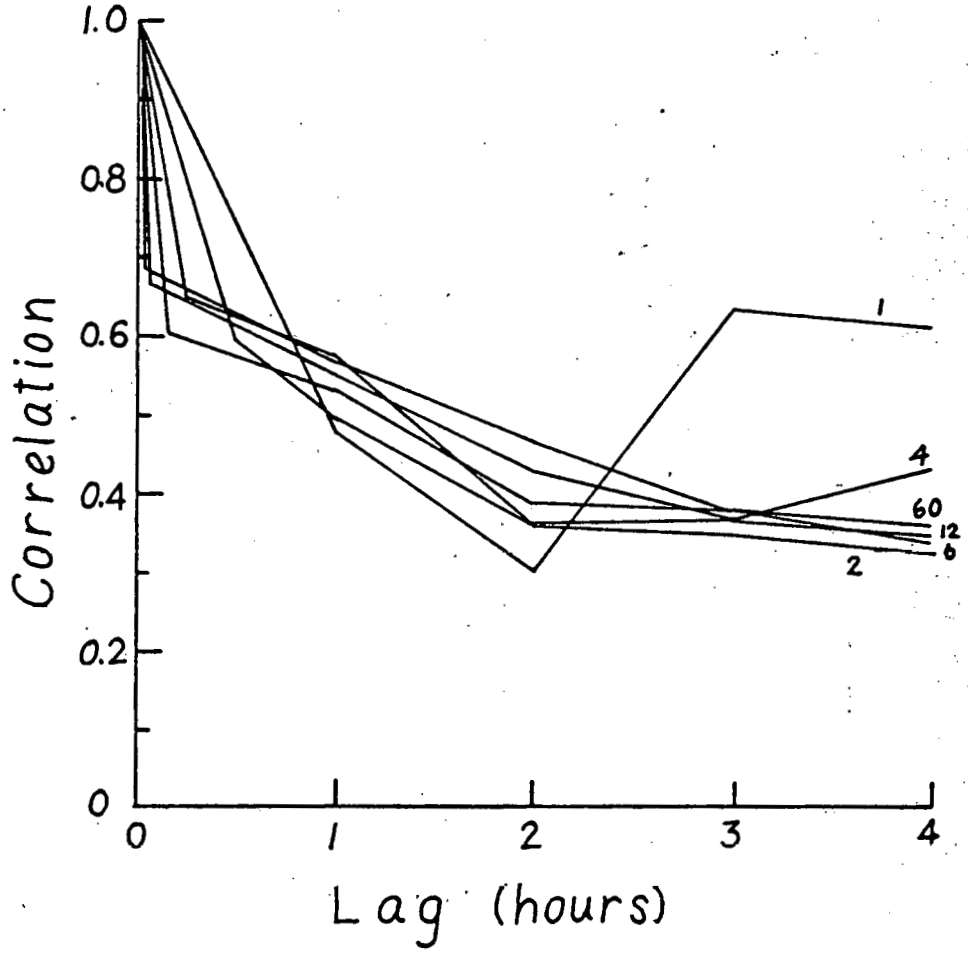

FIGURE 3.6 Effect of Sampling Rate on Autocorrelation Function for One Minute Average Wind Speed, 1978 and 1979 Data (number on curve is samples per hour).

once an hour, a distinct trend exists for averaging time and none for sampling rate.

A run duration analysis was performed, and a definite increase of mean run length with decreasing sampling rate for runs both above and below fixed wind speed levels (run levels) was observed. This is illustrated in Figs. 3.7 and 3.8. For example, the mean run length above 10 m/s ranges from 3.3 minutes (60 samples per hour) to 1.5 hours (1 sample per hour) and the mean run length below that level increases from 14.46 minutes (60 samples per hour) to 10.0 hours (1 sample per hour). However, there is no apparent effect of averaging time on mean run lengths either above or below run levels, as shown in Figs. 3.9 - 3.10. Similar effects were observed in the 1978 data, as shown in Figs. 3.11 - 3.12.

Although the wind speed records obtained were quite limited in duration, a reasonable indication of the possible effects of averaging time and sampling rate is observed. The lack of trend of mean wind speed and variance with averaging time and sampling rate is expected (Doran, Bates, Liddel, and Fox, 1977). The consistency of hourly coefficient of variation with various averaging times is most promising in terms of using the National Weather Service data (one-minute average every hour). The distinct effect of averaging time (but not of sampling rate) on autocorrelation appears to be important and should be taken account of in applications. The effect of sampling rate on run duration is significant, while the apparent lack of trend of averaging time on run duration is somewhat surprising.

The consistent effects of averaging time and sampling rate observed

from the two 24-hour wind data suggest that it may be possible to develop corrective procedures to be used with National Weather Service data. However, further investigation is necessary to substantiate the trends observed here. For the present, one must be very cautious in generalizing models developed from a specific sampling procedure (such as the National Weather Service data). The sensitivity of autocorrelation to averaging time and of run duration to sampling rate is particularly noteworthy.

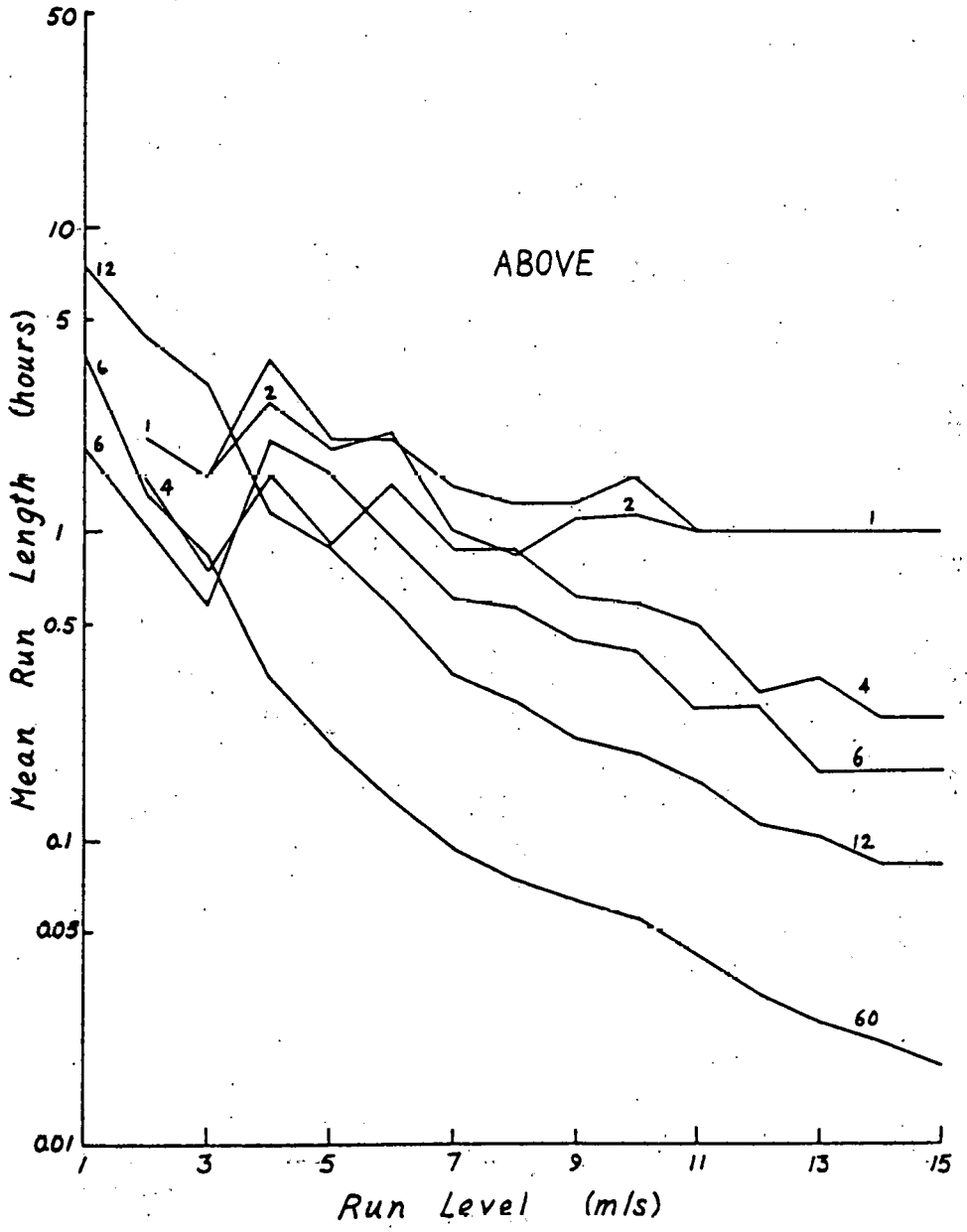

FIGURE 3.7 **Effect of Sampling Rate on Mean Run Lengths Above Wind Levels for One Minute Average Wind Speed, 1979 Data** (number on curve is samples per hour).

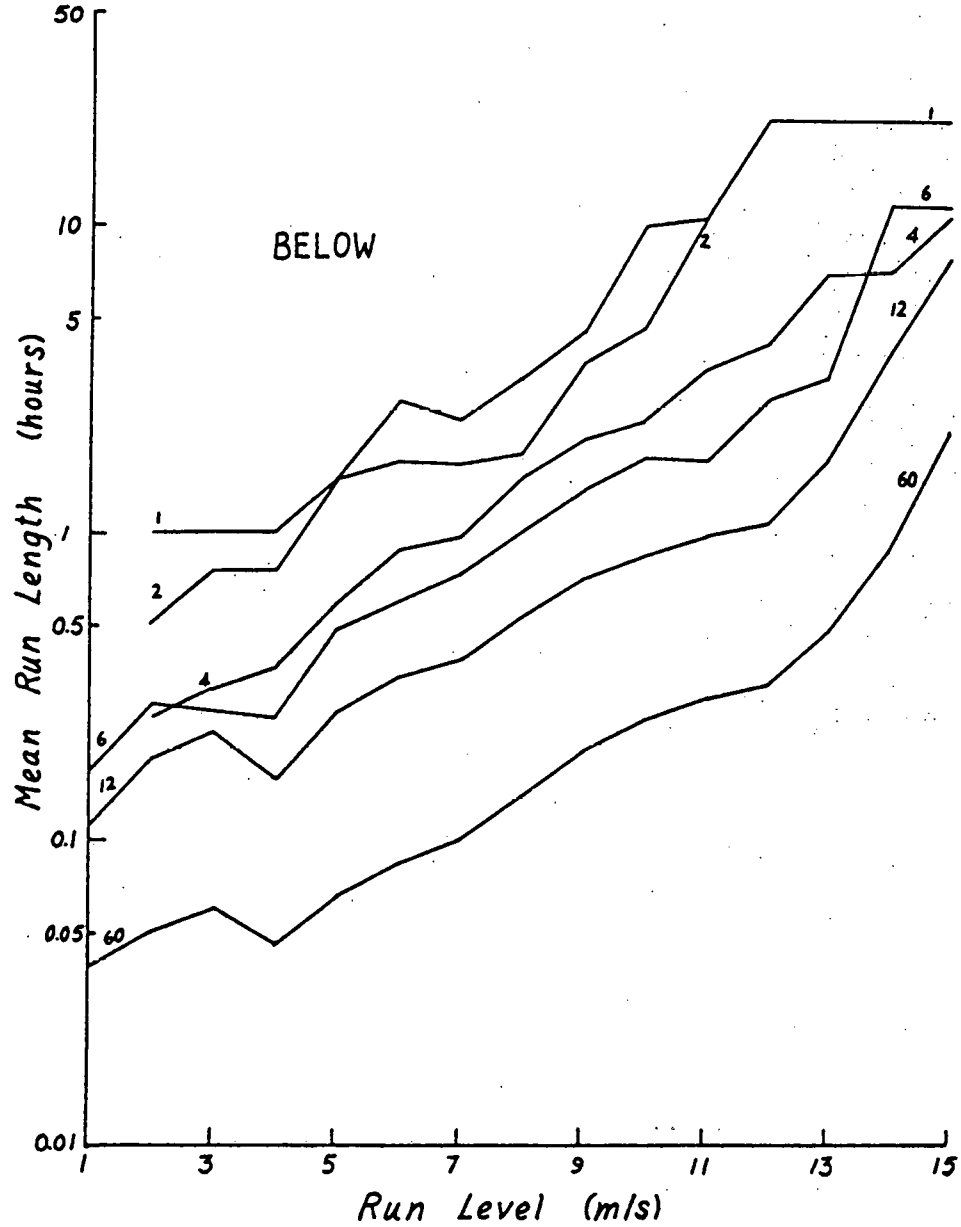

FIGURE 3.8 Effect of Sampling Rate on Mean Run Lengths Below Wind Levels for One Minute Average Wind Speed, 1979 Data (number on curve is samples per hour).

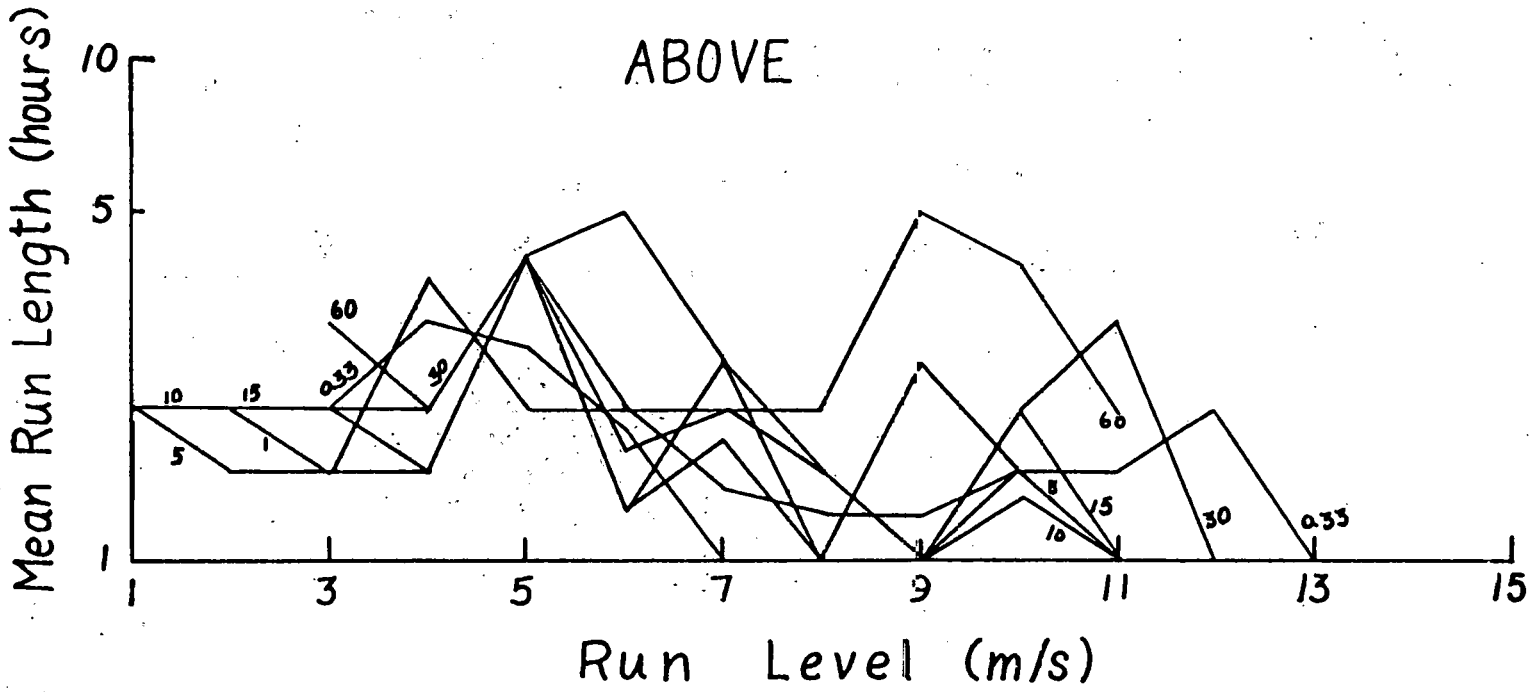

FIGURE 3.9 Effect of Averaging Time on Mean Run Lengths Above Levels for Wind Speed Sampled Once an Hour, 1979 Data (number on curve is averaging time in minutes).

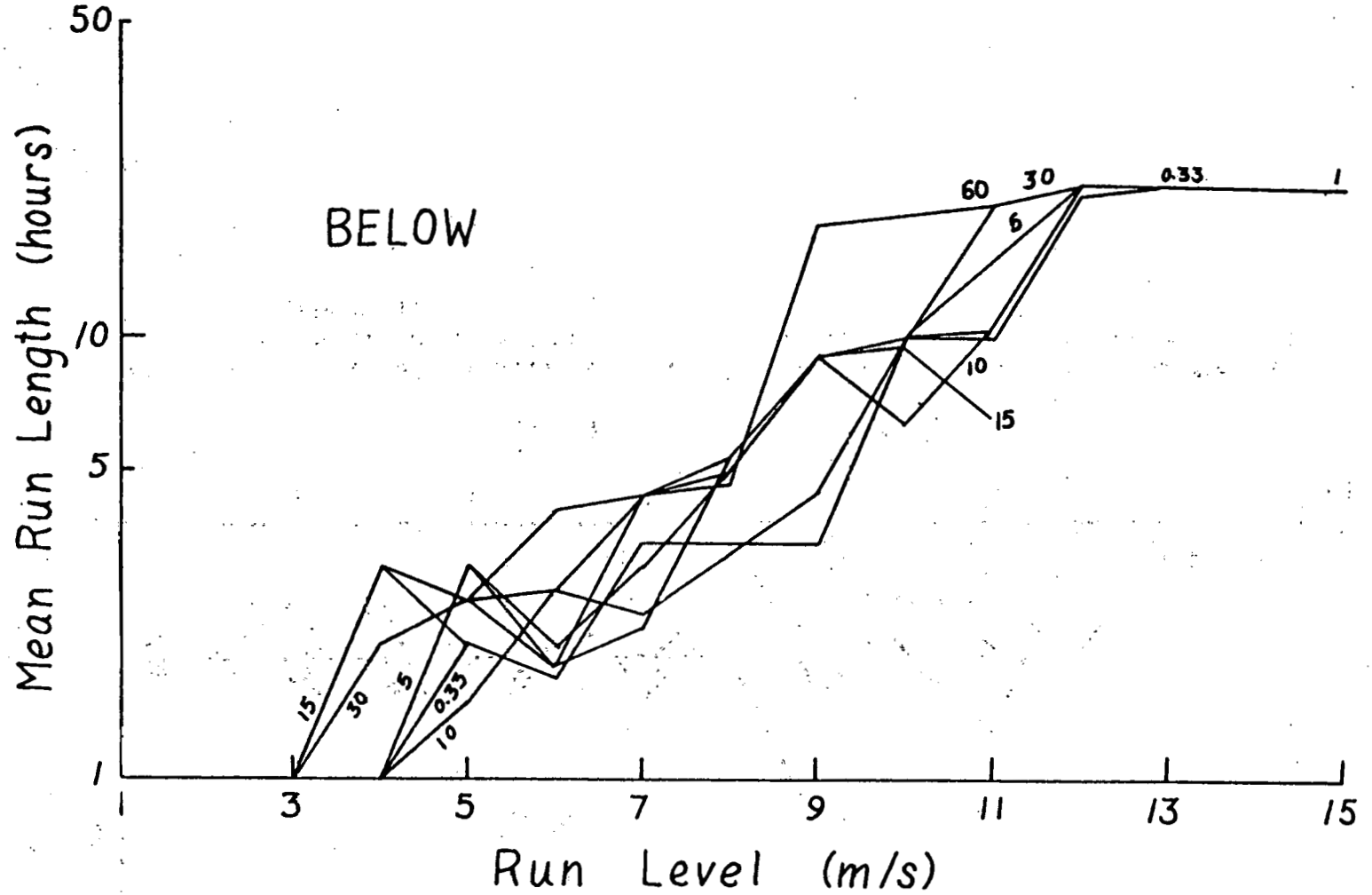

FIGURE 3.10 Effect of Averaging Time on Mean Run Lengths Below Levels for Wind Speed Sampled Once an Hour, 1979 Data (number on curve is averaging time in minutes).

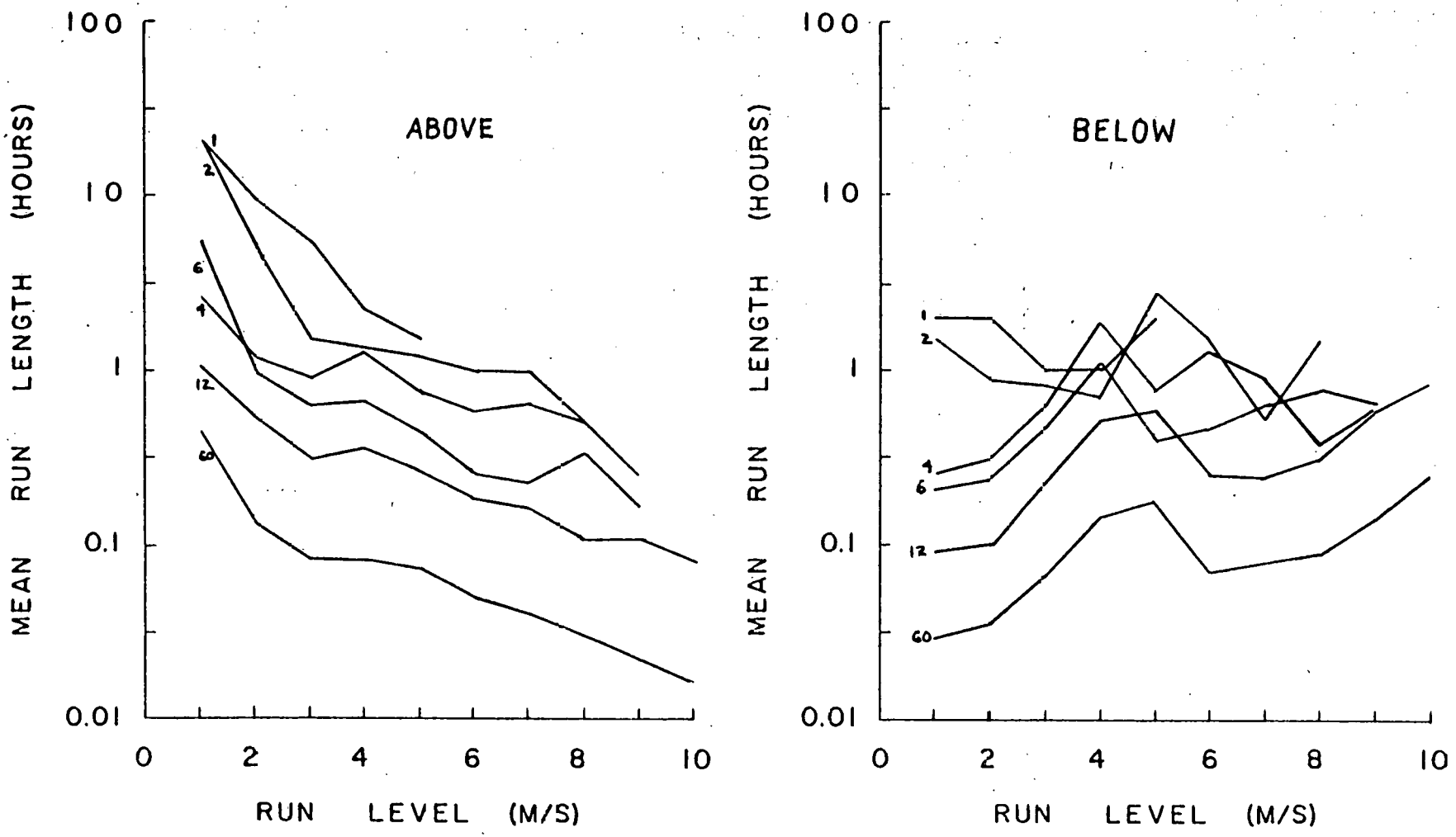

FIGURE 3.11 Effect of Sampling Rate on Mean Run Lengths Above (Left) and Below (Right) Levels for One-Minute Average Wind Speed, 1978 Data (number on curve is samples per hour).

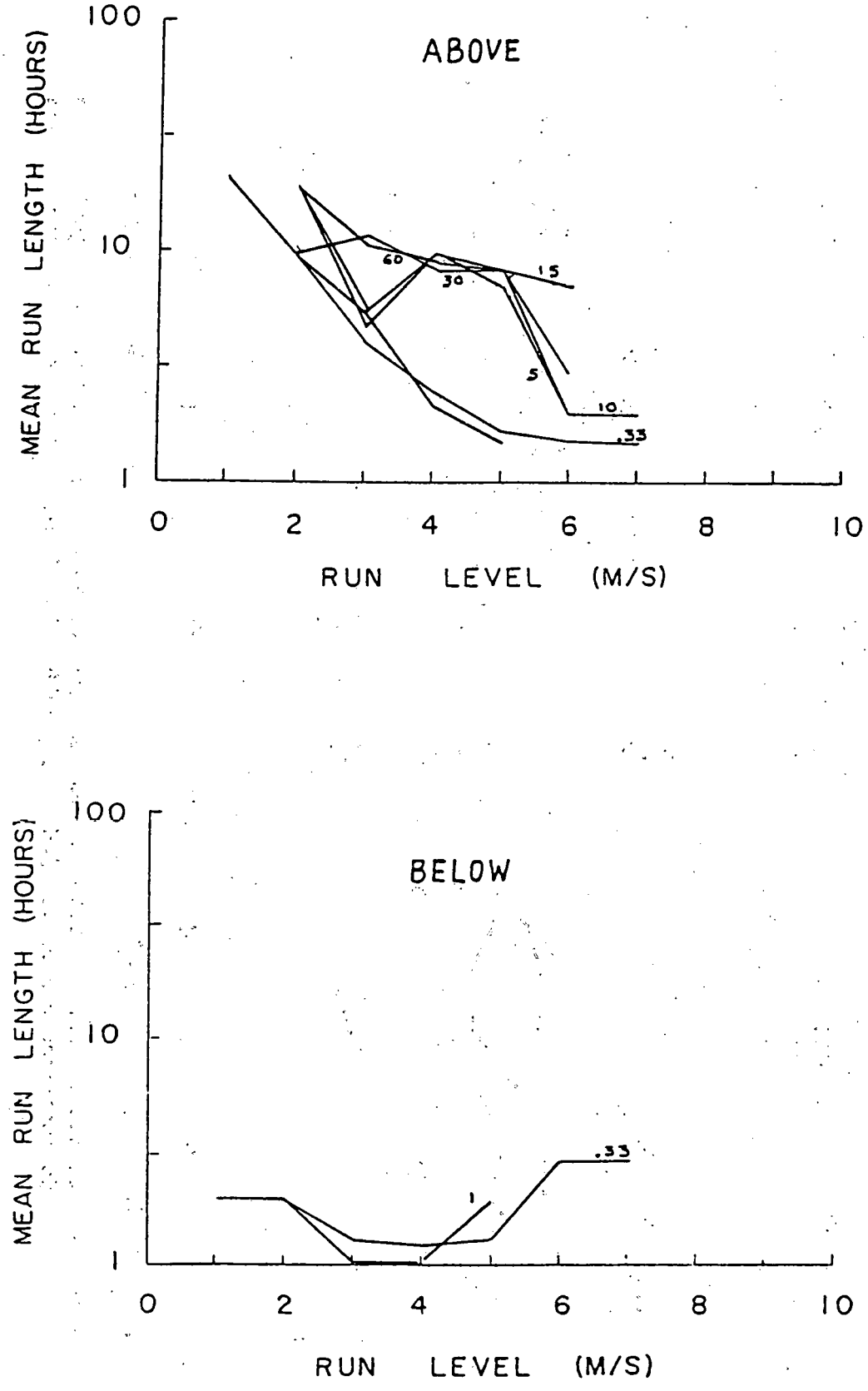

FIGURE 3.12 Effect of Averaging Time on Mean Run Lengths Above (Top) and Below (Bottom) Levels for Wind Speed Sampled Once an Hour, 1978 Data. (number on curve is averaging time in minutes).

CHAPTER 4

SIMULATION OF WIND SPEED AND ARRAY POWER

4.1 SIMULATION OF WIND SPEED

To evaluate long-term wind turbine performance it is possible to extend actual on-site data by Monte Carlo simulation of a time series of hourly wind speeds. The Weibull distribution has been shown (Corotis, 1976) to adequately model hourly wind speed at a site. The Weibull probability density function is given by

$$f_V(v) = (k/c)\ (v/c)^{k-1} \exp[-\ (v/c)^k] \tag{4.1}$$

in which the shape and scale parameters, k and c, respectively, are related to the mean and variance by

$$m_V = c\Gamma\ (1 + 1/k) \tag{4.2}$$

$$\sigma_V^2 = c^2\left\{\Gamma(1 + 2/k) - [\Gamma(1 + 1/k)]^2\right\} \tag{4.3}$$

The simulation of a correlated time series based on the Weibull distribution is very complicated because each hour's wind speed depends on the complete history of previous wind speeds and because the conditional wind speed distribution does not retain the Weibull form. In general, it is necessary to have a complete set of multivariate distributions to completely describe a stochastic process (Crandall and Mark, 1963). An approximate simulation procedure has been developed using an hourly Weibull distribution with a conditional hourly mean and variance, m_i' and $(\sigma_i')^2$ given as follows:

$$m_i' = E[X_i | X_{i-1} = x_{i-1}] = m_{X_i | X_{i-1}}$$

$$= m_{X_i} + \rho\left[\frac{x_{i-1} - m_{X_{i-1}}}{\sigma_{X_{i-1}}}\right] \sigma_{X_i} \tag{4.4}$$

$$(\sigma_i')^2 = \mathrm{Var}[X_i | X_{i-1} = x_{i-1}] = (1 - \rho^2)\, \sigma_{X_i}^2 \tag{4.5}$$

in which ρ is the correlation between X_i and X_{i-1} (here, ρ is a temporal or autocorrelation). Equations (4.4) and (4.5) are exact corrections based on the previous value in the case of a Gaussian distribution (Benjamin and Cornell, 1970). For an exact simulation of a variable at time step i, it is necessary in general to include all previous values. However, in the case of a Guassian distribution, when the autocorrelation function is exponential in form, all prior information is embodied in the last simulated value. In such a situation, Eqs. (4.4) and (4.5) provide the basis for exact generation of a time sequence, which is referred to as a Gauss-Markov process. The autocorrelation function of wind speed has been shown to be exponential (Corotis, 1976, 1977), and this is the basis for developing the approximate simulation procedure for hourly wind speed using Eqs. (4.4) and (4.5) and the Weibull distribution. The correlation, ρ, is taken as the lag one hourly autocorrelation of the site. The unmodified mean speed and variance ($\rho = 0$ for Eqs. (4.4) and (4.5)) are used to initialize the simulation. The computer program, WEISIM (see Appendix A) is written to perform a Monte Carlo simulation based on the Weibull distribution and the approximate procedure discussed previously. The program includes seasonal and diurnal cycles.

Although the simulation based on the approximate procedure appears to be reasonable based on the limited data that were computed, comparison between simulated and observed data from more sites should be made before this procedure can be considered to be verified.

4.2 RELATIONSHIP BETWEEN TURBINE POWER AND WIND SPEED

The available wind power at a site can be shown to vary with the wind velocity cubed (Putnam, 1948; Golding, 1955)

$$\text{Power} = \text{Kinetic Energy} = \frac{1}{2}\rho A v^3 \tag{4.6}$$

where ρ = the density of air, A = projected area swept by the turbine, and v = wind velocity. However, this is an ideal wind speed and generated power relationship; in reality a turbine does not generate any power below cut-in or above cut-out wind speed and generates at full capacity between rated and cut-out wind speed. An example of actual turbine power versus wind speed for a 200-watt turbine (the turbine is designed to have the cut-in, rated and cut-out wind speed of 3.1, 10.3 and 31 m/s, respectively) is shown in Figure 4.1 (Rockwell International, 1978).

In 1976, Justus, Hargraves and Mikhail developed an empirical relationship between wind speed and turbine power with quadratic fit between cut-in and rated wind speed, as given by Eq. (B.8) in Appendix B.

It is interesting to note that for some wind turbines the power computed from Eq. (B.8) will not yield a positive value. It can be shown (see Appendix D) that in order to ensure a positive value of power using Eq. (B.8), the ratio of cut-in speed to rated speed must

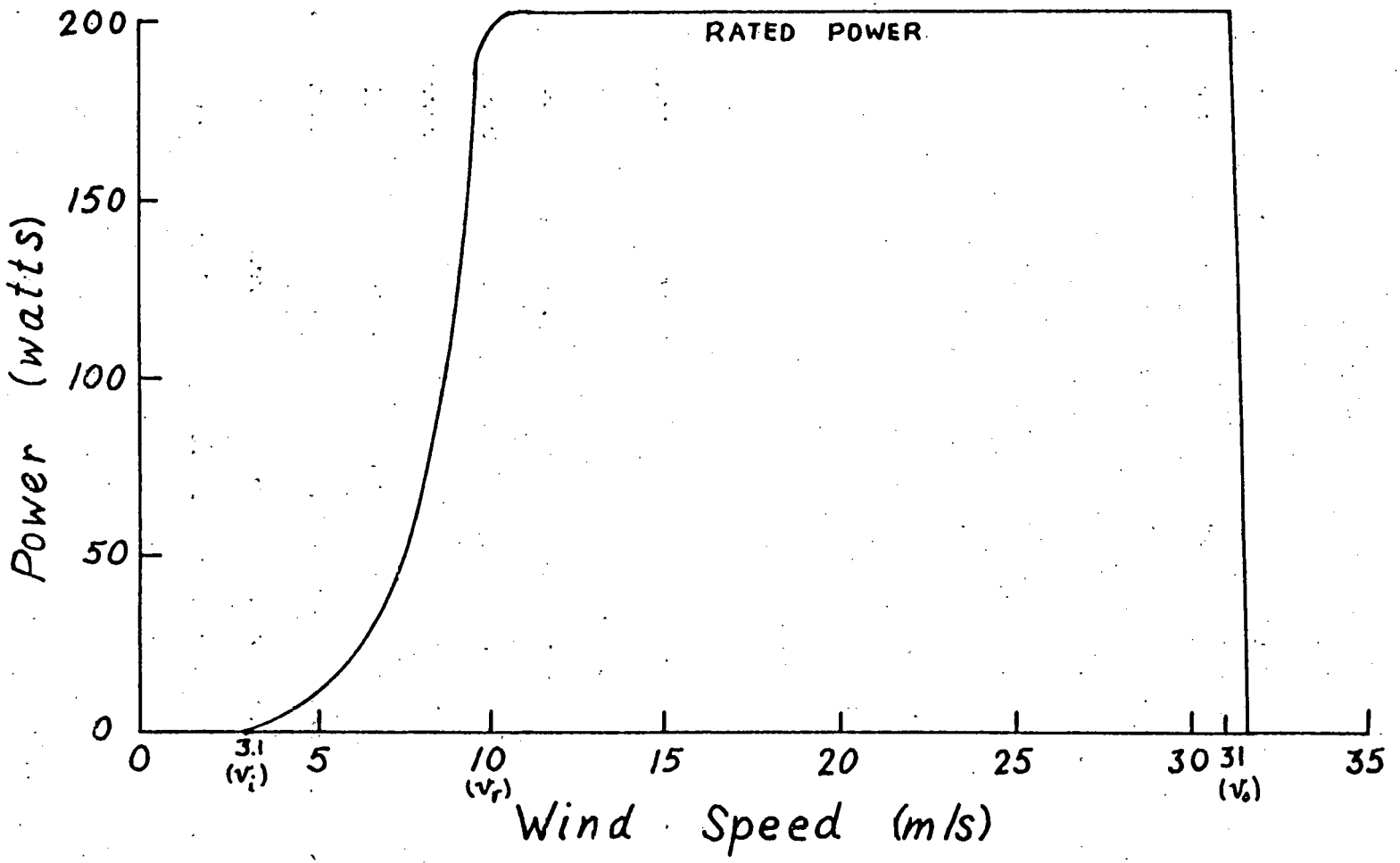

FIGURE 4.1 Actual Wind Turbine Operating Curve for Turbine Capacity of 200 Watts.

be between 0.260 and 0.587.

4.3 DEVELOPMENT OF THE ARRAY POWER SIMULATION

The power output from a spatial array of wind turbines is the sum of the output from each turbine. In 1978, Justus and Mikhail developed an empirical expression which gives a good approximation for the average wind speed (average is used in a spatial sense, not temporal) in a region with spatially correlated wind speeds. The form is basically a modified Weibull distribution with a parameter that is a function of the average correlation between sites within a region (the correlation is a function of the average distance between sites), the Weibull shape parameter for a typical site, and the number of sites. Justus and Mikhail simulate the average regional speed by simulating from a Weibull distribution (or a simplified Rayleigh distribution) for a represenative site (a site that has the same annual mean wind speed as other typical sites within the region it represents) and employing a probability matching technique. Justus and Mikhail have also derived an empirical expression for wind speed at individual sites given the array average speed. They can then simulate the wind speed at each site for the array average speed at a particular point in time (usually an hourly average). A simulation process for an input sequence of a representative site is shown in detail by Cliff, Justus and Elderkin (1978).

There are several advantages to the preceding approach. It uses a Weibull or Rayleigh distribution for wind speed at a single site, provides a sequence of wind speeds at the individual sites over the region, and is shown to be relatively tractable. However,

it contains some empirical approximations and uses a specified rather than simulated sequence, which is somewhat cumbersome. The approach also requires additional computations in order to obtain the array power, and incorporates spatial correlation of non-zero time lags only indirectly. A simplified approach, of commensurate accuracy, is developed herein.

The hourly wind speed at a single site is adequately modelled for wind energy conversion purposes by a Rayleigh distribution (Wentink, 1976; Cliff, 1977; Corotis, 1977; Justus, 1978). The distribution for the mean wind speed over an array varies from Rayleigh (for a one-site array) to Gaussian (for an array of many sites). If the spatial correlation in the array is moderate, then the array average speed will be well modelled by the Gaussian even if the array has only a few sites. The distribution for the array average speed will still be normal, though converging more slowly, for higher values of spatial correlation (hourly values of 0.8 have been observed for winter months in relatively flat terrain). However, given the similar shapes of the Rayleigh and Gaussian distribution (for mean wind speeds between 1 m/s and 10 m/s, the difference in the cumulatives of the two distributions is no more than 4% at any level), the Gaussian will provide a good approximation even for a highly correlated array of a few sites.

The total array power may be expressed as the product of array average power and the number of sites in the array. If the turbine power is linearly related to speed, then the average power is also linearly related to the average speed. Although the power and wind speed are not actually linearly related at a single site, there are

three factors which tend to help make the linearization a reasonable approximation. First, the power curve of array average power versus array average speed will tend to be smoother than the curve for a single site despite the first derivative discontinuity of the single-site turbine power curve at cut-in, rated and cut-out speeds (Justus and Makhail, 1978). Second, the coefficient of variation for array average speed is less than for a single site, and hence a narrower range of the turbine characteristics curve is generally encountered. This effect will diminish considerably with increasing correlation in the array. For instance, the coefficient of variation for a ten-site array will decrease to 32% of a single site when there is no correlation among sites, but will decrease to 68% with 0.4 correlation and only 91% with 0.8 correlation. The third factor is that the linearization can be improved by using a weighted minimum integrated squared error technique in which the weighting function is a Rayleigh distribution of the wind speed itself. The equivalent linearization, which is derived in Appendix B, further ensures that the approximation is a best fit for the range of wind speeds most likely to be observed.

Although the preceding discussion indicates that the use of the Gaussian distribution for array average speed and the equivalent linearization are generally reasonable, it should be cautioned that the approximation can be expected to be much poorer for extremely high or low average wind speeds.

If the power output from turbine j at time i with wind speed v_{ij} is given by

$$P_{ij} = a_j + b_j v_{ij} \tag{4.7}$$

where a_j and b_j are determined in Appendix B, the total power in an array of n turbines at time i will then be

$$P_i = \sum_{j=1}^{n} a_j + \sum_{j=1}^{n} b_j v_{ij} \tag{4.8}$$

with the following mean and variance

$$E[P_i] = \sum_{j=1}^{n} a_j + \sum_{j=1}^{n} b_j E[v_{ij}] \tag{4.9}$$

$$Var[P_i] = \sum_{j=1}^{n} \sum_{k=1}^{n} b_j b_k \, cov[v_{ij}, v_{ik}] \tag{4.10}$$

For simplicity, assume all the wind turbines in the array are the same; that is, they have the same operating characteristics. Also assume that the mean wind speeds at the various sites are similar. In this case a_j and b_j will be independent of site and can be replaced by a and b,respectively. Equations (4.8) - (4.10) become

$$\begin{aligned} P_i &= na + b \sum_{j=1}^{n} v_{ij} \\ &= n(a + b\,\bar{v}_i) \end{aligned} \tag{4.11}$$

$$E[P_i] = na + b \sum_{j=1}^{n} E[v_{ij}] \tag{4.12}$$

$$Var[P_i] = b^2 \sum_{j=1}^{n} \sum_{k=1}^{n} cov[v_{ij}, v_{ik}] \tag{4.13}$$

where $\bar{v}_i$ is the array average wind speed at time i and can be modelled by the Gaussian, as previously discussed. Since P_i is linearly related to $\bar{v}_i$, it can also be described by the Gaussian with the mean and variance given by Eqs. (4.12) and (4.13).

Let $\rho(\tau)$ be defined as the autocorrelation of wind speed at a site for time lag τ, ρ_s the zero-lag spatial correlation and $\rho_s(\tau)$

the time-space correlation of wind speed between sites. Corotis (1976, 1977) has shown that for relatively flat terrain, the hourly spatial correlation is relatively constant for sites that are anywhere from a few kilometers to more than 100 kilometers apart. The wind speed may be assumed to be spatially homogeneous and temporally stationary across the array, and the autocorrelation of the array mean wind speed for time lag τ, $R(\tau)$, may be given as (see Appendix C for derivation)

$$R(\tau) = \frac{\rho(\tau) + (n-1)\ \rho_s(\tau)}{1 + (n-1)\ \rho_s} \tag{4.14}$$

$R(\tau)$ is also the autocorrelation function for the array average power because of the linearity between power and speed.

The studies by Corotis also indicate that the autocorrelation and time-space correlations, $\rho\ (\tau)$ and $\rho_s(\tau)$, decay exponentially with time lag and with similar decay rates. These conditions imply that the autocorrelation, $R(\tau)$, will also decay exponentially.

Following the same reasons discussed in Section 4.1 for the simulation of wind speed at a single site, the Gaussian distribution and the exponential autocorrelation function provide the necessary prerequisites for a Gauss-Markov process. The sequence of array power is simulated from the Gaussian distribution using the parameters given by Eqs. (4.4) and (4.5) with $\rho = R(1)$. However, Eqs. (4.12) and (4.13) are used to initialize the simulation. Computer program ARASIM (see Appendix E) is written to perform the Gaussian simulation for hourly array power based on the preceding discussion and incorporates seasonal and diurnal cycle effects.

4.4 ANALYSES OF ARRAY POWER MODELS

In order to assess the array power model discussed in Section 4.3, statistical analyses were conducted on each of the three array power models, ARASIM (the Gaussian simulation of power), SIMUL (the simulation developed by Cliff, Justus and Elderkin (1978)), and REGIONAL (the actual wind speed collected by National Weather Service). For verification purposes, six wind turbines (45 kW, 100 kW (MOD 0), 200 kW (MOD 0A), 500 kW, 2 MW (MOD 1), 2.5 MW (MOD 2)) and 3 regions (Kansas, Northern Illinois and Wyoming) were studied. The wind turbine operating characteristics (Thomas and Donovan, 1978; Rockwell International, 1978; General Electric Company, 1976; Hunnicutt, Linscott, and Wolf, 1978) and the regions under investigation are summarized in Tables 4.1 and 4.2.

For the REGIONAL results, the data were obtained from the National Climatic Center. The sites are Topeka, Forbes AFB and Olathe NAS in Kansas; Argonne National Laboratory 18', Glenview, Midway, O'Hare and Rockford in northern Illinois; and Cheyenne, Douglas and Laramie in Wyoming. The wind speeds at these sites have been studied extensively by Corotis (1976, 1977, 1979). Due to the variations in record length, the data were extracted for the common period among sites within the region. A linear interpolation was used to replace missing or invalid data. This approximation does not affect the analyses significantly because the number of missing or invalid data in a region is low (a maximum of 0.12% of the record) and it is very unlikely that all sites in a region have a missing datum at the same time. A record of hourly array power was then created for each region and wind turbine by summing the turbine power (computed from Eq. (B.8)) over the region.

TABLE 4.1 Summary of Wind Turbine Operating Characteristics

	OPERATING CHARACTERISTICS			
WIND TURBINES	RATED POWER (KW)	CUT-IN SPEED (m/s)	RATED SPEED (m/s)	CUT-OUT SPEED (m/s)
45 KW	45	2.2	11.2	17.9
MOD 0	100	3.1	6.5	15.3
MOD 0A	200	3.1	8.2	15.3
500 KW	500	3.54	7.27	17.9
MOD 1	2000	4.9	10.8	15.6
MOD 2	2500	3.8	8.9	20.1

TABLE 4.2 Summary of Sites Investigated

LOCATION	LAT. (N) / LONG. (W)	GROUND ELEVATION (meters)	PERIOD OF RECORD	
			TOTAL	UTILIZED
TOPEKA, KS	39° 94' / 95° 38'	285	Jan. 1960- Dec. 1964	Jan. 1960- Dec. 1964
FORBES AFB, KS	38° 57' / 95° 40'	324	Jan. 1960- Dec. 1964	Jan. 1960 Dec. 1964
OLATHE NAS, KS	38° 50' / 94° 53'	335	Jan. 1960- Dec. 1964	Jan. 1960- Dec. 1964
CHEYENNE, WY	41° 09' / 104° 49'	1873	Jan. 1950- Dec. 1954	Jan. 1952 Dec. 1954
DOUGLAS, WY	42° 45' / 105° 23'	1476	Jan. 1950- Dec. 1954	Jan. 1952 Dec. 1954
LARAMIE, WY	41° 19' / 105° 41'	2183	Jan. 1950- Dec. 1954	Jan. 1950 Dec. 1954
ARGONNE NATIONAL LABORATORY 18', IL	41° 43' / 87° 59'	227	July 1949- Mar. 1965	Jan. 1959- Dec. 1964
GLENVIEW, IL	42° 05' / 87° 50'	200	Jan. 1958- Dec. 1964	Jan. 1959- Dec. 1964
MIDWAY, IL	41° 47' / 87° 45'	187	Jan. 1950- Dec. 1973	Jan. 1959- Dec. 1964
O'HARE, IL	41° 59' / 87° 54'	211	Jan. 1950- Dec. 1964	Jan. 1959- Dec. 1964
ROCKFORD, IL	42° 11' / 89° 05'	224	Jan. 1950- Dec. 1954 Jan. 1959- Dec. 1964	Jan. 1959- Dec. 1964

A similar procedure was applied to the SIMUL model where the hourly wind speed in the model was simulated from a sequence of hourly wind speeds at a representative site of each region (Forbes AFB in Kansas, Rockford in northern Illinois and Laramie in Wyoming) for an array size equivalent (in area) to the actual region. Although wind speeds of ten sites were simulated in each array, three sites were actually used for Wyoming and Kansas and five sites for northern Illinois in computing the array power.

The third model, ARASIM, is the Gaussian simulation of hourly array power. The model input is outlined in Appendix E. The data are the averages of the statistics at individual sites over the array. The diurnal cycle factors were linearly interpolated between the 6-hour period statistics from the WINDATB (Corotis, 1977) analysis to obtain the hourly effect. The monthly correlations were also linearly interpreted between seasons from the correlations analyses previously done.

Computer programs WINDATB, AUTOCOR and PERSIST (Corotis, 1976,1977), which compute the statistical analyses for wind speed, were modified slightly to compute the statistical analyses for array power. The modified programs were renamed as WINDATR, RUTOCOR and PERIR for WINDATB, AUTOCOR and PERSIST, respectively. A brief description of the modified programs is given in Appendix F. The modification basically consisted of deleting the computation for velocity-cubed statistics and renaming the velocity statistics as power statistics. A power unit, PUN, is introduced which is defined in every analysis from the input data. For convenient resolution it is recommended that PUN should be greater than or equal to one-thirtieth of the total array power.

The basic statistics to compare among models are the mean, variance and coefficient of variation of the data. Table 4.3 summarizes the mean, standard deviation and coefficient of variation for the array power data. The mean array powers for the ARASIM are somewhat lower than the REGIONAL with only a few exceptions. The coefficients of variation are quite consistent with the REGIONAL. Overall, the ARASIM model shows good agreement with the REGIONAL, and in many cases, it even fits better than the SIMUL.

Histograms for all the models were computed to assess the fitting of the array power frequency distribution. Selected typical histograms, winter and summer seasons for MOD 0A (200kW) for the three regions, are presented in Figures 4.2-4.4. Except for the extreme ranges, the ARASIM fits reasonably well to the REGIONAL. The cumulative density at 25 and 75% of the total array power for the winter and summer seasons for all the data are shown in Table 4.4. The two approximate models vary from the REGIONAL quite irregularly, but the cumulative densities are not significantly different.

Another important area of comparison is the autocorrelation function. Besides comparing the fit among models, it is necessary to verify that the autocorrelation function decays exponentially, one of the characteristics required by the Gauss-Markov process. A list of correlation times (the time that it takes the autocorrelation function to decay to 1/e of its original value) for winter and summer is given in Table 4.5. The correlation times for the ARASIM in winter are higher than the REGIONAL and for the summer are lower, while the correlation times for the SIMUL are lower for both seasons. Figures

4.5-4.6 show the autocorrelation function for MOD 0A in the various regions. It is observed that the correlation function does decay exponentially, with the effect of the diurnal cycle superimposed. The correlation functions for the ARASIM are usually higher than the REGIONAL in the winter and lower in the summer. For the first few lag hours, the correlations agree very well with the exact correlations. The SIMUL, on the other hand, has lower correlation values than the REGIONAL, and the function decays considerably in the first few lag hours. The higher correlations for the ARASIM may be due to the estimated correlation function, R(1), given by Eq. (4.14). The assumptions made for the spatial and time-space correlations may have overestimated the correlation function. However, further investigation is needed to substantiate the observations or to adjust the correlation function.

Mean run lengths below 25% and above 75% of total array power in each region were tabulated and are presented in Table 4.6 to compare the persistence among the various models. The mean run lengths for the ARASIM are longer than the REGIONAL while the SIMUL are shorter in general. One may notice the substantial difference between ARASIM and REGIONAL below 25% of total array power in the summer at Kansas region. However, the overall variation is reasonable. Graphs of mean run length versus run levels were drawn for all turbines and regions. Some selected graphs are shown in Figures 4.8-4.10 which provide an overall summary of the run duration fit among the models. It is observed that the complete curve for the ARASIM fits the REGIONAL reasonably well. The SIMUL fits well only at the low run

levels for runs below the fixed run levels, and the difference increases with higher run level. Hence, the statistics shown in Table 4.6 are somewhat limited, reflecting the particular level of array power being compared. However, Table 4.6 still provides adequate information for comparison. In general, the ARASIM model gives a reasonable approximate to the REGIONAL results. The overestimated mean run lengths below high run levels may be related to the high autocorrelation.

Based on the preceding analyses and discussion, it is reasonable to say that the approximate approach (ARASIM) developed here is a good approximation to the exact model. In many occasions, the ARASIM is shown to give a better fit than the SIMUL. In addition, the ARASIM has several computational advantages over the SIMUL: the hourly array power is simulated directly, the program is efficient, computing time does not increase with the number of sites in an array, and the method consistently incorporates autocorrelation and spatial correlation. However, there are some areas in the ARASIM model that require attention: the relatively consistent high autocorrelations, and the capability of modelling an array with different wind turbines.

TABLE 4.3a Basic Array Power Statistics for Kansas Region

TURBINE RATED POWER	SEASON	REGIONAL			ARASIM			SIMUL		
		MEAN (KW)	STD. DEV. (KW)	σ/m	MEAN (KW)	STD. DEV. (KW)	σ/m	MEAN (KW)	STD. DEV. (KW)	σ/m
45 KW	ANNUAL	15.83	23.62	1.492	14.97	20.70	1.383	11.43	20.57	1.800
	WINTER	18.54	24.42	1.317	18.94	22.24	1.174	13.63	21.96	1.611
	SPRING	21.86	27.81	1.272	20.70	24.31	1.174	15.16	23.92	1.578
	SUMMER	9.53	15.47	1.623	7.76	12.11	1.561	6.56	13.61	2.075
	FALL	13.41	21.38	1.594	12.53	16.91	1.349	10.37	19.43	1.874
MOD 0 (200 KW)	ANNUAL	109.35	104.60	0.956	103.92	94.20	0.906	86.87	100.66	1.159
	WINTER	126.25	106.01	0.840	123.28	92.78	0.753	100.17	103.36	1.032
	SPRING	131.72	106.72	0.810	129.42	91.47	0.707	104.40	105.97	1.015
	SUMMER	80.75	88.27	1.093	67.45	80.87	1.199	62.49	85.42	1.367
	FALL	98.98	102.81	1.039	95.95	90.47	0.943	80.62	97.81	1.213
MOD 0A (200 KW)	ANNUAL	148.32	172.28	1.162	130.98	157.88	1.205	111.90	155.82	1.393
	WINTER	173.05	177.39	1.025	161.02	165.50	1.028	131.30	163.03	1.242
	SPRING	189.52	186.18	0.982	171.32	167.51	0.978	140.48	171.26	1.219
	SUMMER	100.32	130.85	1.304	75.72	115.79	1.529	73.30	119.81	1.635
	FALL	130.60	164.18	1.257	116.28	145.26	1.249	102.75	149.71	1.457
500 KW	ANNUAL	450.60	489.90	1.087	406.42	443.62	1.092	345.30	454.72	1.317
	WINTER	525.22	502.76	0.957	496.58	449.39	0.905	403.42	472.18	1.170
	SPRING	562.20	513.56	0.913	529.20	445.05	0.841	427.50	490.09	1.146
	SUMMER	314.10	389.81	1.241	237.60	352.15	1.482	233.02	365.65	1.569
	FALL	401.70	475.57	1.184	363.68	419.14	1.152	317.92	439.11	1.381
MOD 1 (2 MW)	ANNUAL	667.50	114.00	1.669	495.50	1017.75	2.054	464.25	956.25	2.060
	WINTER	787.00	1156.02	1.469	666.00	1125.44	1.690	561.50	1026.07	1.827
	SPRING	951.25	1318.50	1.386	743.25	1215.60	1.636	634.75	1118.15	1.762
	SUMMER	376.00	717.59	1.908	192.25	553.68	2.880	244.25	626.25	2.564
	FALL	555.25	1006.04	1.812	381.25	845.91	2.219	417.00	899.24	2.156
MOD 2 (2.5 MW)	ANNUAL	1503.50	1961.25	1.304	1251.75	1778.75	1.421	1100.25	1739.00	1.581
	WINTER	1763.50	2029.98	1.151	1588.50	1890.78	1.190	1305.00	1833.08	1.405
	SPRING	1988.25	2175.85	1.094	1715.50	1933.65	1.127	1420.75	1949.94	1.372
	SUMMER	961.00	1413.86	1.471	639.25	1214.96	1.901	672.75	1268.29	1.885
	FALL	1302.50	1843.91	1.416	1068.25	1606.84	1.504	1004.25	1664.16	1.657

TABLE 4.3b Basic Array Power Statistics for Northern Illinois Region

TURBINE RATED POWER	SEASON	REGIONAL			ARASIM			SIMUL		
		MEAN (KW)	STD. DEV. (KW)	σ/m	MEAN (KW)	STD. DEV. (KW)	σ/m	MEAN (KW)	STD.DEV. (KW)	σ/m
45 KW	ANNUAL	23.03	33.81	1.468	24.67	33.16	1.344	25.05	34.04	1.359
	WINTER	31.15	39.32	1.262	34.98	38.80	1.109	28.51	35.11	1.231
	SPRING	25.92	34.86	1.346	27.48	34.52	1.256	29.17	36.66	1.257
	SUMMER	12.02	20.94	1.742	11.93	19.36	1.623	16.90	26.97	1.596
	FALL	23.22	32.88	1.416	24.58	30.39	1.236	25.69	34.21	1.331
MOD 0 (100 KW)	ANNUAL	180.95	166.62	0.921	173.95	154.70	0.889	185.55	162.78	0.877
	WINTER	225.08	175.87	0.781	226.02	152.80	0.676	206.72	162.62	0.787
	SPRING	196.88	160.63	0.816	187.12	148.15	0.792	204.88	161.84	0.790
	SUMMER	117.88	134.39	1.140	103.75	130.02	1.253	141.50	150.81	1.066
	FALL	185.15	165.92	0.896	180.42	150.28	0.833	189.68	162.38	0.856
MOD 0A (200 KW)	ANNUAL	232.98	264.28	1.134	217.42	259.48	1.193	243.58	258.42	1.061
	WINTER	301.90	293.16	0.971	296.00	286.06	0.966	274.60	263.31	0.959
	SPRING	257.45	262.28	1.019	237.32	256.27	1.080	274.75	264.65	0.963
	SUMMER	137.13	189.39	1.381	115.72	184.04	1.590	176.20	224.27	1.273
	FALL	237.30	260.60	1.098	222.80	253.12	1.136	249.52	259.25	1.039
500 KW	ANNUAL	725.32	771.52	1.064	678.22	728.55	1.074	748.42	749.70	1.002
	WINTER	928.72	838.90	0.903	917.78	760.70	0.829	841.05	757.27	0.900
	SPRING	796.42	754.09	0.947	741.08	703.56	0.949	839.32	758.18	0.903
	SUMMER	439.88	583.30	1.326	362.78	560.51	1.545	549.98	669.60	1.217
	FALL	741.82	765.61	1.032	697.95	712.42	1.021	766.05	750.58	0.980
MOD 1 (2 MW)	ANNUAL	938.40	1589.20	1.694	799.60	1624.40	2.032	1035.20	1587.20	1.533
	WINTER	1308.80	1865.86	1.426	1240.40	1980.18	1.596	1189.20	1651.23	1.389
	SPRING	1068.00	1650.65	1.546	912.00	1697.43	1.861	1220.00	1712.26	1.403
	SUMMER	443.20	958.65	2.163	285.20	855.20	2.999	670.80	1243.80	1.854
	FALL	943.20	1542.93	1.636	771.20	1531.12	1.985	1063.60	1596.90	1.501
MOD 2 (2.5 MW)	ANNUAL	2281.60	2943.20	1.290	2066.00	2916.00	1.411	2420.80	2905.20	1.200
	WINTER	3032.40	3335.34	1.100	2944.40	3308.78	1.124	2748.00	2979.56	1.084
	SPRING	2542.40	2955.32	1.162	2287.60	2906.90	1.271	2772.00	3026.60	1.092
	SUMMER	1252.40	1995.47	1.593	966.80	1914.45	1.980	1687.60	2437.05	1.444
	FALL	2317.60	2891.42	1.248	2089.20	2840.17	1.359	2484.80	2922.93	1.176

TABLE 4.3c Basic Array Power Statistics for Wyoming Region

TURBINE RATED POWER	SEASON	REGIONAL			ARASIM			SIMUL		
		MEAN (KW)	STD.DEV. (KW)	σ/m	MEAN (KW)	STD.DEV. (KW)	σ/m	MEAN (KW)	STD.DEV. (KW)	σ/m
45 KW	ANNUAL	33.22	33.77	1.016	31.77	31.86	1.003	33.50	36.53	1.090
	WINTER	47.12	37.37	0.793	46.95	37.29	0.794	44.24	39.15	0.885
	SPRING	34.38	33.56	0.976	32.42	30.69	0.947	35.02	36.63	1.046
	SUMMER	20.00	23.29	1.164	17.95	20.48	1.141	22.86	29.28	1.281
	FALL	31.72	32.57	1.027	30.16	28.01	0.929	32.09	36.45	1.136
MOD 0 (100 KW)	ANNUAL	152.91	93.83	0.614	167.75	86.35	0.515	157.54	108.20	0.687
	WINTER	181.02	90.17	0.498	207.15	72.08	0.348	182.34	106.30	0.583
	SPRING	163.20	93.20	0.571	173.62	82.21	0.473	164.41	105.78	0.643
	SUMMER	125.87	87.78	0.697	125.05	84.15	0.673	134.82	103.66	0.769
	FALL	142.48	93.43	0.656	166.28	80.12	0.482	149.06	110.22	0.739
MOD 0A (200 KW)	ANNUAL	239.18	182.12	0.762	238.42	184.22	0.773	240.90	200.65	0.833
	WINTER	302.95	183.06	0.604	321.25	184.19	0.573	294.78	204.08	0.692
	SPRING	254.18	182.83	0.719	246.50	179.81	0.729	251.35	198.10	0.788
	SUMMER	178.72	158.41	0.886	155.18	151.01	0.973	189.92	181.33	0.955
	FALL	222.88	177.07	0.794	233.00	170.44	0.731	228.52	201.57	0.882
500 KW	ANNUAL	695.78	486.38	0.699	721.42	445.95	0.618	707.70	545.48	0.771
	WINTER	871.28	475.42	0.546	938.78	381.40	0.406	852.45	542.72	0.637
	SPRING	738.08	485.32	0.658	750.90	427.36	0.569	739.20	536.82	0.726
	SUMMER	528.22	429.69	0.813	492.52	411.31	0.835	569.78	503.23	0.883
	FALL	650.78	477.76	0.734	709.42	412.21	0.581	672.15	552.17	0.821
MOD 1 (2 MW)	ANNUAL	1437.00	1535.00	1.068	1242.75	1598.25	1.286	1425.75	1633.50	1.146
	WINTER	2052.50	1679.16	0.818	2013.75	1876.70	0.932	1896.25	1744.38	0.920
	SPRING	1492.75	1537.08	1.030	1269.50	1543.90	1.216	1489.25	1635.43	1.098
	SUMMER	854.00	1112.74	1.303	553.75	986.12	1.781	965.75	1347.17	1.395
	FALL	1364.75	1471.75	1.078	1153.00	1417.26	1.229	1361.00	1619.72	1.190
MOD 2 (2.5 MW)	ANNUAL	2745.25	2337.00	0.851	2518.75	2186.50	0.868	2732.50	2526.50	0.925
	WINTER	3697.00	2419.05	0.654	3581.50	2176.80	0.608	3474.50	2603.11	0.749
	SPRING	2875.50	2325.64	0.809	2615.00	2128.04	0.814	2856.00	2512.03	0.880
	SUMMER	1815.25	1853.41	1.001	1473.00	1723.22	1.170	2006.75	2177.40	1.085
	FALL	2582.75	2262.53	0.876	2433.25	2012.85	0.827	2605.75	2530.71	0.971

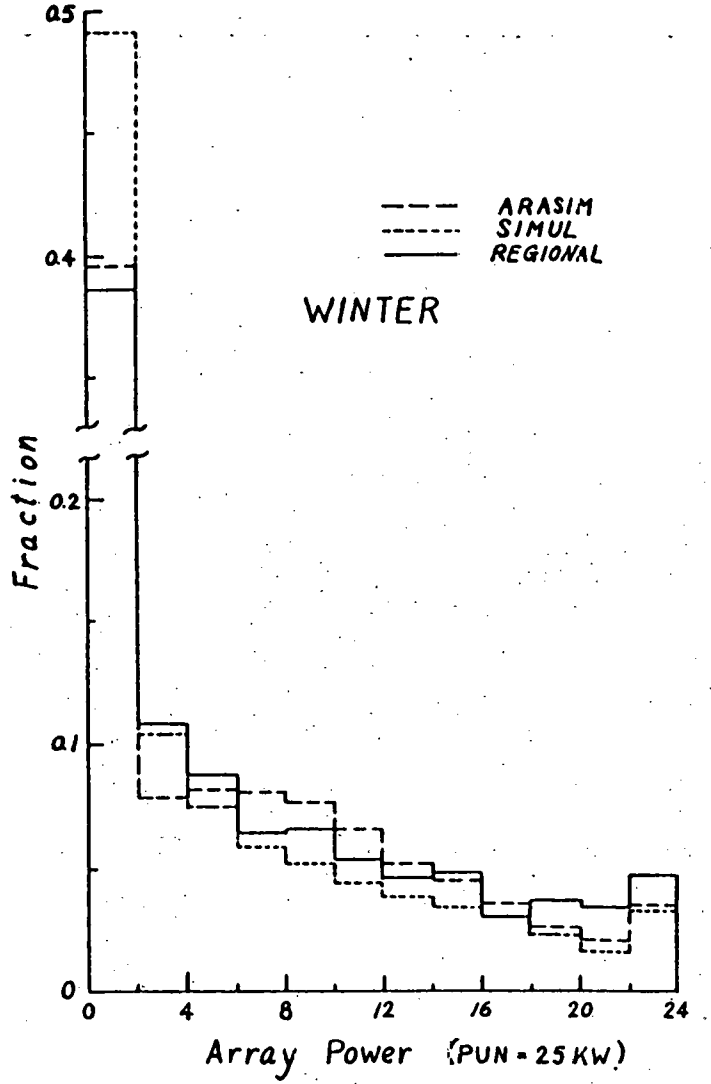

FIGURE 4.2a Histograms of Array Power for MOD 0A (200 KW) in Kansas Region for Winter.

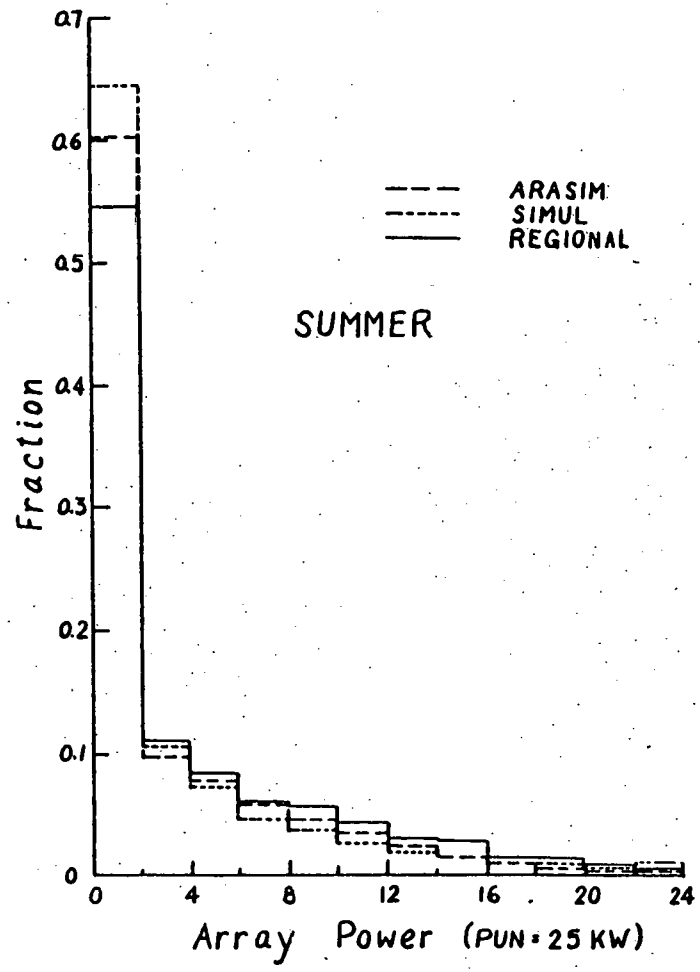

FIGURE 4.2b Histograms of Array Power for MOD 0A (200 KW) in Kansas Region for Summer.

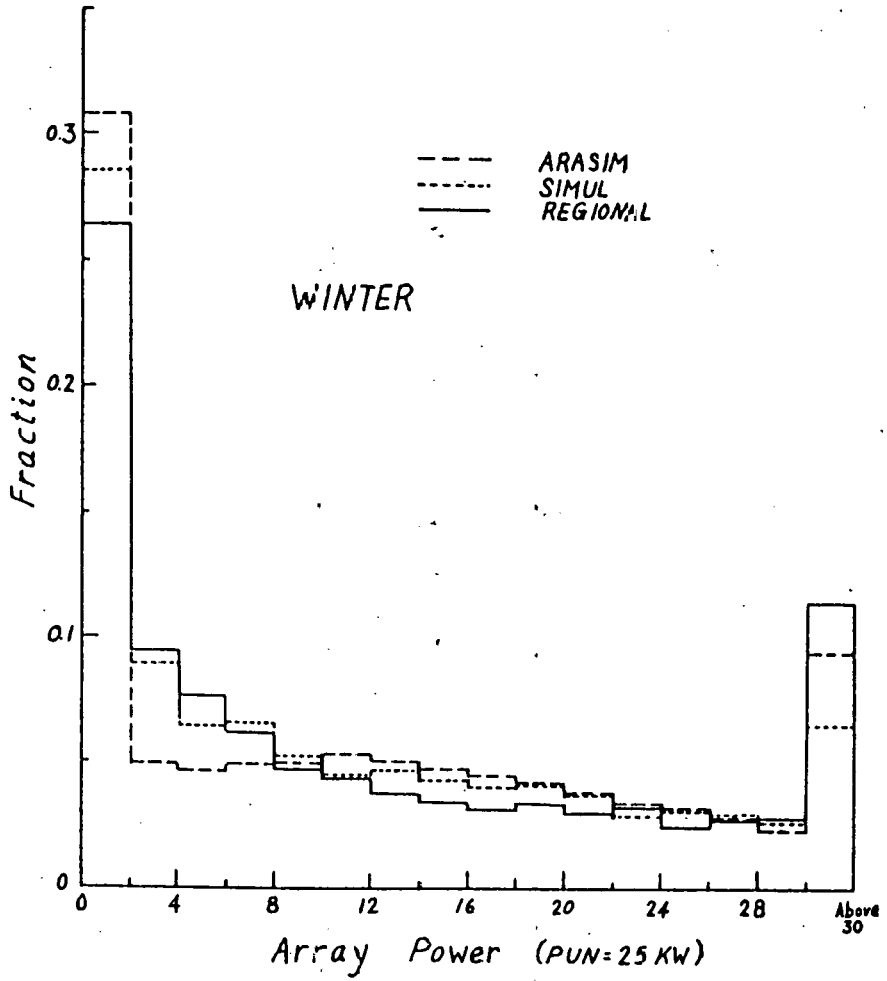

FIGURE 4.3a Histograms of Array Power for MOD 0A (200 KW) in Northern Illinois for Winter Season.

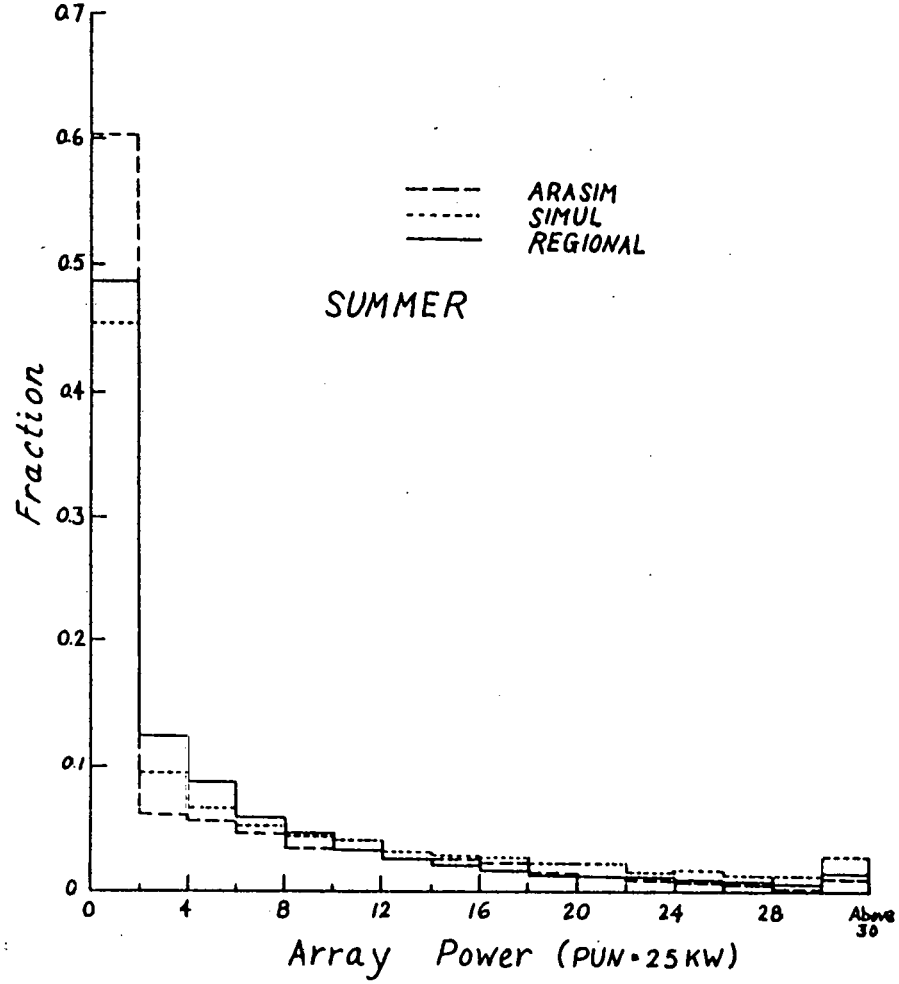

FIGURE 4.3b Histograms of Array Power for MOD 0A (200 KW) in Northern Illinois for Summer Season.

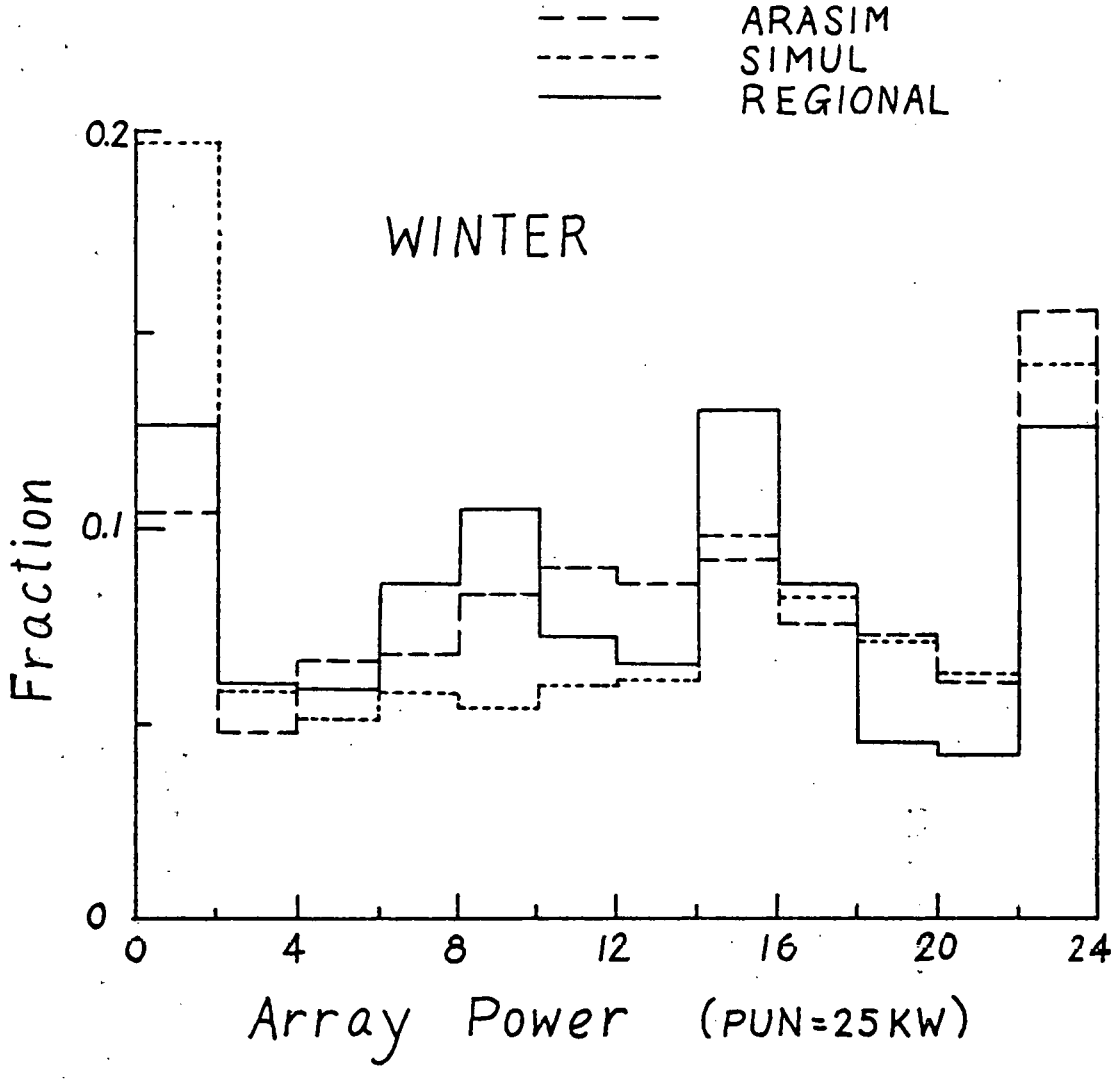

FIGURE 4.4a Histograms of Array Power for MOD 0A (200 KW) in Wyoming Region for Winter Season.

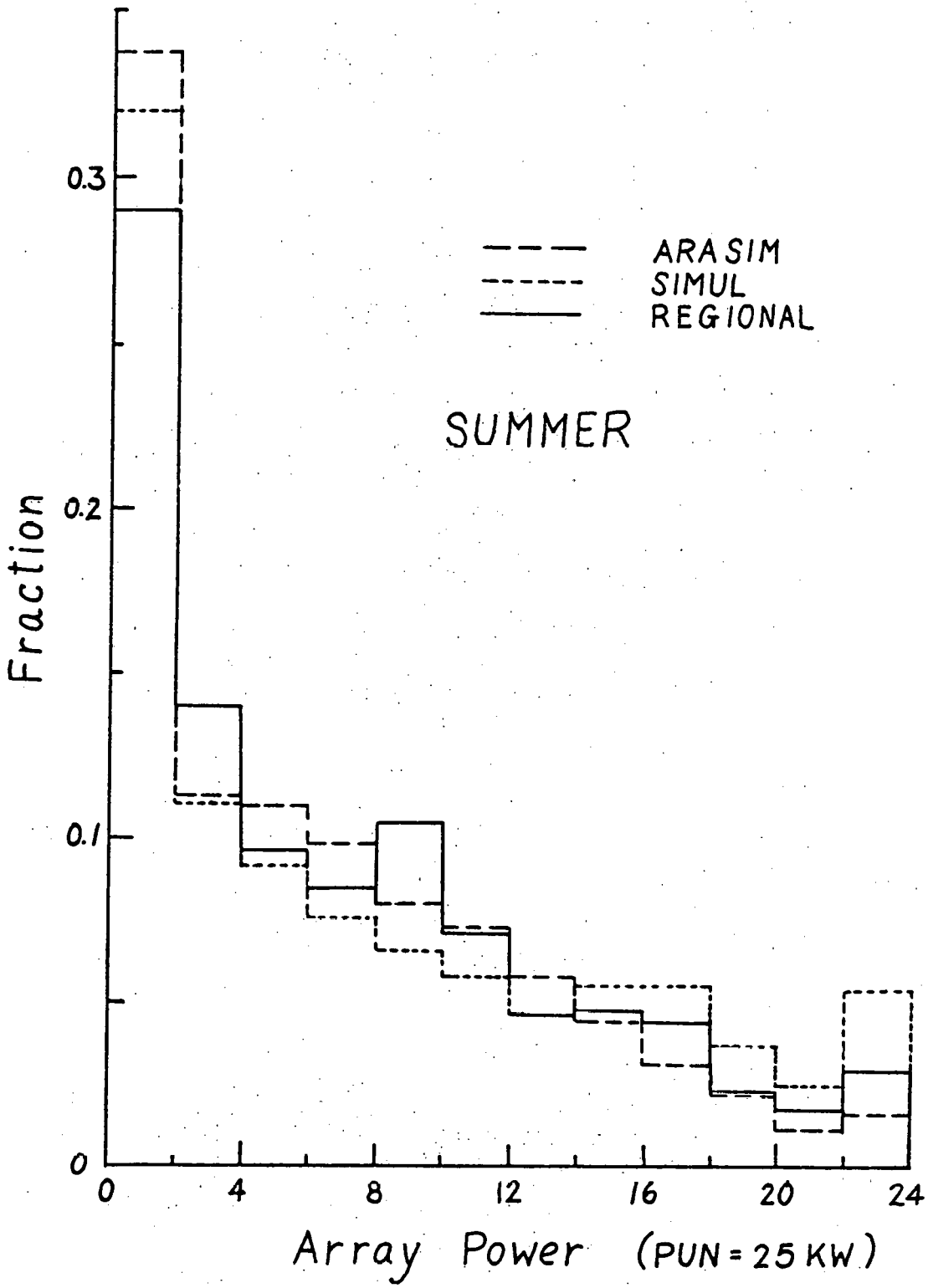

FIGURE 4.4b Histograms of Array Power for MOD 0A (200 KW) in Wyoming Region for Summer Season.

TABLE 4.4 Cumulative Density of Array Power Output at Indicated Percentages of Total Array Power

TURBINE RATED POWER	SIMULATION MODEL	WYOMING REGION				KANSAS REGION				NORTHERN ILLINOIS			
		WINTER		SUMMER		WINTER		SUMMER		WINTER		SUMMER	
		25%	75%	25%	75%	25%	75%	25%	75%	25%	75%	25%	75%
45 KW	REGIONAL	.497	.890	.827	.991	.834	.986	.944	.999	.813	.984	.960	.999
	ARASIM	.480	.897	.854	.997	.828	.992	.968	.999	.756	.992	.960	1.000
	SIMUL	.507	.888	.789	.971	.892	.987	.964	.998	.832	.993	.921	.998
MOD 0 (100 KW)	REGIONAL	.151	.647	.349	.824	.439	.740	.599	.893	.346	.687	.597	.909
	ARASIM	.057	.528	.328	.847	.383	.806	.647	.933	.252	.755	.613	.932
	SIMUL	.225	.556	.376	.741	.538	.812	.693	.915	.356	.750	.535	.863
MOD 0A (200 KW)	REGIONAL	.247	.785	.527	.929	.573	.881	.739	.971	.552	.885	.811	.983
	ARASIM	.218	.710	.562	.950	.555	.917	.794	.985	.507	.910	.810	.989
	SIMUL	.310	.725	.525	.883	.668	.929	.823	.978	.557	.935	.726	.971
500 KW	REGIONAL	.157	.620	.382	.854	.470	.788	.626	.927	.470	.780	.735	.949
	ARASIM	.068	.578	.387	.888	.429	.847	.700	.955	.402	.839	.754	.966
	SIMUL	.238	.558	.408	.780	.570	.857	.726	.944	.469	.849	.649	.927
MOD 1 (2 MW)	REGIONAL	.441	.900	.779	.988	.798	.893	.920	.998	.791	.981	.952	.999
	ARASIM	.482	.865	.993	.993	.816	.983	.955	.999	.779	.980	.957	.999
	SIMUL	.492	.904	.757	.970	.864	.986	.950	.997	.808	.992	.906	.998
MOD 2 (2.5 MW)	REGIONAL	.288	.740	.609	.946	.658	.914	.815	.983	.635	.936	.873	.993
	ARASIM	.271	.778	.683	.969	.658	.940	.871	.992	.608	.946	.876	.996
	SIMUL	.363	.720	.617	.898	.746	.947	.879	.986	.645	.968	.794	.988

TABLE 4.5 Correlation Time (in Hours) for Array Power

TURBINE RATED POWER	SIMULATION MODEL	WYOMING REGION		KANSAS REGION		NORTHERN ILLINOIS	
		WINTER	SUMMER	WINTER	SUMMER	WINTER	SUMMER
45 KW	REGIONAL	6	4	8	7	11	7
	ARASIM	7	4	9	5	16	6
	SIMUL	4	2	7	6	7	4
MOD 0 (100 KW)	REGIONAL	5	4	8	7	10	7
	ARASIM	7	5	10	6	17	6
	SIMUL	3	2	7	6	8	5
MOD 0A (200 KW)	REGIONAL	5	4	9	7	11	7
	ARASIM	7	4	10	6	17	6
	SIMUL	3	2	7	6	8	5
500 KW	REGIONAL	6	4	8	7	10	7
	ARASIM	7	5	10	6	17	6
	SIMUL	4	2	7	6	8	5
MOD 1 (2 MW)	REGIONAL	6	4	8	7	11	6
	ARASIM	7	4	8	4	13	5
	SIMUL	3	2	6	5	7	6
MOD 2 (2.5 MW)	REGIONAL	7	4	9	7	11	7
	ARASIM	7	4	9	5	17	6
	SIMUL	4	3	7	6	8	5

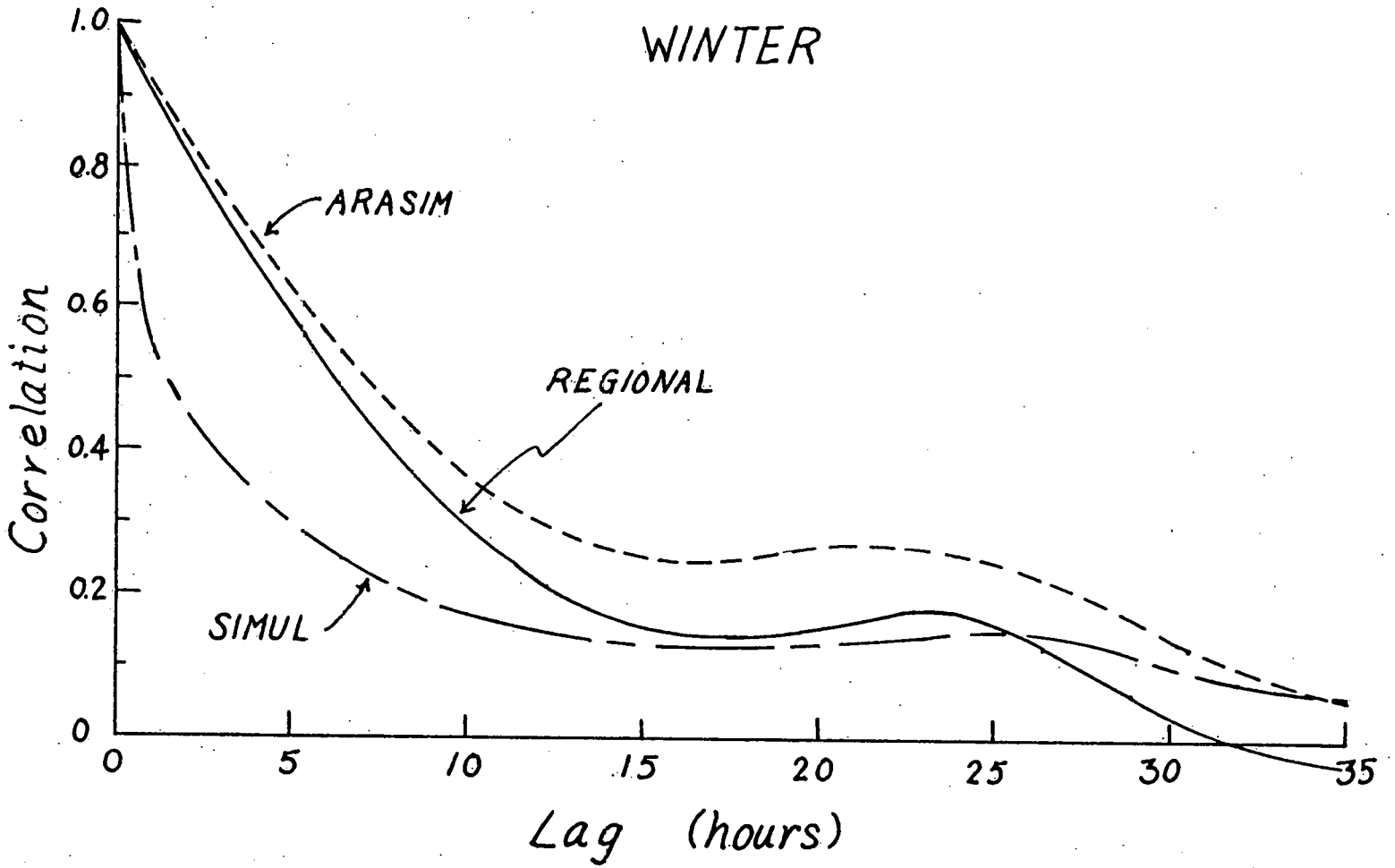

FIGURE 4.5a Autocorrelation Function for MOD 0A (200 KW) in Kansas Region for Winter Season.

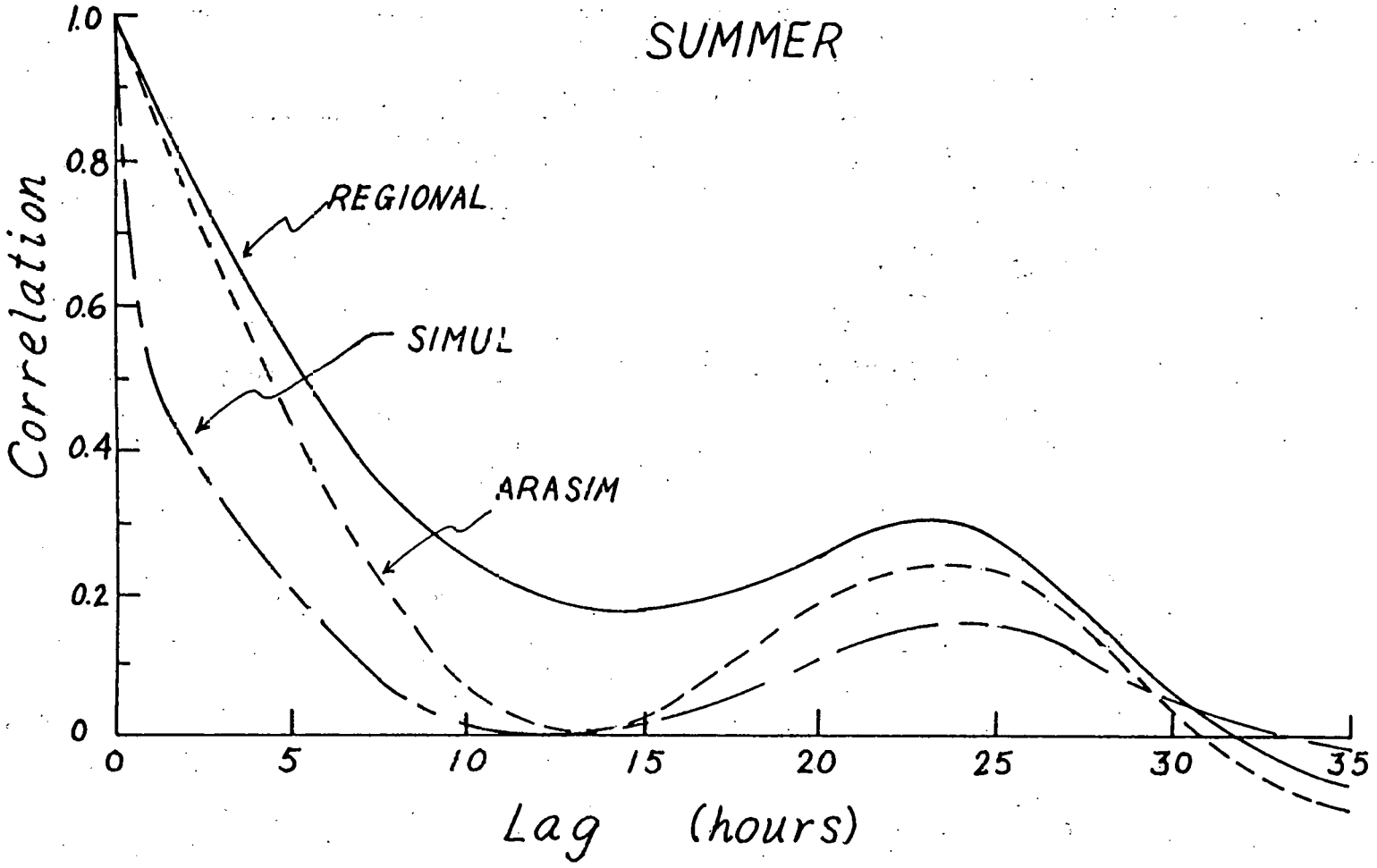

FIGURE 4.5b Autocorrelation Function for MOD 0A (200 KW) in Kansas Region for Summer Season.

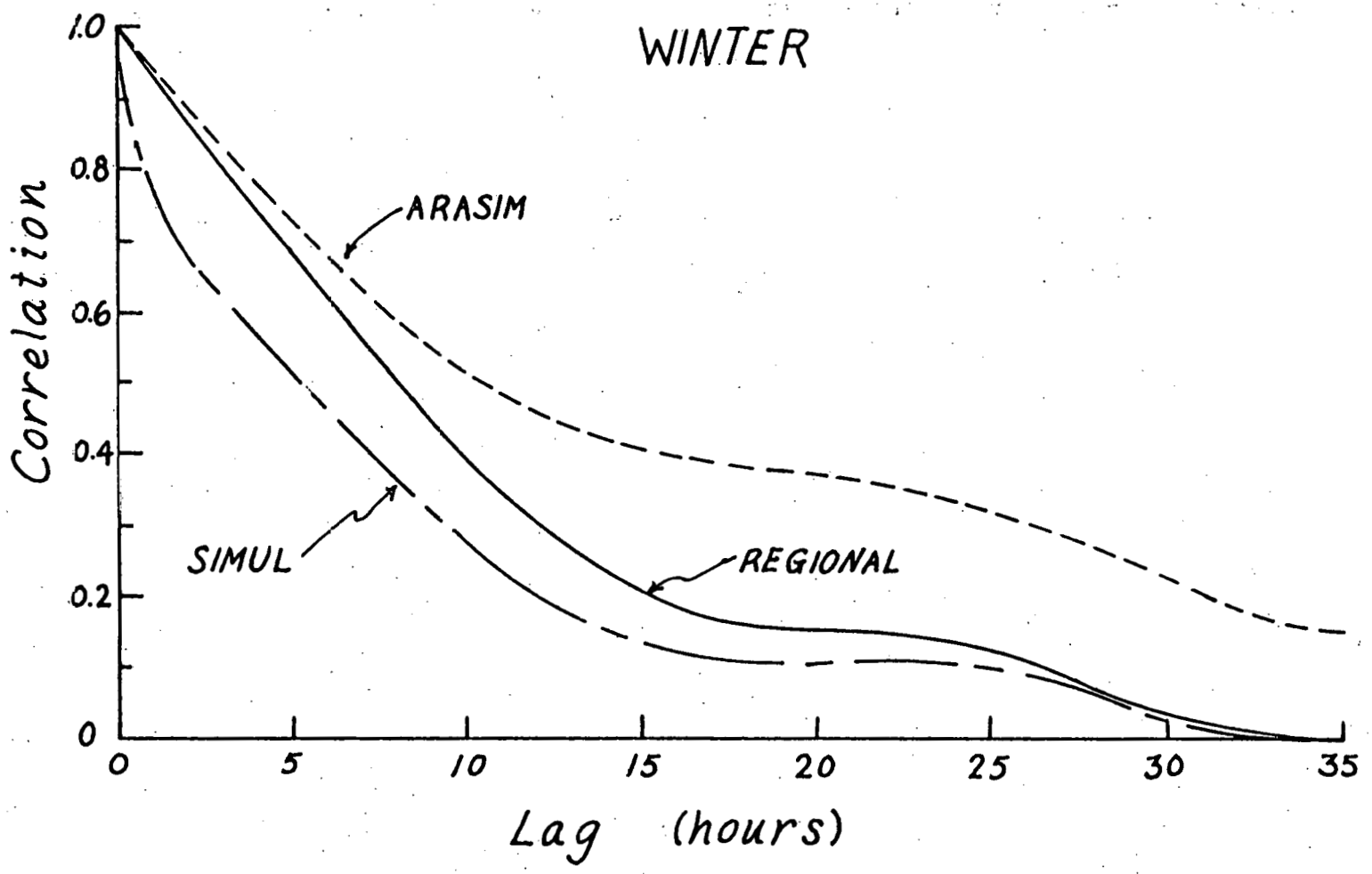

FIGURE 4.6a Autocorrelation Function for MOD 0A (200 KW) in Northern Illinois for Winter Season.

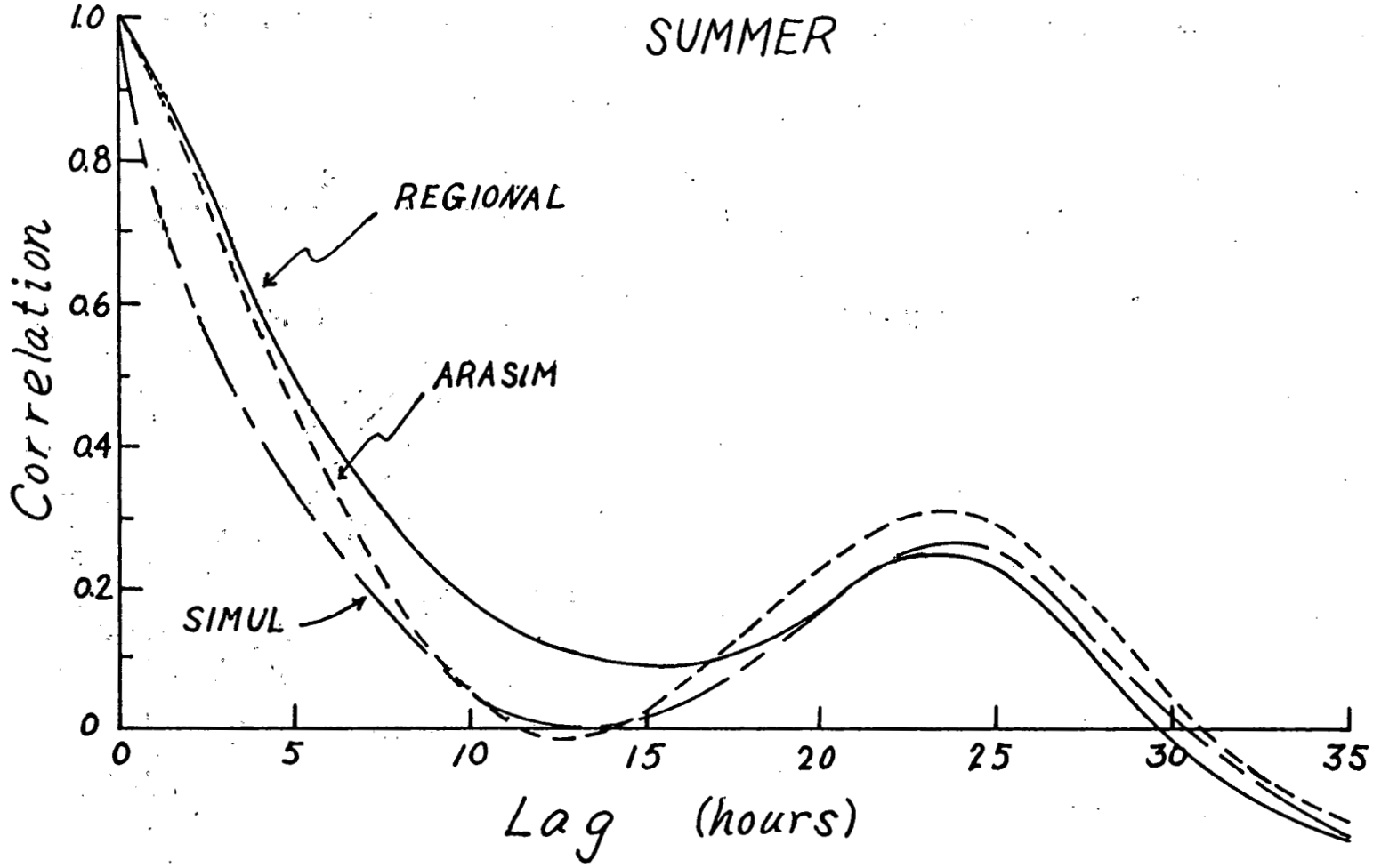

FIGURE 4.6b Autocorrelation Function for MOD 0A (200 KW) in Northern Illinois for Summer Season.

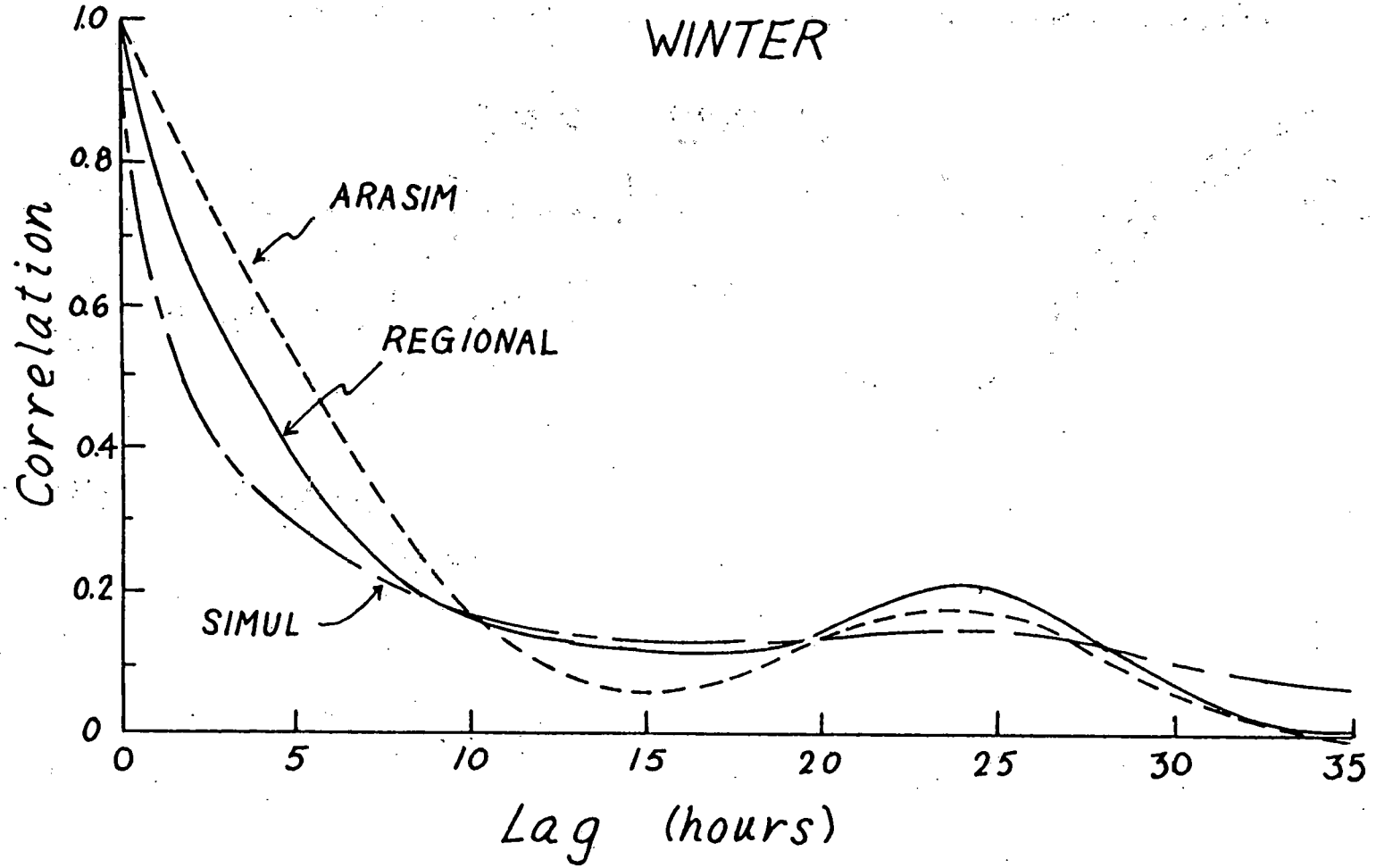

FIGURE 4.7a Autocorrelation Function for MOD 0A (200 KW) in Wyoming Region for Winter Season.

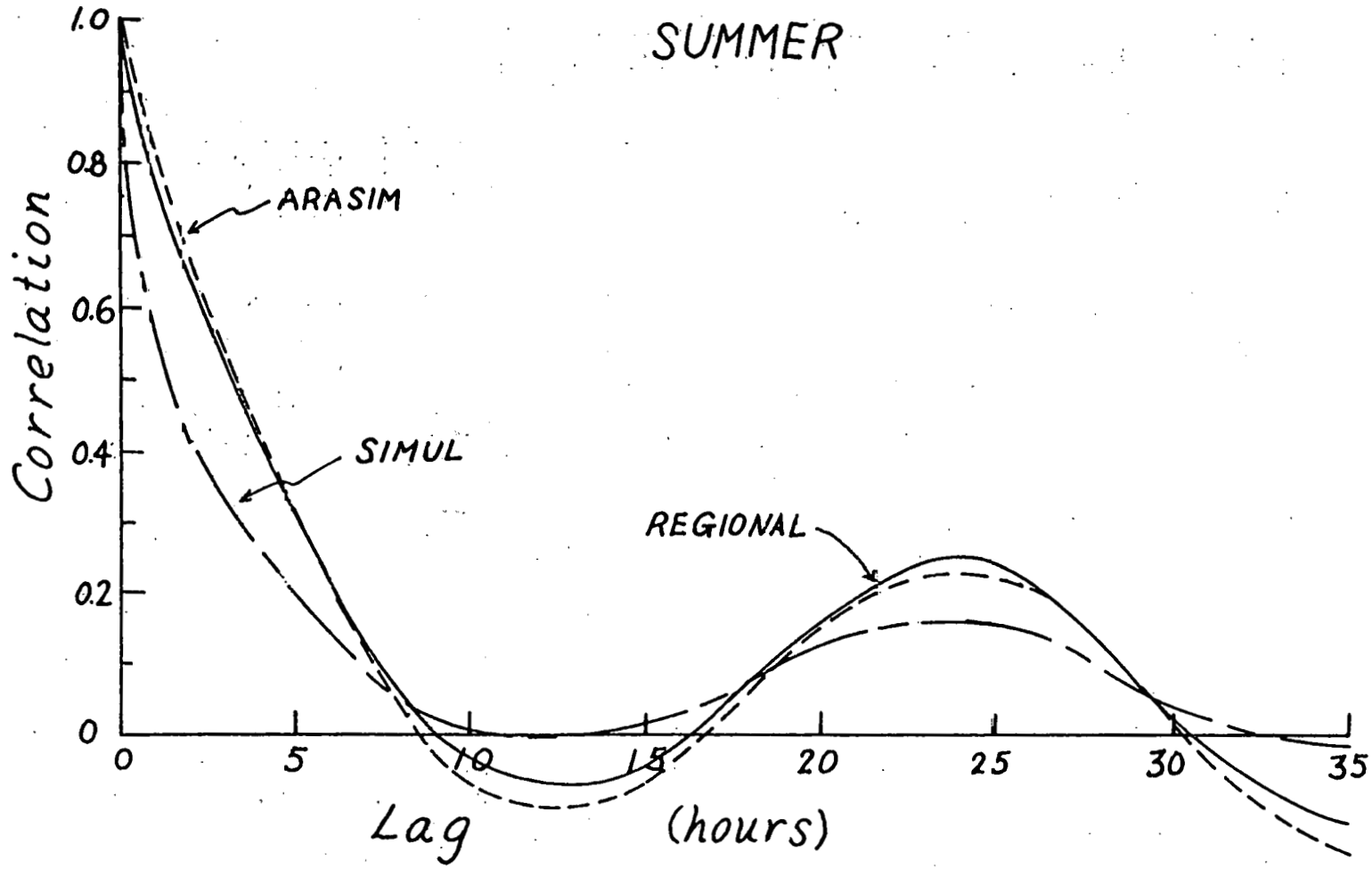

FIGURE 4.7b Autocorrelation Function for MOD 0A (200 KW) in Wyoming Region for Summer Season.

TABLE 4.6 Mean Run Length (in Hours) Above and Below Indicated Percentage of Total Array Power

TURBINE RATED POWER	SIMULATION MODEL	WYOMING REGION				KANSAS REGION				NORTHERN ILLINOIS			
		WINTER		SUMMER		WINTER		SUMMER		WINTER		SUMMER	
		BELOW 25%	ABOVE 75%	BELOW 25%	ABOVE 75%	BELOW 25%	ABOVE 75%	BELOW 25%	ABOVE 75%	BELOW 25%	ABOVE 75%	BELOW 25%	ABOVE 75%
45 KW	REGIONAL	6.501	2.358	12.986	1.706	22.442	2.559	45.621	3.333	25.771	3.231	76.405	1.375
	ARASIM	7.143	3.009	18.970	1.636	23.417	3.000	80.598	1.000	19.819	2.784	72.118	-
	SIMUL	3.958	1.326	7.557	1.143	17.996	1.366	42.603	1.211	11.103	1.237	20.580	1.174
MOD 0 (100 KW)	REGIONAL	2.620	3.500	3.413	2.597	7.514	5.326	8.298	3.523	7.604	7.933	9.578	4.177
	ARASIM	2.624	6.910	4.006	3.003	6.971	4.610	10.045	3.320	6.097	6.420	10.749	3.429
	SIMUL	2.678	2.483	2.612	1.843	5.922	2.261	7.410	1.821	4.198	2.462	5.150	1.973
MOD 0A (200 KW)	REGIONAL	3.410	2.525	5.299	2.112	9.889	3.865	12.300	2.779	12.297	4.264	18.645	2.936
	ARASIM	4.132	4.764	5.985	2.205	9.836	3.742	17.130	2.278	10.179	4.390	20.937	2.127
	SIMUL	2.908	1.743	3.500	1.450	7.419	1.700	11.313	1.426	5.793	1.515	8.089	1.336
500 KW	REGIONAL	2.793	7.182	3.520	2.604	7.773	5.406	8.455	3.303	10.215	6.207	13.608	3.464
	ARASIM	2.796	6.228	4.428	2.690	7.860	4.691	12.083	2.721	8.276	5.435	16.938	2.948
	SIMUL	2.820	2.687	2.787	1.857	6.201	2.112	8.230	1.650	4.944	1.994	6.530	1.565
MOD 1 (2 MW)	REGIONAL	5.326	2.060	10.406	1.711	19.620	2.367	31.844	2.571	23.775	3.024	63.651	1.308
	ARASIM	7.218	3.229	17.247	1.679	21.266	3.033	56.167	1.200	21.369	3.581	68.640	1.000
	SIMUL	3.607	1.218	3.607	1.218	14.745	1.336	32.965	1.240	10.213	1.262	18.352	1.185
MOD 2 (2.5 MW)	REGIONAL	4.143	3.753	6.337	2.238	12.282	3.719	17.600	2.563	15.081	3.768	28.150	2.636
	ARASIM	4.569	3.989	8.707	2.000	12.301	3.354	24.958	2.070	11.950	3.971	29.082	2.192
	SIMUL	3.267	1.936	4.367	1.443	8.962	1.765	15.389	1.402	6.695	1.358	10.033	1.264

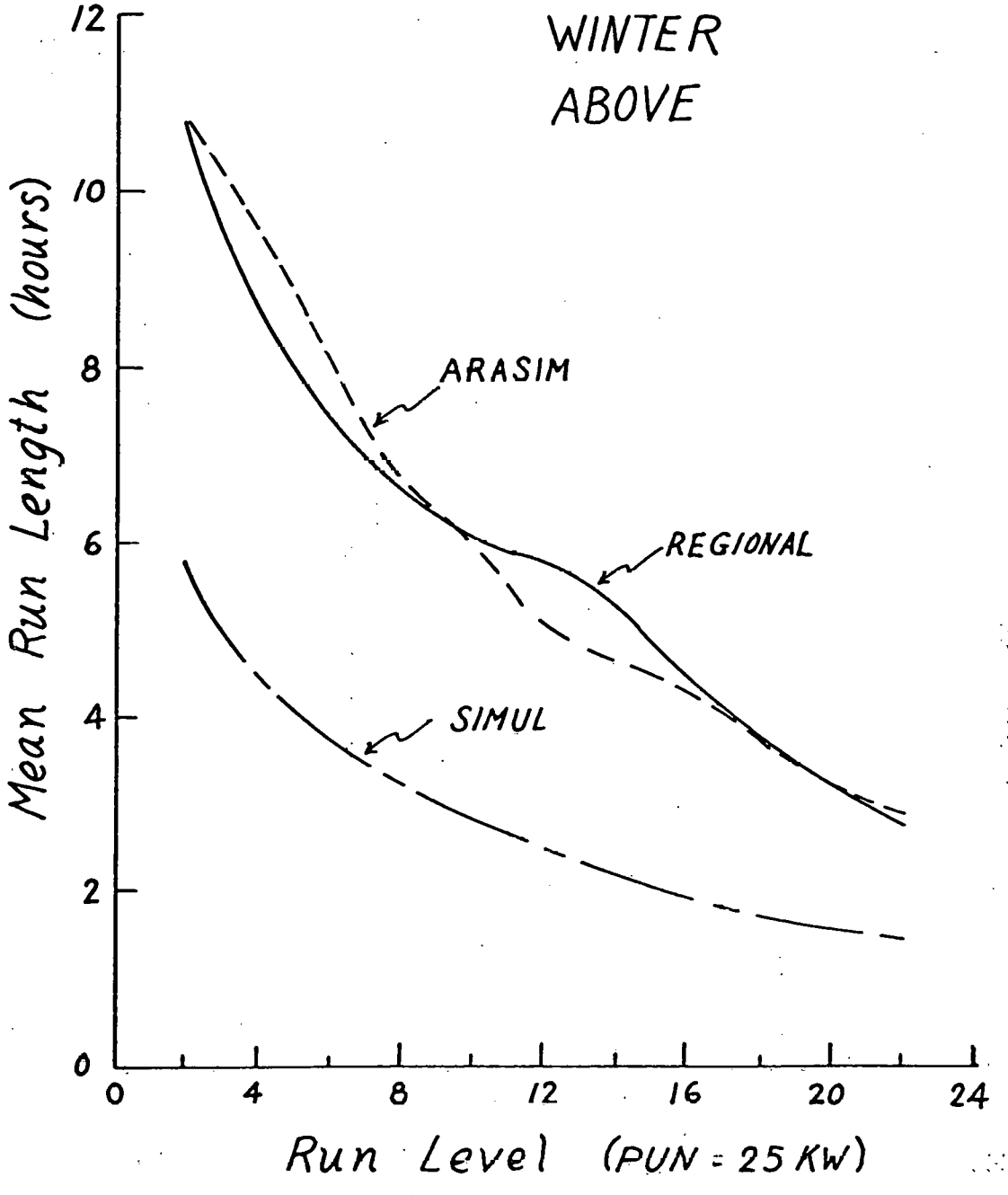

FIGURE 4.8a Mean Run Lengths Above Fixed Run Levels for MOD 0A (200 KW) in Kansas Region for Winter Season.

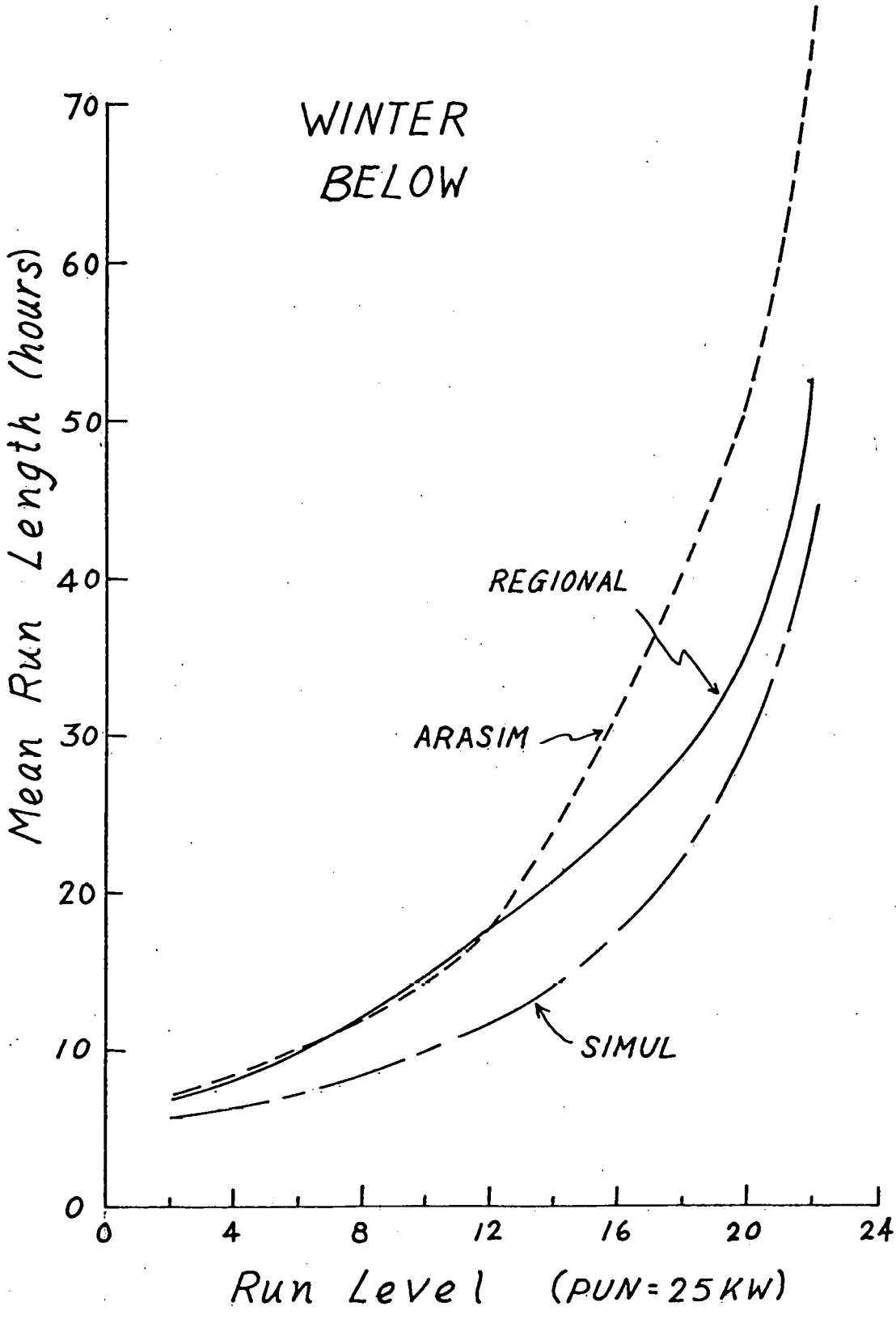

FIGURE 4.8b Mean Run Lengths Below Fixed Run Levels for MOD 0A (200 KW) in Kansas Region for Winter Season.

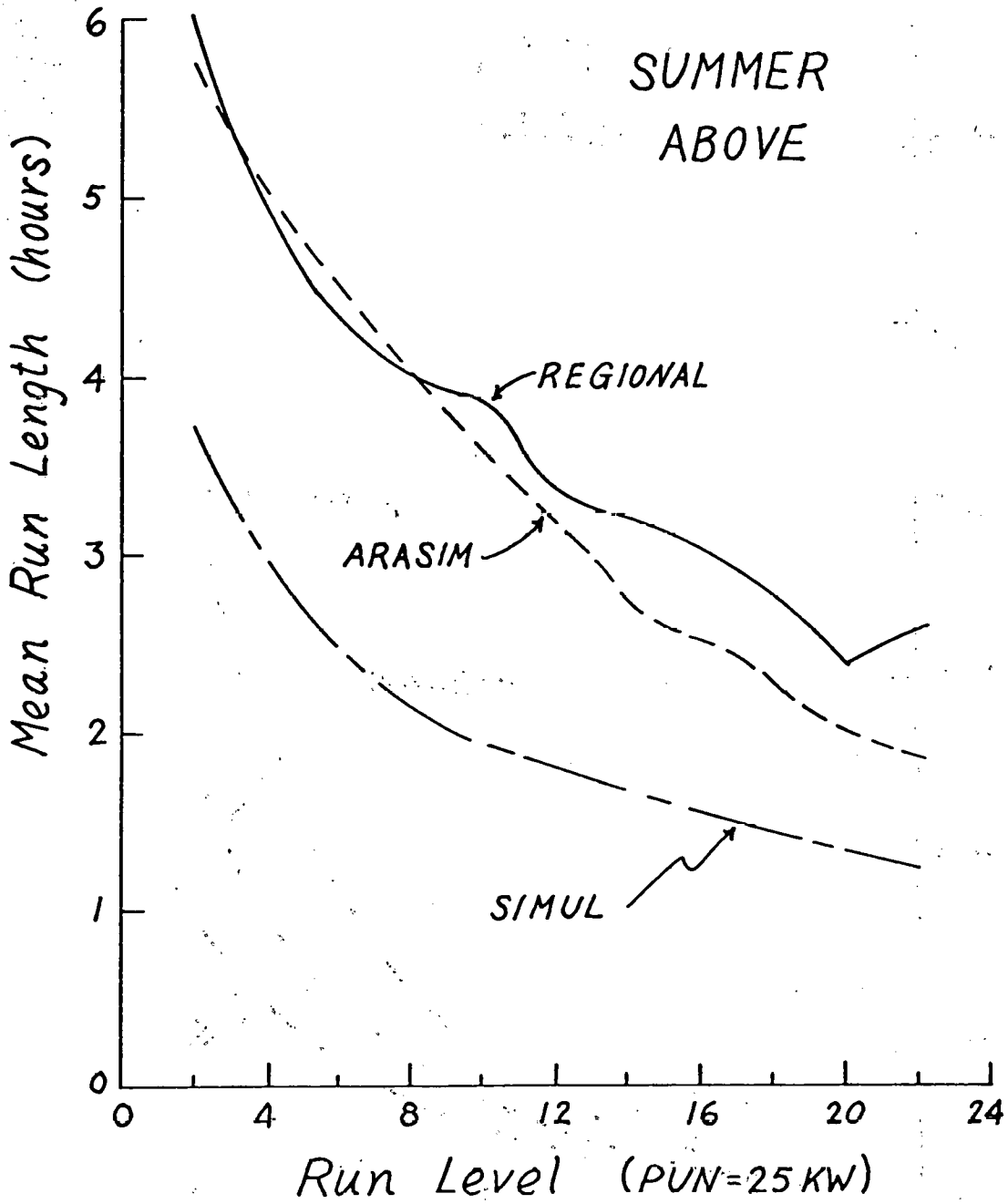

FIGURE 4.8c Mean Run Lengths Above Fixed Run Levels for MOD 0A (200 KW) in Kansas Region for Summer Season.

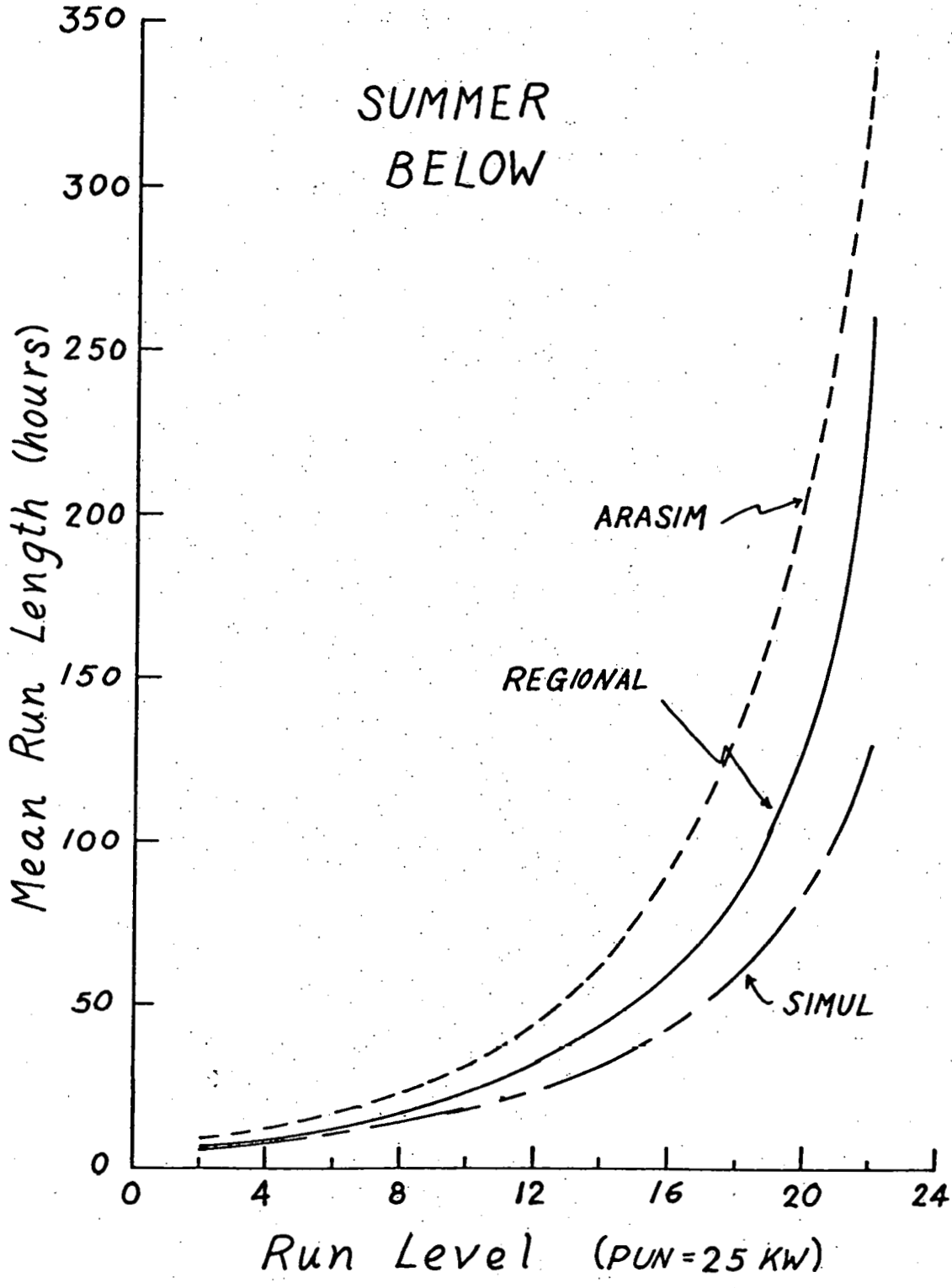

FIGURE 4.8d Mean Run Lengths Below Fixed Run Levels for MOD 0A (200 KW) in Kansas Region for Summer Season.

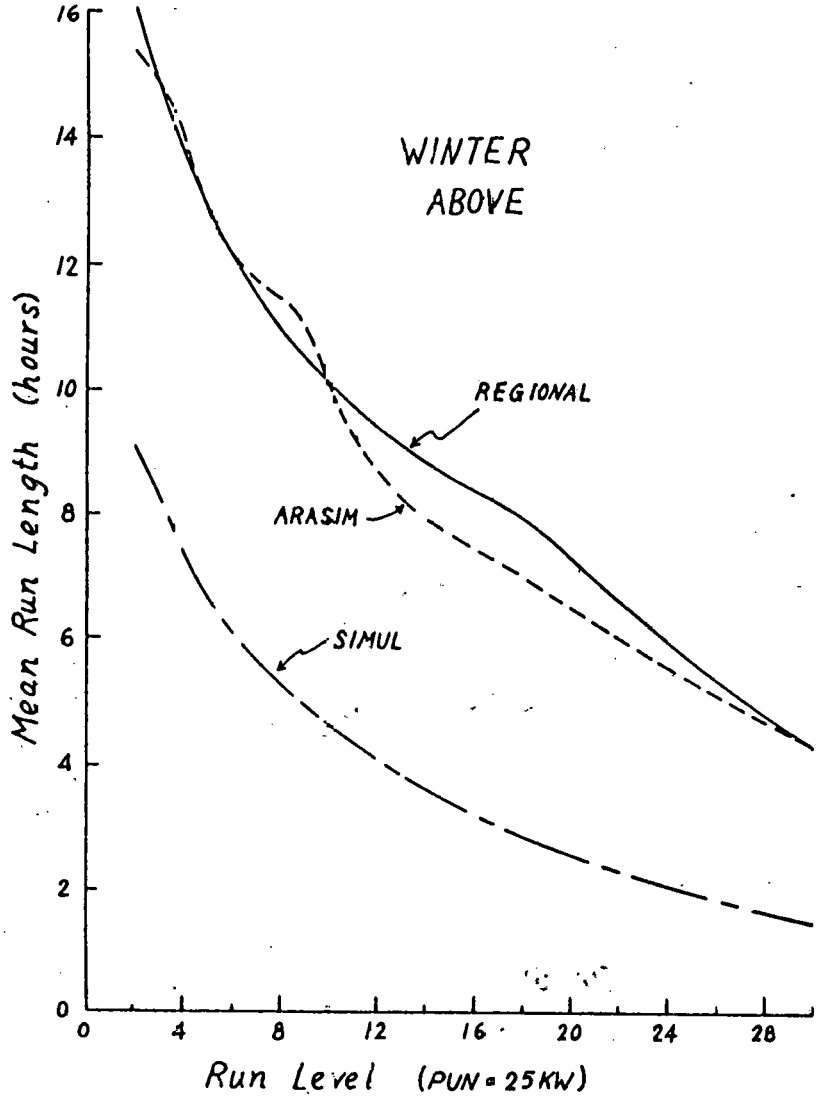

FIGURE 4.9a Mean Run Lengths Above Fixed Run Levels for MOD 0A (200 KW) in Northern Illinois for Winter Season.

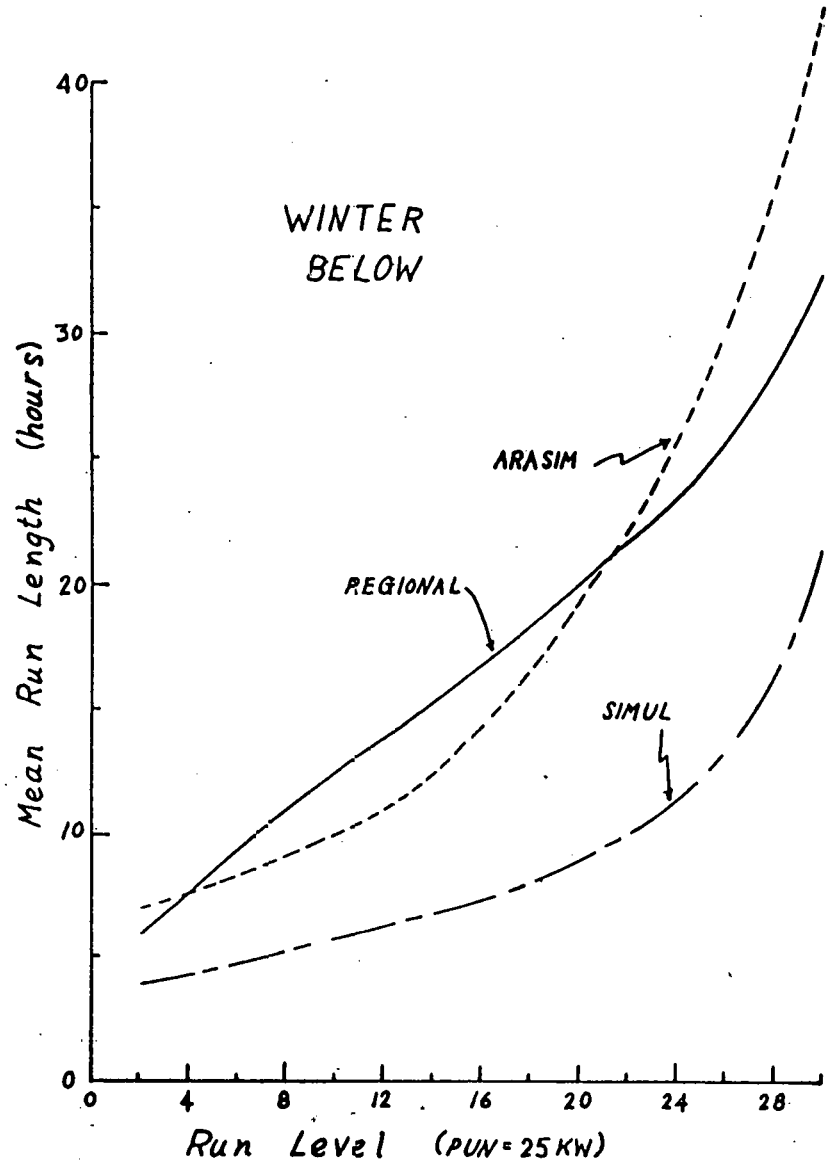

FIGURE 4.9b Mean Run Lengths Below Fixed Run Levels for MOD 0A (200 KW) in Northern Illinois for Winter Season.

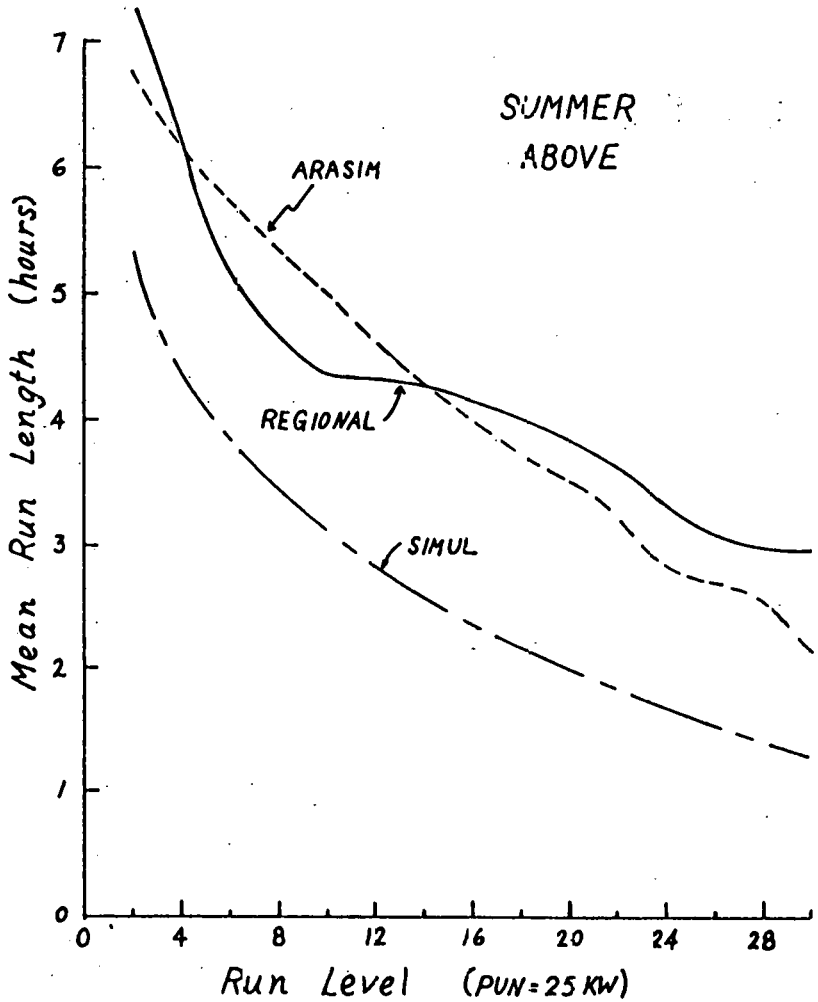

FIGURE 4.9c Mean Run Lengths Above Fixed Run Levels for MOD 0A (200 KW) in Northern Illinois for Summer Season.

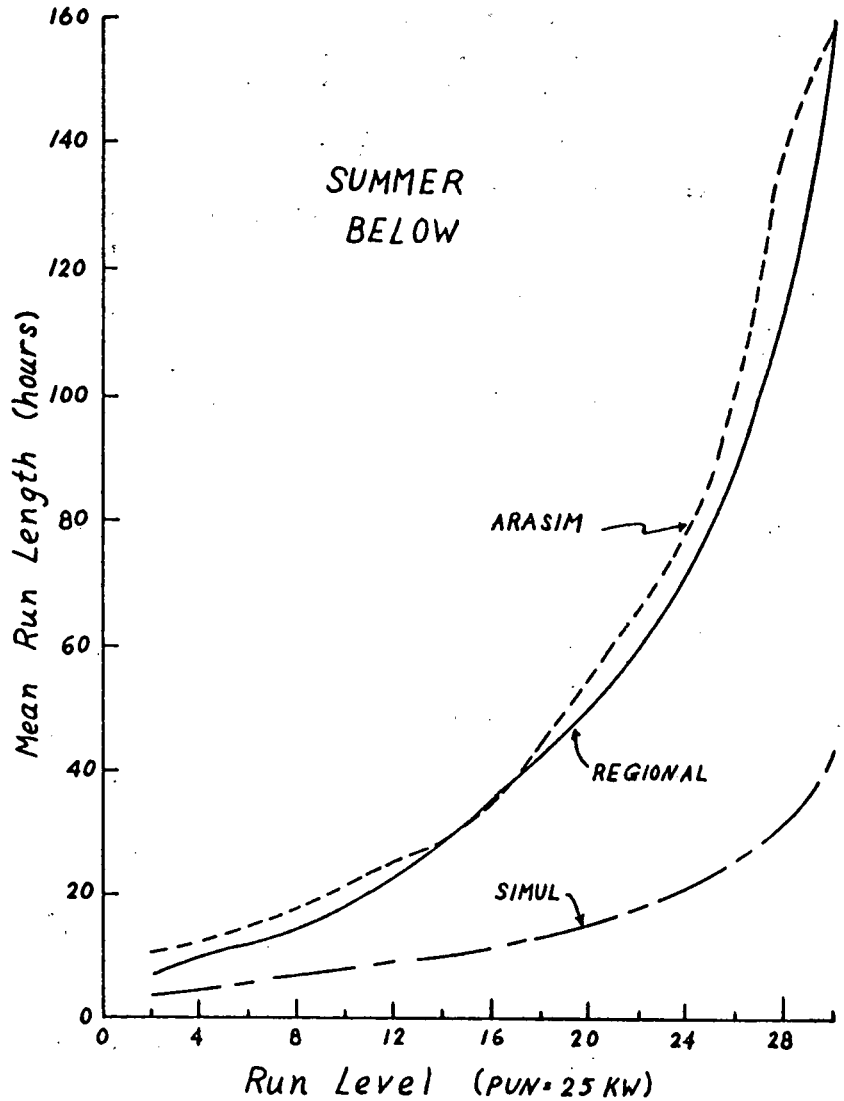

FIGURE 4.9d Mean Run Lengths Below Fixed Run Levels for MOD 0A (200 KW) in Northern Illinois for Summer Season.

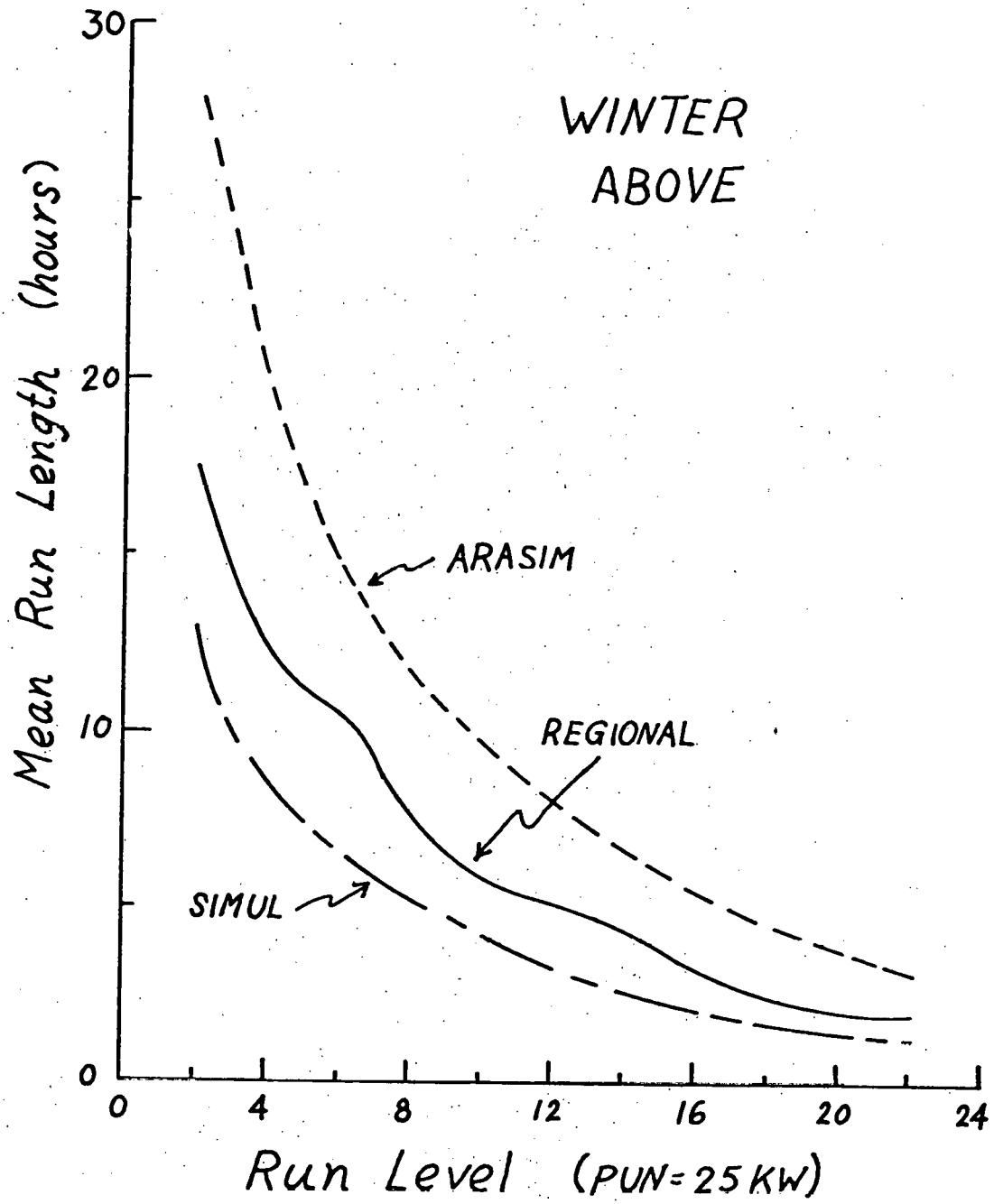

FIGURE 4.10a Mean Run Lengths Above Fixed Run Levels for MOD 0A (200 KW) in Wyoming Region for Winter Season.

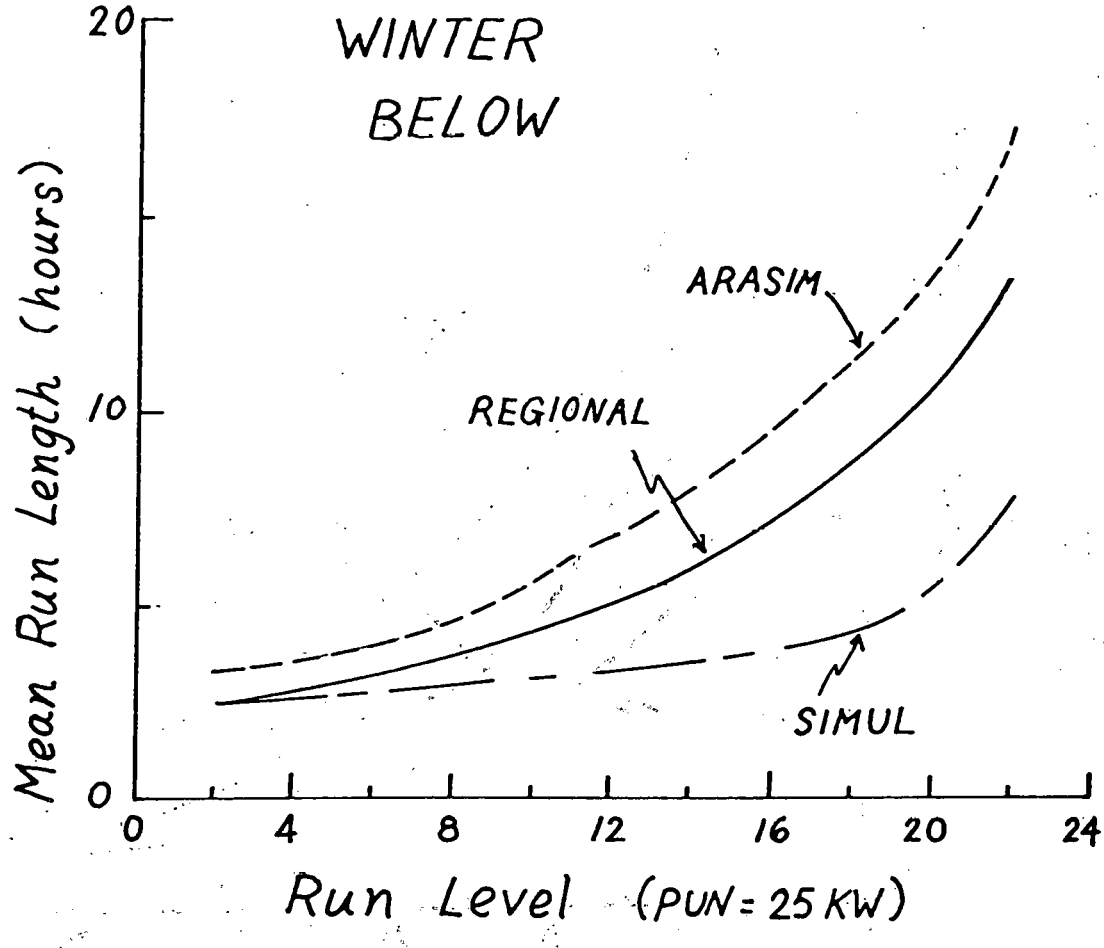

FIGURE 4.10b Mean Run Lengths Below Fixed Run Levels for MOD 0A (200 KW) in Wyoming Region for Winter Season.

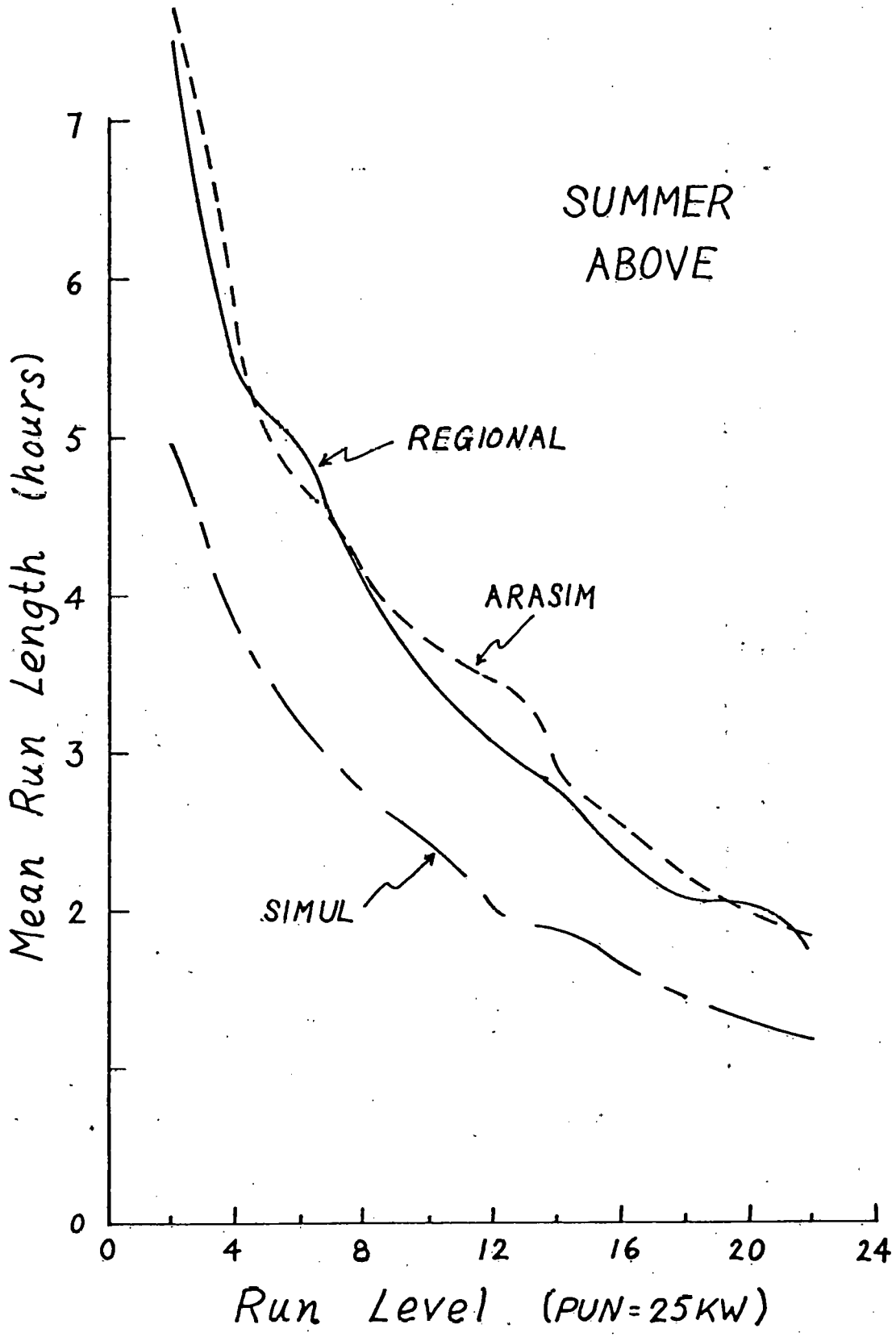

FIGURE 4.10c Mean Run Lengths Above Fixed Run Levels for MOD 0A (200 KW) in Wyoming Region for Summer Season.

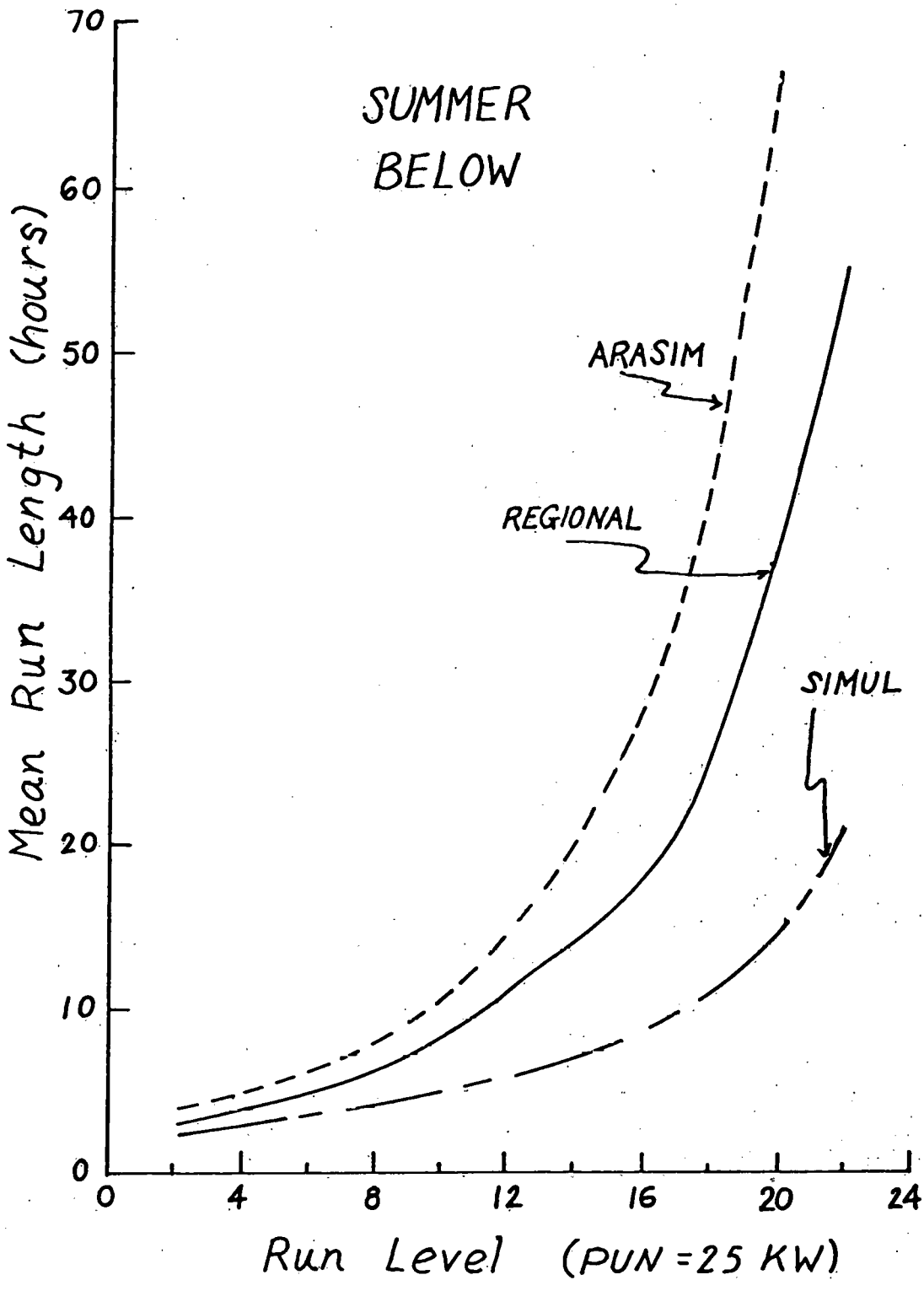

FIGURE 4.10d Mean Run Lengths Below Fixed Run Levels for MOD 0A (200 KW) in Wyoming Region for Summer Season.

CHAPTER 5

BAYESIAN WIND SPEED DISTRIBUTION

5.1 INTRODUCTION TO BAYESIAN ANALYSIS

The classical approach to parameter estimation is based on the assumption that the parameters are unknown constants. The estimators, which are obtained using only sample statistics, lead to confidence intervals to express the range of errors. Estimation using only observed data may be limiting, especially when intuitive or subjective information is available since there exists no formal basis for its incorporation using classical methods. Such problems can be treated rigorously using Bayesian analysis.

The Bayesian approach to parameter estimation is to model the unknown parameters as random variables. Through Bayes' theorem, the uncertainty associated with the estimated parameters can be formally combined with the inherent randomness of the basic random variable. Using this approach, information based on previous experience and sampling can be combined systematically to provide a more realistic distribution of the basic random variable.

A common situation is one in which the underlying probability distribution of a basic random variable, denoted by X, is known with a high degree of certainty, but has parameters which are not precisely known. The unknown parameters will be denoted by θ and considered a single parameter for simplicity. The first step is to treat θ as a random variable and choose a prior distribution of θ, $f'_{\theta}(\theta)$, which best quantifies all available intuitive and judgemental beliefs. Now if

the outcome of n observations of the random variable, X, becomes available, then the posterior distribution of θ, $f''_\theta(\theta)$ can be obtained from Bayes' theorem (Benjamin and Cornell, 1970) as follows:

$$f''_\theta(\theta) = N \cdot L(\theta/x_1, x_2, \ldots : x_n) \cdot f'_\theta(\theta) \tag{5.1}$$

where N = a normalizing constant

$L(\theta/x_1, x_2, \ldots x_n)$ = Likelihood of the sample given θ

$f'_\theta(\theta)$ = Prior distribution of θ

$f''_\theta(\theta)$ = Posterior distribution of θ given the sample observations $x_1, x_2, \ldots\ldots x_n$

For the sampling process which involves n independent observations of the random variable, X, the likelihood function can be written as

$$L(\theta/x_1, x_2, \ldots\ldots x_n) = \prod_{i=1}^{n} f_X(x_i/\theta) \tag{5.2}$$

Equation (5.1) can now be written in the form

$$f''_\theta(\theta) = N \cdot \prod_{i=1}^{n} f_X(x_i/\theta) \cdot f'_\theta(\theta) \tag{5.3}$$

where, $f_X(x_i/\theta)$ = Probability distribution of the basic random variable, X given θ

In the above expression, it is assumed that both the prior and posterior distributions of θ are continuous. A similar expression is applicable when a discrete probability mass function is assumed for the prior. When the number of observations is relatively large, i.e., in comparison with information upon which the prior is based, then the prior distribution is termed diffuse. The resulting posterior distribution is virtually free of the prior information and is said to be data-based.

The posterior distribution of θ deals with the statistical uncertainty in the parameter of the modelled distribution of the basic random variable, X. The distribution of X presents the inherent uncertainty in the value of the random variable, which can be combined with the uncertainty of the parameter, θ, to obtain a compound or Bayesian distribution of X. This distribution will have a larger variance than that for the modelled distribution alone, since it contains both the statistical and inherent uncertainties.

5.2 BAYESIAN DISTRIBUTION OF WIND SPEED

The basic random variable, i.e., the wind speed, V, has been modelled by a Rayleigh distribution, which is of the form

$$f_V(v) = (\pi/2 \cdot m^2) \cdot v \cdot \exp(-\pi \cdot v^2/4 \cdot m^2) \qquad (5.4)$$

The mean wind speed, m, is a parameter of the Rayleigh distribution and is approximated by a random variable which will be denoted M. M is assumed to behave as a random variable with its own prior distribution, $f'_M(m)$. The choice of the prior is very important, and the following criteria are generally used:

- The distribution should be mathematically tractable to allow the posterior to be easily determined, i.e., obtainable in a closed form given the prior and the sample data.
- The distribution should be flexible enough to be capable of expressing the user's prior information and beliefs.
- The parameters of the distribution should be readily interpretable.

A frequently used method of satisfying the above conditions is to choose a form of the prior distribution for the parameter that is proportional to the kernal of the likelihood function, i.e., the portion obtained by neglecting the factors independent of the parameter. Such a prior which is compatible with the sample likelihood function is termed a conjugate prior distribution. Also, the use of a conjugate prior ensures a posterior distribution that is of the same form as the prior.

The Rayleigh distribution of wind speed can be written as a special form of the Weibull probability density function,

$$f_V(v) = (c/\alpha) \cdot (v/\alpha)^{c-1} \cdot \exp(-(v/\alpha)^c) \qquad (5.5)$$

where, $v > 0$

$c = 2$ (shape parameter)

$\alpha = 2\ m/\sqrt{\pi}$

Let $\lambda = \alpha^{-c} = \alpha^{-2} = \pi/4\ m^2$. Substituting in (5.5) yields

$$f_V(v) = 2 \cdot \lambda \cdot v \cdot e^{-\lambda v^2} \qquad (5.6)$$

The likelihood function for λ given n observations of the wind speed is $L(\lambda/v_1,v_2,\ldots v_n) = \lambda^n \cdot 2^n \cdot \exp(-\lambda \sum_{i=1}^{n} v_i^2)$. The kernal of this function (i.e., factors dependent on λ) is used to find a natural conjugate prior distribution for the parameter λ, assumed to be a random variable. A prior distribution similar in form and proportional to the kernal of the likelihood function is the Gamma-1 probability density function

$$f'_{\lambda}(\lambda/r', y) = \frac{y^{r'} \cdot \lambda^{r'-1} \cdot e^{-\lambda y}}{(r' - 1)!} \tag{5.7}$$

where, r' and y are the shape and scale parameters, respectively, and $(r' - 1)!$ is to be interpreted as $\Gamma(r')$ when r' is non-integer.

A parameter of greater interest than λ is the mean wind speed, since it is recognizable and more easily characterized. A prior distribution for the mean wind speed, M, which will be a natural conjugate of the Rayleigh distribution is derived from the Gamma-1 distribution of λ.

$$\lambda = \frac{\pi}{4m^2} \tag{5.8}$$

Therefore $$\frac{d\lambda}{dm} = \frac{-\pi}{2m^3} \tag{5.8a}$$

The derived distribution of M is given by

$$f'_{M}(m) = f\ (\pi/4m^2) \cdot \left|\frac{d\lambda}{dm}\right| \tag{5.9a}$$

which can be evluated using (5.7) and (5.8a):

$$f'_{M}(m) = \frac{y^{r'} \cdot (\pi/4m^2)^{r'-1} \cdot \exp(-\pi y/4m^2))}{(r' - 1)!} \cdot \frac{\pi}{2m^3}$$

$$= \frac{2 \cdot (\pi \cdot y/(4m^2)^{r'} \cdot \exp(-\pi y/(4m^2))}{m \cdot (r' - 1)!} \tag{5.9b}$$

Letting $y' = (\pi y/4)$ in the above expression gives the final form of the prior distribution of the mean wind speed,

$$f'_{M}(m) = \frac{2}{\sqrt{y'}} \cdot \frac{(y'/m^2)^{r'+1/2} \cdot \exp(-y'/m^2)}{(r' - 1)!} \tag{5.10}$$

The posterior distribution of the mean after n observations of

the wind speed is of the form given by 5.3, i.e.

$$f_M''(m) = N \cdot \prod_{i=1}^{n} f_V(v|m) \cdot f_M'(m) \tag{5.11}$$

where N = Normalizing constant $= \left(\int_0^\infty \prod_{i=1}^{n} f_V(v|m) \cdot f_M'(m)\, dm\right)^{-1}$

$$\prod_{i=1}^{n} f_V(v|m) = \prod_{i=1}^{n} v_i \cdot \exp\left((-\pi/4m^2) \sum_{i=1}^{n} v_i^2\right) \tag{5.12a}$$

Cancelling terms and letting $y_1 = \frac{\pi}{4} \cdot \sum_{i=1}^{n} v_i^2$ yields

$$f_M''(m) = \frac{(1/m^2)^{n+r'+1/2} \cdot \exp(-y_1 + y')/m^2)}{\int (1/m^2)^{n+r'+1/2} \cdot \exp(-y_1 + y')/m^2)\, dm} \tag{5.12b}$$

By letting $r'' = n + r' + 1/2$ and $y'' = y_1 + y'$, this becomes

$$f_M''(m) = \frac{(1/m^2)^{r''} \cdot \exp(-y''/m^2)}{(1/y'')^{r''} \int_0^\infty (y''/m^2)^{r''} \cdot \exp(-y''/m^2)\, dm} \tag{5.13}$$

and by letting $t = m^2$, one obtains

$$f_M''(m) = \frac{(1/m^2)^{r''} \cdot \exp(-y''/m^2)}{(1/y'')^{r''} \cdot 1/2y''^{-1/2} \int_0^\infty (y''/t)^{r''+1/2} \cdot \exp(-y''/t)\, dt} \tag{5.14}$$

On solving the integral, this becomes

$$f_M''(m) = \frac{(1/m^2)^{r''} \cdot \exp(-y''/m^2)}{1/2 \cdot (1/y'')^{r''+1/2} \cdot (r'' + 1/2 - 2)! \cdot y''} \tag{5.15}$$

Upon further simplification, the final form of the posterior distribution of the mean wind speed is given by

$$f_M''(m) = \frac{2}{(y'')^{1/2}} \cdot \frac{(y''/m^2)^{r''} \cdot \exp(-y''/m^2)}{(r'' - 3/2)!} \tag{5.16}$$

The posterior distribution of the mean wind speed contains both the prior information and the observed data. This can now be formally combined with the modelled Rayleigh distribution of the wind speed to obtain the Bayesian distribution of the wind speed

$$f_V^*(v) = \int_0^\infty f_V(v|m) \cdot f_M''(m)\, dm$$

$$= \int_0^\infty \frac{\pi}{2m^2} \cdot v \cdot \exp(-\pi v^2/4m^2) \cdot$$

$$\cdot \frac{2}{(y'')^{1/2}} \cdot \frac{(y''/m^2)^{r''} \cdot \exp(-y''/m^2)}{(r'' - 3/2)!}\, dm \qquad (5.17)$$

Rearranging, this becomes

$$f_V^*(v) = \frac{\pi \cdot v \cdot (y'')^{r'' - 1/2}}{(r'' - 3/2)!} \cdot \int_0^\infty (1/m^2)^{r''+1}$$

$$\cdot \exp(-\pi v^2/4m^2 - y''/m^2)\, dm \qquad (5.17a)$$

by letting $A = (\pi v^2/4 + y'')$, this becomes

$$f_V^*(v) = \frac{\pi \cdot v \cdot (y'')^{r'' - 1/2}}{(r'' - 3/2)!} \cdot \int_0^\infty (1/m^2)^{r''+1} \cdot \exp(-A/m^2)\, dm \qquad (5.18)$$

and by multiplying and dividing by $A^{r'' + 3/2}$ and letting $t = m^2$, one obtains

$$= \frac{\pi \cdot v \cdot (y'')^{r''- 1/2}}{(r'' - 3/2)!} \cdot (1/A)^{r''+1} \cdot 1/2\, A^{-1/2} \int_0^\infty (A/t)^{r''+ 3/2}$$

$$\cdot \exp(-A/t)\, dt \qquad (5.19)$$

On solving the integral, this becomes

$$f_V^*(v) = \frac{\pi \cdot v \cdot (y'')^{r''-1/2}}{(r''-3/2)!} \cdot (1/A)^{r''+3/2} \cdot (r''-1/2)! \cdot A \qquad (5.20)$$

Further simplification leads to the final form of the Bayesian distribution of the wind speed,

$$f_V^*(v) = \frac{\pi \cdot v \cdot (y'')^{r''-1/2}}{2 \cdot (\pi v^2/4 + y'')^{r''+1/2}} \cdot (r''-1/2) \qquad (5.21)$$

Equation (5.21) is free of the mean wind speed, M, which served as the parameter of the original Rayleigh distribution. It is a function of r'' and y'', the modified shape and scale parameters, respectively, of the posterior distribution of the mean wind speed.

5.3 APPLICATIONS

The distribution of the mean wind speed that is chosen prior to the observations of the wind speed at a site is dictated by subjective judgment about the nature of the mean. The probability density of the prior distribution with parameters r' and y' is given by Equation (5.10) below

$$f_M'(m|r',y') = \frac{2}{(y')^{1/2}} \cdot \frac{(y'/m^2)^{r'+1/2} \cdot \exp(-y'/m^2)}{(r'-1)!} \qquad (5.10)$$

The mean and variance of this distribution are given by

$$E(M) = \frac{y'^{1/2} \cdot (r'-3/2)!}{(r'-1)!} \qquad (5.22)$$

$$\text{Var}(M) = \frac{y' \, (r' - 2)! \, (r' - 1)! - (r' - 3/2)!}{(r' - 1)!)^2} \qquad (5.22b)$$

Subjective judgment about either the mean or the variance of the mean wind speed can be used in Equations (5.22a) and (5.22b), which will enable prior information to be quantified in terms of the parameters, r' and y', of the prior distribution. This form of the prior distribution is very flexible and allows even limited information to be expressed by properly choosing r' and y'.

Example

Assume that the prior estimate of the mean wind speed at a site is 4.7 m/s. Equation (5.22a) can be applied to obtain a relation between the parameters r' and y'. Further, if information about the variance, σ^2, is known, such as $\sigma^2 = 3(\text{m/s})^2$, Equation 5.22b can be used as well. This yields values of $r' = 3$ and $y' = 50$, which fully characterizes the prior distribution of the mean and is written below:

$$f'_M(m \mid r' = 3, \; y' = 50) = 1.25 \times 10^5 \cdot (1/m^2)^{3.5} \cdot \exp(-50/m^2) \qquad (5.23)$$

Suppose now just one observation of the process (i.e., the wind speed) becomes available, viz. $v_1 = 4.5$ m/s. The posterior distribution of the mean wind speed, M, is given by Equation (5.16)

$$f''_M(m) = \frac{2}{(y'')^{1/2}} \cdot \frac{(y''/m^2)^{r''} \cdot \exp(-y''/m^2)}{(r'' - 3/2)!} \qquad (5.16)$$

where, $r'' = n + r' + 1/2$

$= 1 + 3 + 1/2 = 4.5$

$$y'' = \frac{\pi}{4} \cdot \sum_{i=1}^{n} v_i^2 + y'$$

$$= \frac{\pi}{4} \cdot (4.5)^2 + 50 = 65.9043$$

The posterior distribution can now be written as

$$f_M''(m|r'' = 4.5,\ y'' = 65.9043) = 6.2883 \times 10^6 \cdot (1/m^2)^{4.5} \cdot \exp(-65.9043/m^2) \qquad (5.24)$$

Instead of just one observation, suppose the following 10 observations of the wind speed in meters per second were taken at the same site as before:

4.5, 4.9, 6.8, 7.1, 5.2, 5.9, 6.2, 6.0, 5.6, 5.8

Then, $r'' = 10 + 3 + 1/2 = 13.5$ (5.25a)

$$y'' = (\pi/4) \cdot 342.2 + 50 = 318.7632 \qquad (5.25b)$$

The posterior distribution can now be written for this case as

$$f_M''(m|r'' = 13.5,\ y'' = 318.7632) = 1.4648 \times 10^{24} \cdot (1/m^2)^{13.5} \cdot \exp(-318.7632/m^2) \qquad (5.26)$$

Consider the case where the following fifty observations of the process are available as speed in meters per second:

4.5, 4.9, 6.8, 7.1, 5.2, 5.9, 6.2, 6.0, 5.6, 5.8,
5.3, 5.3, 5.9, 6.2, 6.0, 6.0, 6.2, 6.5, 4.8, 4.9,
5.2, 4.9, 4.5, 4.3, 4.9, 4.9, 4.8, 6.0, 5.6, 6.0, $\bar{v} = 5.808$
6.5, 6.7, 5.8, 5.9, 5.6, 5.4, 6.0, 6.4, 6.7, 5.9
5.7, 5.9, 6.9, 7.1, 7.2, 7.2, 7.0, 6.5, 5.0, 4.8

For this set of observations,

$r'' = 50 + 3 + 1/2 = 53.5$ (5.27a)

$$y'' = (\pi/4) \cdot 1716.64 + 50 = 1398.2458 \qquad (5.27b)$$

The posterior distribution using these parameters is given by

$$f_M''(m \mid r'' = 53.5,\ y'' = 1398.2458) = 1.2892 \times 10^{99} \cdot (1/m^2)^{53.5} \cdot \exp(-1398.2458/m^2) \qquad (5.28)$$

The prior distribution (Eq.(5.23)) and the posterior distributions of each case (Eqs. (5.24),(5.26) and(5.28)) have been sketched in Fig. 5.1.

Once the posterior distribution has been obtained, the Bayesian distribution of the wind speed, $f_V^*(v)$ can be determined from Eq. 5.21:

$$f_V^*(v) = \frac{\pi \cdot v \cdot (y'')^{r''} - 1/2 \cdot (r'' - 1/2)}{2 \cdot ((\pi v^2/4) + y'')^{r'' + 1/2}}$$

Case 1: Before sampling, i.e., when n = 0;

$$r'' = n + r' + 1/2 = r' + 1/2 = 3.5 \qquad (5.29a)$$

$$y'' = y' = 50 \qquad (5.29b)$$

Substituting in Eq.(5.21) yields,

$$f_V^*(v) = \frac{5.8905 \times 10^5 \cdot v}{(0.785\ v^2 + 50)} \qquad (5.30)$$

Case 2: After 1 observation of the wind speed, i.e. n = 1:

$r'' = 4.5$, $y'' = 65{,}9043$. Substituting in Eq.(5.21) gives

$$f_V^*(v) = \frac{1.1853 \times 10^8 \cdot v}{(0.785\ v^2 + 65.9043)} \qquad (5.31)$$

Case 3: After 10 observations of the process, i.e., n = 10:

Substitution of $r'' = 13.5$ and $y'' = 318.7632$ in Eq.(5.21) gives

$$f_V^*(v) = \frac{7.1639 \times 10^{33} \cdot v}{(0.787\ v^2 + 318.7632)} \qquad (5.32)$$

Case 4: After 50 observations of the process, i.e., n = 50:

$r'' = 53.5$, $y'' = 1398.2458$. Substituting in Eq.(5.21) yields

$$f_V^*(v) = 0.05954 \cdot v \cdot \left| \frac{1398.2458}{0.785\, v^2 + 1398.2458} \right| \qquad (5.33)$$

The Bayesian distributions of the wind speed given by Eqs. (5.30), (5.31),(5.32)and(5.33)are shown in Fig.5.2.

From procedures reported earlier, the number of equivalent independent hours of data per day upon which are based the observed statistics is given by

$$N_{hrs/day} = \frac{\sigma_{hr}^2}{\sigma_{day}^2} \qquad (5.34)$$

where, σ_{hr}^2 = variance of hourly speed

σ_{day}^2 = variance of daily average speed

Similarly the number of independent hours per month is given by

$$N_{hrs/month} = \frac{\sigma_{hour}^2}{\sigma_{month}^2} \qquad (5.35)$$

where, σ_{month}^2 = variance of monthly average speed

The calculation of equivalent independent readings gave approximately 2-3 hours per day and 50-64 hours per month. This suggests that 14-21 independent hours per week or 150-200 hours per season would be obtained from hourly data records.

If in the above example, the samples of wind speed at a site are

hourly records, then 10 independent hourly observations (n = 10) is equivalent to sampling for approximately one week and 50 independent observations (n = 50) is equivalent to sampling for approximately one month.

The process of obtaining a posterior distribution of the mean wind speed after one observation is nothing but an updating of the prior distribution with the new information. Thus, each posterior distribution can be thought of as an updated prior for the subsequent set of observations. This process is seen in Fig. 5.1 as a shifting of each posterior distribution to the right, i.e., in a direction strongly influenced by each new data set. Further, the posterior after 50 observations also shows a lesser spread than the posterior after 10 observations, whose spread is less than that of the posterior after just one observation. If 150-200 observations (representing a whole season) were used, the posterior would most likely show a sharp peak with a very small spread about the mean of the observations. A whole year's equivalent data (approximately 600-800) would yield a posterior with an even lesser spread, a very sharp peak, and be almost totally data-based. In a similar manner, Fig. 5.2 shows a continuous updating of the Bayesian distribution of wind speed with an increase in the number of observations. When the number of independent observations of wind speed is equivalent to that of a year (i.e., approximately 600-800), the Bayesian distribution of wind speed will approximate a Rayleigh distribution obtained using only the observational data. However, the Bayesian distribution will have a larger variance since it contains the uncertainty in the mean as well as elements of the assumed prior. Additional data from subsequent years will continue to reduce the uncertainty in the mean.

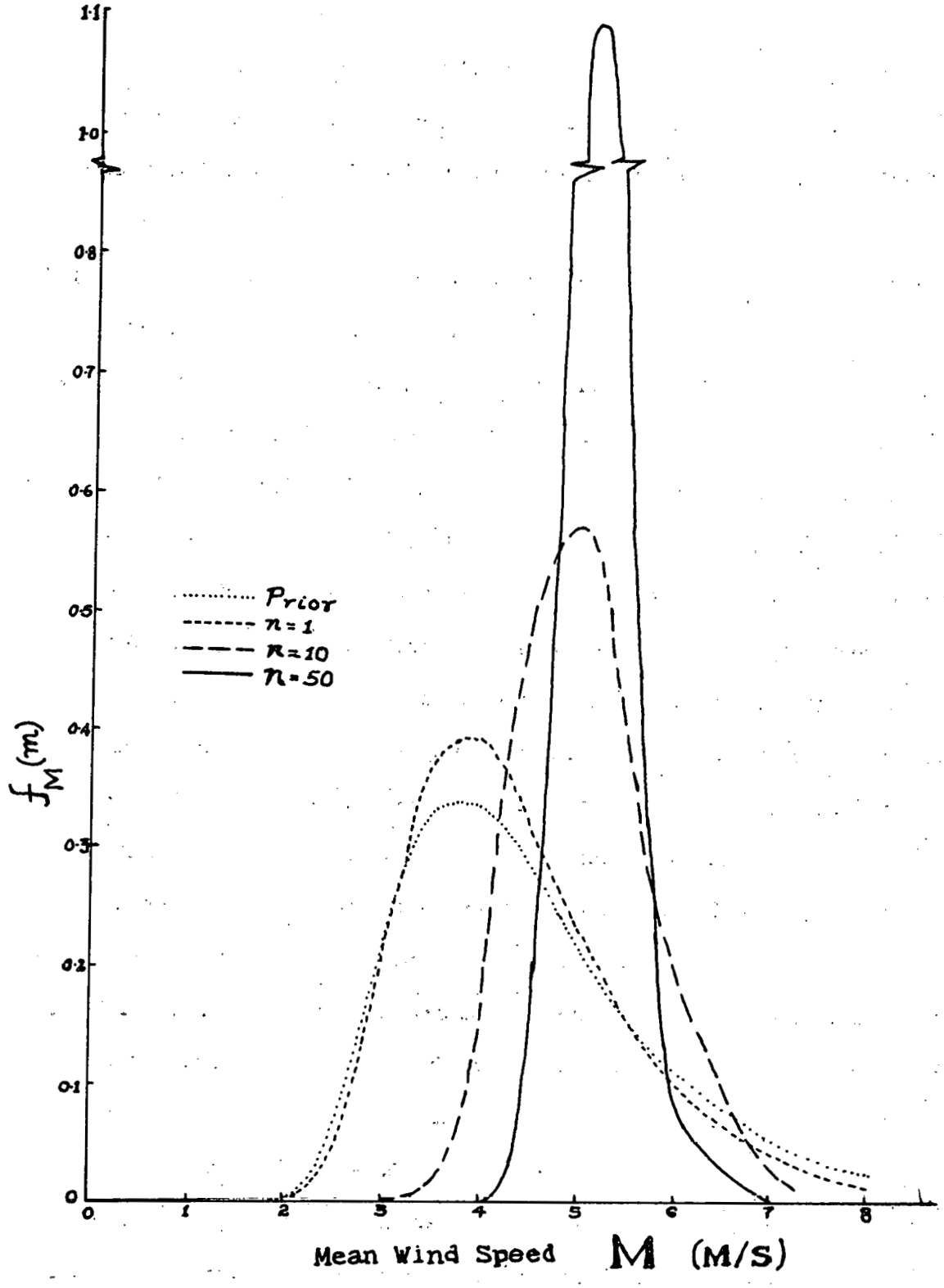

FIGURE 5.1 Prior and Posterior Distribution of Mean Wind Speed.

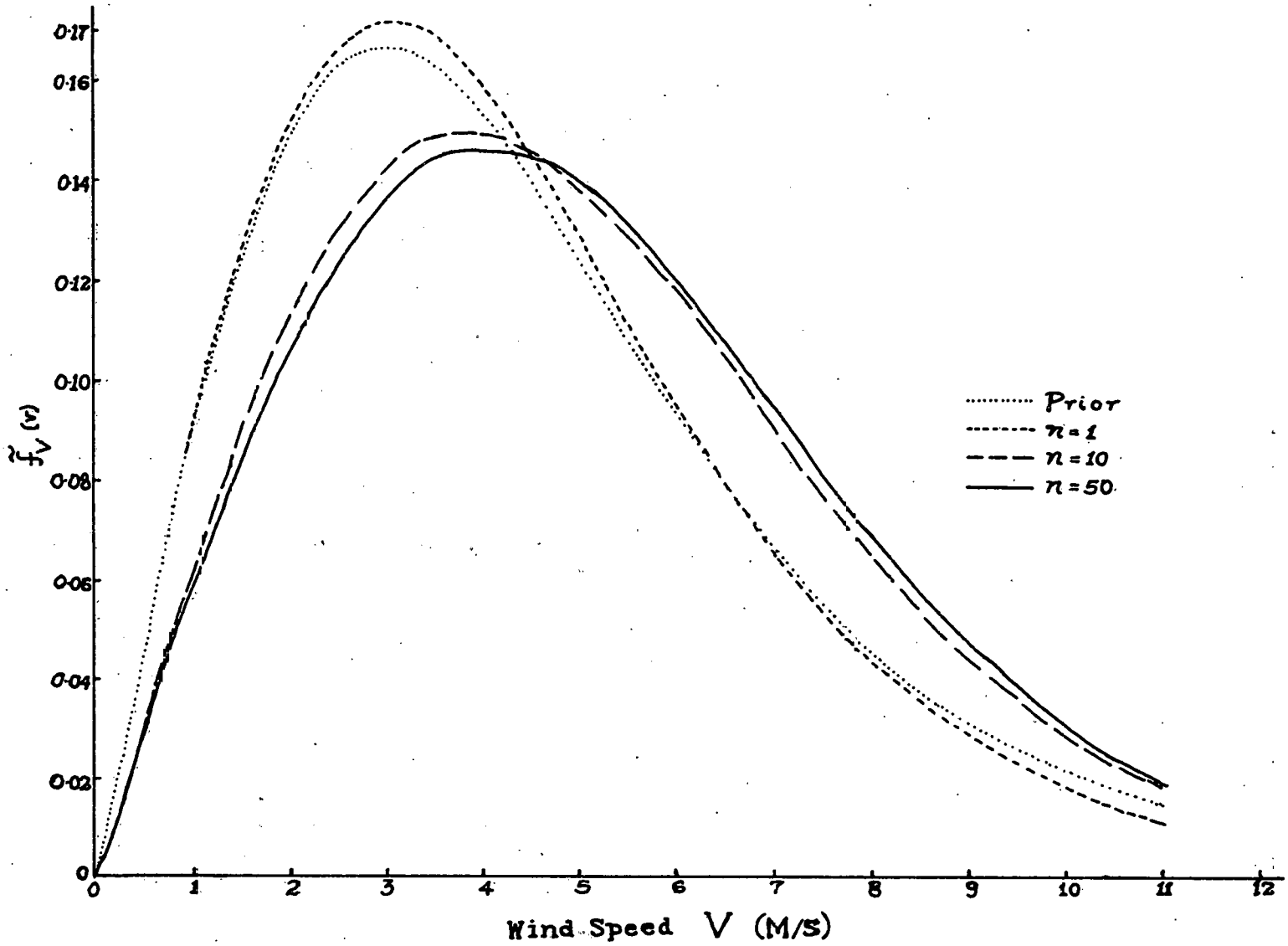

FIGURE 5.2 Bayesian Distribution of Wind Speed

CHAPTER 6

ADDITIONAL ANALYSIS OF NATIONAL WEATHER SERVICE SITES

6.1 ANALYSIS OF NEW DATA

In order to validate models from previous reports (Corotis, 1976, 1977, 1979), hourly wind data were obtained from eight relatively windy sites throughout the U.S. and five clustered sites in New Hampshire. A summary of the sites is given in Appendix G. All records consist of one-minute average wind speeds sampled once an hour.

Table 6.1 gives the summary of wind statistics for all the sites. The hourly standard deviations are high, except for Cape Hatteras, as compared to the Rayleigh standard deviation of 52% of the mean. Three sites in New Hampshire (Manchester, Lebanon and West Lebanon) have extremely high standard deviations relative to the mean, with the coefficient of variation exceeding 100% (actually the last two sites are essentially the same location).

The number of equivalent independent readings for the sites is shown in Table 6.2. The number of independent hours per day was determined from a variance analysis using WINDATB (Corotis, 1977) and ranges from 1.7 to 3.9 for the winter; from 1.9 to 4.2 in the spring; from 1.9 to 4.2 in the summer and from 1.7 to 4.3 in the fall. These values are consistent with the general guidelines of 2-4 found for previous sites. From an autocorrelation analysis using AUTOCOR (Corotis, 1976), the number of independent days per month is seen from Table 6.2 to be in the range of 10 to 25 days in the winter; 12 to 28 days in the spring; 17 to 30 days in the summer and 10 to 24 days in

TABLE 6.1 Summary of Wind Statistics

SITE	SEASON	WIND SPEED (m/s)	HOURLY STD. DEV. (m/s)	COEFF. OF VARIATION
Livingston Montana 1948 - 1954	Winter	8.51	5.22	0.61
	Spring	5.80	3.36	0.58
	Summer	4.81	3.05	0.63
	Fall	7.73	4.83	0.62
Dunkirk New York 1949 - 1953	Winter	5.98	3.69	0.62
	Spring	4.56	3.06	0.67
	Summer	4.16	2.57	0.62
	Fall	5.80	3.27	0.56
Cape Hatteras North Carolina 1957 - 1964	Winter	5.63	2.50	0.44
	Spring	5.26	2.14	0.41
	Summer	4.65	2.10	0.45
	Fall	5.14	2.40	0.47
Dalhart Texas 1948 - 1954	Winter	6.83	3.88	0.57
	Spring	7.35	3.96	0.54
	Summer	6.27	3.07	0.49
	Fall	6.16	3.39	0.55
Laguardia New York 1948 - 1961	Winter	5.20	2.65	0.51
	Spring	5.57	2.83	0.51
	Summer	5.22	2.69	0.51
	Fall	5.56	2.86	0.51
North Platte Nebraska 1948 - 1964	Winter	5.11	3.04	0.59
	Spring	4.92	2.93	0.60
	Summer	5.22	3.12	0.60
	Fall	4.83	2.89	0.60
Mount Shasta California 1950 - 1951	Winter	3.72	2.48	0.67
	Spring	3.29	2.38	0.72
	Summer	3.75	2.57	0.69
	Fall	3.44	2.42	0.70

TABLE 6.1 Summary of Wind Statistics (continued)

SITE	SEASON	MEAN SPEED (m/s)	HOURLY STD. DEV. (m/s)	COEFF. OF VARIATION
Blue Canyon California 1948 - 1951	Winter	4.81	3.05	0.63
	Spring	4.61	3.09	0.67
	Summer	5.00	3.07	0.61
	Fall	4.88	2.99	0.61
Concord New Hampshire 1948 - 1964	Winter	3.40	2.58	0.76
	Spring	3.05	2.28	0.75
	Summer	2.29	1.89	0.82
	Fall	2.75	2.36	0.86
Manchester New Hampshire 1951 - 1967	Winter	2.48	2.65	1.07
	Spring	2.26	2.38	1.06
	Summer	2.04	2.21	1.08
	Fall	2.17	2.32	1.07
Portsmouth New Hampshire 1956 - 1974	Winter	3.91	2.75	0.70
	Spring	3.49	2.33	0.67
	Summer	2.85	1.94	0.68
	Fall	3.36	2.45	0.73
Lebanon New Hampshire 1959 - 1964	Winter	2.35	2.49	1.06
	Spring	2.42	2.45	1.01
	Summer	1.81	2.21	1.22
	Fall	1.95	2.39	1.23
W. Lebanon New Hampshire 1949 - 1958	Winter	2.44	2.65	1.09
	Spring	2.56	2.55	1.00
	Summer	1.94	2.29	1.18
	Fall	2.11	2.47	1.17

TABLE 6.2 Equivalent Independent Readings

SITE	WINTER			SPRING			SUMMER			FALL		
	HR/ DAY	DAY/ MONTH	DURA-TION (MTHS)	HR/ DAY	DAY/ MONTH	DURA-TION (MTHS)	HR/ DAY	DAY/ MONTH	DURA-TION (MTHS)	HR/ DAY	DAY/ MONTH	DURA-TION (MTHS)
Livingston Montana 1948 - 1954	1.7	18.5	3.3	2.5	24.0	1.5	3.3	22.1	1.5	1.7	16.7	3.7
Dunkirk New York 1949 - 1953	1.9	17.3	3.1	2.1	21.9	2.7	2.1	24.2	2.0	2.0	17.0	2.6
Cape Hatteras North Carolina 1957 - 1964	1.9	15.8	1.8	1.9	18.9	1.2	1.9	18.0	1.7	1.7	13.7	2.6
Dalhart Texas 1948 - 1954	2.4	25.3	1.4	2.6	23.4	1.3	2.8	25.5	0.9	2.5	24.1	1.4
Laguardia New York 1948 - 1961	3.1	9.8	2.3	2.9	17.9	1.3	3.0	17.3	1.4	3.0	10.1	2.3
North Platte Nebraska 1948 - 1964	3.9	11.5	2.1	4.2	12.3	1.8	3.9	18.4	1.3	4.3	12.1	1.9
Mount Shasta California 1950 - 1951	3.7	13.9	2.3	3.7	16.5	2.3	3.5	26.1	1.4	4.1	12.6	2.6

TABLE 6.2 Equivalent Independent Readings (continued)

SITE	WINTER			SPRING			SUMMER			FALL		
	HR/ DAY	DAY/ MONTH	DURA-TION (MTHS)	HR/ DAY	DAY/ MONTH	DURA-TION (MTHS)	HR/ DAY	DAY/ MONTH	DURA-TION (MTHS)	HR/ DAY	DAY/ MONTH	DURA-TION (MTHS)
Blue Canyon California 1948 - 1951	2.4	12.7	3.6	2.1	28.3	2.0	2.4	30.4	1.4	2.3	13.1	3.3
Concord New Hampshire 1948 - 1964	2.1	19.5	3.8	3.4	21.0	2.1	4.2	17.1	2.5	2.2	21.0	4.4
Manchester New Hampshire 1951 - 1967*	2.3	15.9	8.8	3.2	18.9	5.0	3.5	20.5	4.4	3.0	17.2	5.9
Portsmouth New Hampshire 1956 - 1974	1.9	19.1	3.7	2.9	20.7	2.0	3.2	22.7	1.7	2.0	18.1	3.9
Lebanon New Hampshire 1959 - 1964	2.6	23.7	5.0	4.0	18.3	3.8	4.1	21.9	4.5	2.3	19.4	8.9
W. Lebanon New Hampshire 1949 - 1958	2.3	22.5	6.2	3.5	21.0	3.7	3.8	19.2	5.2	2.6	23.4	6.2

*WINDATB Recorded From 1951 - 1967; AUTOCOR Recorded From 1951 - 1955.

the fall. These are also consistent with the previous guidelines of 10-25.

The required number of months of site data collection for 90% confidence that the observed seasonal average wind speed is within 10% of the true long-term average was computed. Except for the New Hampshire sites and the winter and fall of Livingston and Blue Canyon, a single season of data collection is adequate. For all sites except those with coefficients of variation above one, no more than two seasons of data are required.

Comparisons between the observed histograms and the Rayleigh distribution for all sites are summarized in Table 6.3 in terms of the cumulative probability at 4m/s and 10m/s. The Rayleigh fits quite well to the observed data in general, with differences in the cumulatives at 4m/s of less than 0.1 (except for the sites with coefficients of variation exceeding one). Differences at 10m/s are less than 0.04. It should be cautioned, however, that this table only provides selected information limited to the particular levels of wind speed used for comparison.

The cross-correlation values were computed for sites in the state of New Hampshire and are given in Table 6.4. The hourly, daily, monthly and annual correlation values are generally consistent with previous results (Corotis, 1979). They are slightly lower than for regions with generally smooth terrain (northern Illinois, northeast Kansas, and southeast New England) and slightly higher than for southeast Wyoming, which is quite mountainous. The annual correlation between Lebanon and Portsmouth is anomalous, and may be due to the

TABLE 6.3 Summary of Fit for the Rayleigh Model

SITE	SEASON	P[v < 4 m/s]		P[v < 10 m/s]	
		OBSERVED	RAYLEIGH	OBSERVED	RAYLEIGH
Livingston Montana 1948 - 1954	Winter	0.201	0.153	0.676	0.647
	Summer	0.451	0.421	0.947	0.967
Dunkirk New York 1949 - 1953	Winter	0.320	0.296	0.877	0.888
	Summer	0.499	0.516	0.983	0.989
Cape Hatteras North Carolina 1957 - 1964	Winter	0.253	0.341	0.963	0.926
	Summer	0.356	0.401	0.972	0.960
Dalhart Texas 1948 - 1954	Winter	0.216	0.235	0.829	0.812
	Summer	0.215	0.272	0.938	0.927
Laguardia New York 1948 - 1961	Winter	0.199	0.240	0.834	0.820
	Summer	0.367	0.422	0.886	0.862
North Platte Nebraska 1948 - 1964	Winter	0.467	0.424	0.929	0.968
	Summer	0.454	0.469	0.979	0.981
Mount Shasta California 1950 - 1951	Winter	0.507	0.574	0.987	0.995
	Summer	0.709	0.807	0.999	1.000

TABLE 6.3 Summary of Fit for the Rayleigh Model (continued)

SITE	SEASON	P[v < 4 m/s]		P[v < 10 m/s]	
		OBSERVED	RAYLEIGH	OBSERVED	RAYLEIGH
Blue Canyon California	Winter	0.444	0.417	0.996	0.966
1948 - 1951	Summer	0.606	0.640	0.999	0.998
Concord New Hampshire	Winter	0.610	0.662	0.985	0.999
1948 - 1964	Summer	0.808	0.907	0.999	1.000
Manchester New Hampshire	Winter	0.543	0.617	0.964	0.998
1951 - 1967	Summer	0.710	0.874	0.998	1.000
Portsmouth New Hampshire	Winter	0.540	0.561	0.969	0.994
1956 - 1974	Summer	0.712	0.786	0.998	1.000
Lebanon New Hampshire	Winter	0.689	0.898	0.998	1.000
1959 - 1964	Summer	0.773	0.978	1.000	1.000
W. Lebanon New Hampshire	Winter	0.694	0.878	0.995	1.000
1949 - 1958	Summer	0.766	0.963	0.999	1.000

TABLE 6.4 Cross Correlation Values in New Hampshire

SITES	WINTER			SUMMER			ANNUAL
	HOURLY	DAILY	MONTHLY	HOURLY	DAILY	MONTHLY	
Concord-Lebanon 1/1/59 - 12/31/64	0.60	0.78	0.65	0.57	0.67	0.50	0.43
Concord-Portsmouth 1/1/59 - 12/31/64	0.72	0.87	0.47	0.58	0.69	0.66	0.48
Lebanon-Portsmouth 1/1/59 - 12/31/64	0.51	0.70	0.30	0.46	0.51	0.66	-0.29
Concord-Manchester 4/1/51 - 9/30/55	0.76	0.88	0.34	0.67	0.70	0.24	0.48

anemometer change at Portsmouth.

6.2 CALIBRATION OF PERSISTENCE MODEL

Previous research (Corotis, 1979) has led to the development of a power-exponential composite probability distribution for the length of time (run duration) the wind speed remains above or below fixed wind speed levels (referred to as run levels). The cumulative distribution for run lengths in hours is given by

$$F_T(t) = \begin{cases} 1 - (t/t_0)^{1-b} & t_0 \leq t \leq t_1 \\ 1 - A\, e^{-\lambda t} & t_1 \leq t \leq \infty \end{cases} \tag{6.1}$$

in which

$$t_0 = 0.5 \text{ hours} \tag{6.2a}$$

$$t_1 = 0.5\ (0.25)^{1/(1-b)} \tag{6.2b}$$

$$A = 0.25\ e^{b-1} \tag{6.2c}$$

$$\lambda = 2(b-1)\ (0.25)^{1/(1-b)} \tag{6.2d}$$

The mean run duration consistent with Equation (6.1) is

$$m_t = 0.5\ \{\alpha^{-1}[1 - (0.25)^{\alpha}] + [b/(b-1)]\ (0.25)^{\alpha}\} \tag{6.3}$$

in which

$$\alpha = \frac{2-b}{1-b} \tag{6.4}$$

The one free parameter in the power-exponential model is b, which has been found (Corotis, 1979) to be highly correlated to the ratio of the run level to the seasonal mean wind speed at a site. A nonlinear

regression has been performed for b using data from all sites with hourly data analyzed in the present and previous reports (Corotis, 1976; 1977; 1979), except for those sites with very short records or significant anemometer changes. There were about 30 sites and 120 sets of seasonal data. The regression was performed for b versus the ratio of run level to mean speed, for ratios ranging from 0.4 to 2.5. There were about 5 data points for each seasonal set.

For the b parameter for runs above a fixed run level, the simple linear equation

$$b_{above} = 1.348 + 0.211 \text{ (Run Level/Mean Speed)} \qquad (6.5)$$

was chosen over the second and third order equations tested because the improvement in fit with the higher order curves was minor.

For runs below a fixed run level, a nonlinear regression up to the fourth order was performed and it was found that the following quadratic equation fit the data well

$$b_{below} = 1.868 - 0.393 \text{ (Run Level/Mean Speed)} + 0.063 \text{ (Run Level/Mean Speed)}^2 \qquad (6.6)$$

A standard F-test was used to assess the fit of the regression curves, and they were significant at all levels. Figure 6.1 shows Equations (6.5) and (6.6) as well as all the data points.

Mean run durations were found from observed data for all the sites used in the regression and graphed versus the ratio of run level to mean speed (between 0.4 and 2.5). The power-exponential run duration model was calibrated with b parameter values from Equations

(6.5) and (6.6) and computed mean run durations compared to observed values. Reasonable agreement is obtained for all sites with hourly coefficients of variation close to or slightly above that predicted by the Rayleigh (52%). When the coefficient of variation is less than about 45%, the power-exponential model for runs above fixed wind speed levels is only good for levels greater than the site mean speed, and for runs below fixed wind speed levels is only good for levels less than about 1.3 times the site mean wind speed. For hourly coefficients of variation between 45% and about 80% the power-exponential model appears to be good over the full range tested (wind speed levels from 0.4 to 2.5 times the site mean wind speed). For coefficients of variation above about 80%, the model is in substantial error for runs below fixed wind speed levels more than about 1.5 times the site mean wind speed. In general, the model fits as well for sites with relatively high mean wind speeds (4-8 m/s) as it does for the less windy sites.

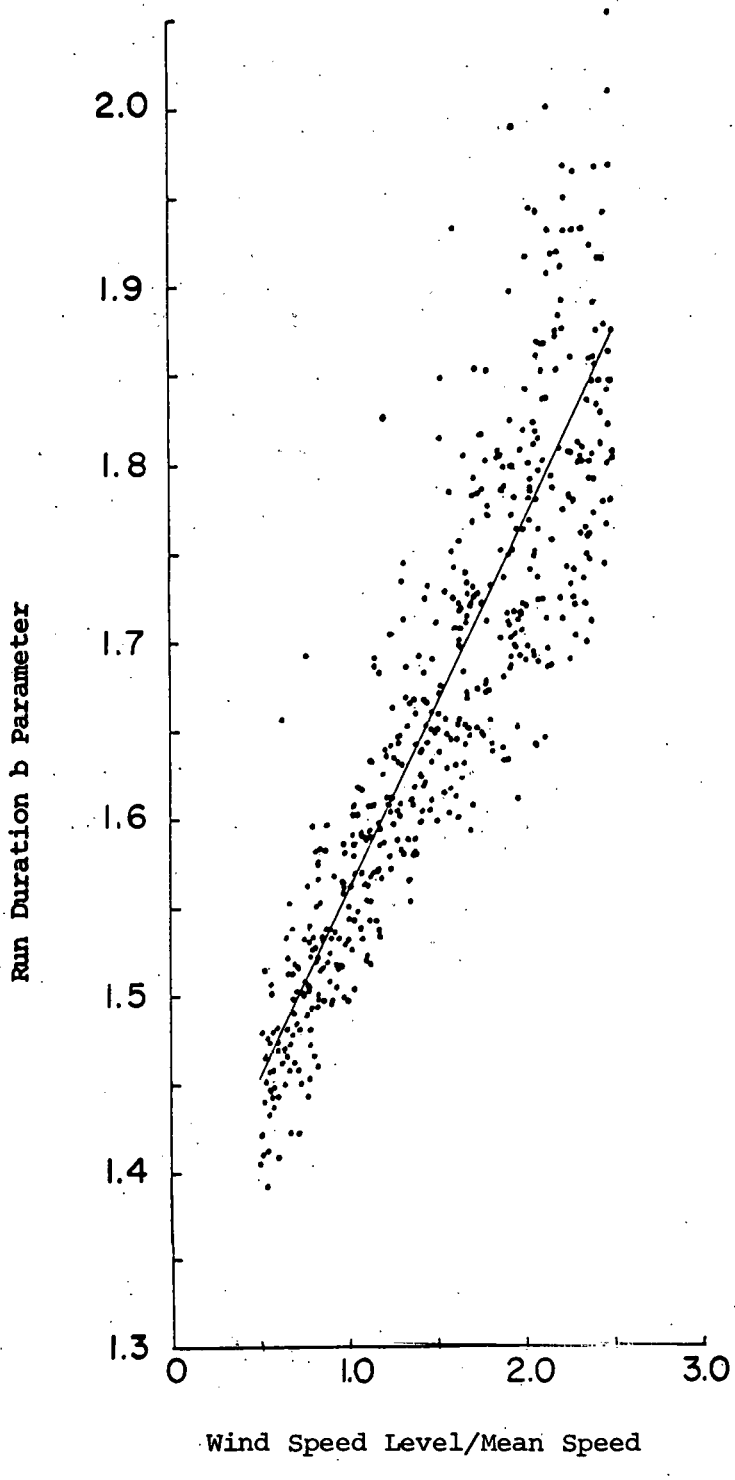

FIGURE 6.1a. Run Duration b Parameter for Runs Above Fixed Wind Speed Levels.

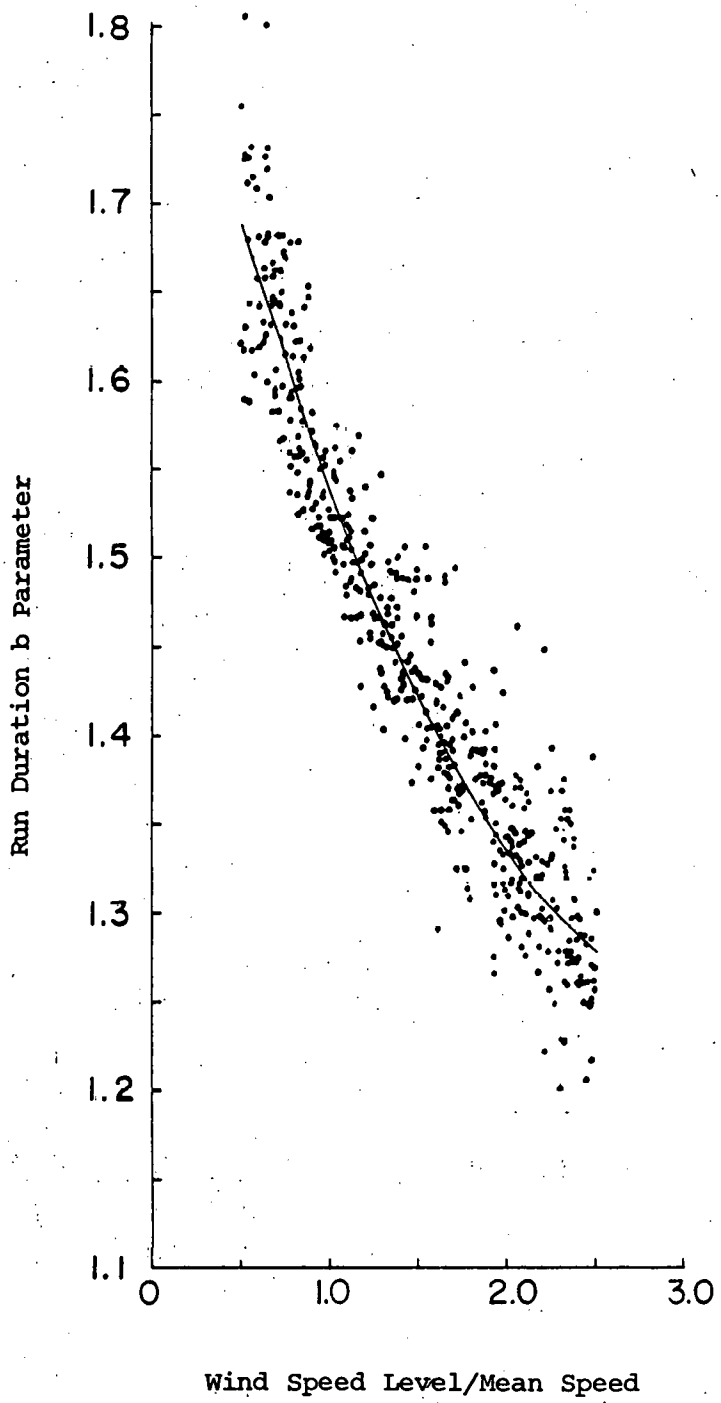

FIGURE 6.1b. Run Duration b Parameter for Runs Below Fixed Wind Speed Levels.

CHAPTER 7

CONCLUSIONS

This study has shown that when the wind speed is composed of horizontal vector components that are orthogonal, independent and of unequal variance, the probability distribution of the wind speed is well modelled by the one parameter (mean wind speed) Rayleigh distribution. A slight shift of the Rayleigh distribution to the right of the derived distribution suggests that the Rayleigh may fit better with the mode of the observed data than with the mean (except in the extreme upper tail region). The Rayleigh distribution also gives a reasonable approximation when the vector components are correlated and of unequal variance. The density function is found to be symmetric with respect to the sign of the correlation between components. This observation is especially significant and advantageous in computing the derived density function (Eq. (2.19)).

There is no apparent effect of sampling rate or averaging time on the mean of the wind speed, and the effect on the variance is relatively minor for sampling rates and averaging times of practical interest. A distinct increase in autocorrelation with averaging times is observed, as well as an increase in mean wind speed persistence (run duration) with decreasing sampling rate. Although the sampling effects observed from two 24-hour records are consistent, they are not considered to be conclusive. Further investigation is necessary to substantiate these trends.

The application of a modified Weibull distribution in combination

with the lag-one autocorrelation for sequential hourly wind speed simulation leads to a simple and versatile procedure. Although the simulation model appears to agree well with actual hourly wind speeds, comparison with more observed data is required before the simulation can be considered to be fully verified.

The ARASIM model that is developed for the time series simulation of power from a regional array of wind turbines is shown to give a good approximation to the array power output based on historical data, and in many cases gives better agreement than a somewhat more complicated model. From the analyses that were used to evaluate the fitting of the simulated array power models to the observed data, it is shown that the array power means and variances of the ARASIM model agree reasonably well with the REGIONAL. The analysis shows that the autocorrelation function decays exponentially, which allows the application of the Gauss-Markov process. The consistency of higher correlation for the ARASIM model in the winter and lower correlation in the summer than the REGIONAL results may be due to the estimation procedures used and the assumption that the spatial and time-space correlation are relatively consistent throughout a region. The mean run durations for the ARASIM model are consistently longer than the REGIONAL results and may be due to the high autocorrelation. Although the model developed herein is considered to be a good model, further development is required to better approximate the spatial and autocorrelation functions and the array power for a variety of wind turbines. It is also recommended that the ARASIM and the REGIONAL results be compared with data from regions having more sites.

The concept of Bayesian statistics is seen to be an appropriate and practical procedure for incorporating the uncertainty associated with finite sampling duration into the basic wind speed model. While further development and application analysis are needed, it appears that the sampling uncertainty is strongly dominated by the inherent variability for a year or more of field data.

Data from relatively windy NCC sites is seen to generally confirm the use of the probability models previously developed, including minimum survey duration, the Rayleigh distribution for wind speed, and the power-exponential distribution for run duration. Some care in the use of general models must be exercised at those sites with unusual topography or exceptional variability of wind.

REFERENCES

Benjamin, J.R. and Cornell, C.A. (1970), *Probability, Statistics and Decision for Civil Engineers*, McGraw Hill, New York.

Breiman, L. (1969), *Probability and Stochastic Processes*, Houston Mifflin Co., Boston.

Cliff, W.C. (1977), "The Effect of Generalized Wind Characteristics on Annual Power Estimates from Wind Turbine Generators", Battelle, PNL-2436 Report, ERDA Contract No. EY-76-C-06-1830.

Cliff, W.C., Justus, C.G. and Elderkin, C.E. (1978), "Simulation of the Hourly Wind Speeds for Randomly Dispersed Sites", Battelle PNL 2523 Report, ERDA Contract No. EY-76-C-06-1830, May.

Corotis, R.B. (1976), "Stochastic Modelling of Site Wind Characteristics", Final Report, ERDA/NSF/00357-76/1, Northwestern University, Evanston, Illinois, November.

Corotis, R.B. (1977), "Stochastic Modelling of Site Wind Characteristics", Final Report, ERDA/RLO/2342-77/2, Northwestern University, Evanston, Illinois, September.

Corotis, R.B. (1979), "Survey Methodology and Reliability Analysis for Site Wind Characteristics", Final Report, DOE/RLO/2342-79/1, Northwestern University, Evanston, Illinois, January.

Crandall, S.H. and Mark, W.D. (1963), *Random Vibration in Mechanical System*, Academic Press, New York.

Crutcher, H.L. and Baer, L. (1962), "Computation for Elliptical Wind Distribution Statistics", *Journal of Applied Meteorology*, Vol. 1, No. 4, December, pp. 522-530.

Doran, J.C., Bates, J.A., Liddell, P.J. and Fox, T.D. (1977), "Accuracy of Wind Power Estimates", Battelle PNL-2442, ERDA Contract No. EY-76-C-06-1830, October.

General Electric Company (1976), "Design Study of Wind Turbines 50 KW To 3000 KW For Electric Utility Applications", Volume I-Summary Report, ERDA/NASA/9403-76/1, September.

Golding, E.W. (1955), *The Generation of Electricity By Wind Power*, E. & F.N. Spon Ltd., London.

Hald, A. (1952), *Statistical Theory with Engineering Applications*, John Wiley and Sons, Inc., New York, pp. 585-612.

Hunnicutt, C.L., Linscott, B. and Wolf, R.A. (1978), "An Operating 200-KW Horizontal Axis Wind Turbine", DOE/NASA/1004-78/14, NASA Lewis Research Center, Cleveland, Ohio.

Justus, C.G. (1975), "National Wind Energy Statistics for Large Arrays of Aerogenerators", Progress Report No. 1, NSF Grant GAE75-00547, Georgia Institute of Technology, Atlantic, Georgia, October.

Justus, C.G. (1976), "Wind Energy Statistics for Large Arrays of Wind Turbines (New England and Central U.S. Regions)", Final Report, ERDA/NSF-0054/76/1, Georgia Institute of Technology, Atlanta, Georgia, August.

Justus, C.G., Hargraves, W.R. and Mikhail, A.S. (1976), "Reference Wind Speed Distributions and Height Profiles For Wind Turbine Design and Performance Evaluation Applications", ORO/5108-76/4, Georgia Institute of Technology, Atlanta, Georgia, August.

Justus, C.G., Hargraves, W.R. (1977), "Wind Energy Statistics for Large Arrays of Wind Turbines (Great Lakes and Pacific Coast Regions)", Annual Progress Report, RLO/2439-77/2, Georgia Institute of Technology, Atlanta, Georgia, May.

Justus, C.G. (1978), *Winds and Wind System Performance*, Franklin Institute Press, Philadelphia, Pennsylvania, pp. 92-93.

Justus, C.G. and Mikhail, A.S. (1978), "Energy Statistics for Large Wind Turbine Arrays", RLO/2439-78/3, Georgia Institute of Technology, Atlanta, Georgia, May.

Peterson, E.W. and Hennessey, J.P. (1978), "On the Use of Power Laws for Estimates of Wind Power Potential", *Journal of Applied Meteorology*, Vol. 17, No. 3, March.

Putnam, P.C. (1948), *Power From The Wind*, Van Nostrand Reinhold Company, New York.

Reed, J.W. (1975), "Wind Power Climatology of the United States", U.S. ERDA, Contract AT(29-1)-789, Sandia Laboratories, Albuquerque, New Mexico, June.

Reed, J.W. (1978), "Wind Speed Distribution Changes with Height at Selected Weather Stations", DOE Contract AT(29-1)-789, Sandia Laboratories, Albuquerque, New Mexico, August.

Reed, J.W. (1979), "Wind Power Climatology of the United States--Supplement", DOE Contract DE-AC04-76DP00789, Sandia Laboratories, Albuquerque, New Mexico, April.

Rockwell International (1978), "A Guide To Commercially Available Wind Machines", DOE/RFP-2836/3533/78/3, Rocky Flats Plants, Golden, Colorado, April.

Thomas, R.L. and Donovon, R.M. (1978), "Large Wind Turbine Generators", DOE/NASA/1059-78/1, NASA Lewis Research Center, Cleveland, Ohio, February.

Wentink, T.C. (1974), "Wind Power Potential of Alaska: Part I. Surface Wind Data from Specific Coastal Sites", NSF/RANN Grant GI-43098, University of Alaska, Fairbanks, Alaska, August.

Wentink, T.C. (1976), "Study of Alaskan Wind Power and Its Possible Applications", Final Report, NSF/RANN/SE/AER74-00239/FR-76/1, University of Alaska, Fairbanks, Alaska, February.

Wentink, T.C. (1976). "Wind Power Potential of Alaska: Part II. Wind Duration Curve Fits and Output Power Estimates for Typical Windmills", RLO/2229/T12-76/1, University of Alaska, Fairbanks, Alaska, August.

Won, D.J. (1979), "Survey Methodology and Reliability Analysis for Site Wind Characteristics", thesis presented to Northwestern University, at Evanston, Illinois, in partial fulfillment of the requirements for the degree of Master of Science, June.

APPENDIX A

PROGRAM "WEISIM"

The WEISIM program simulates the hourly wind speed at a single site. The simulation utilizes an approximate procedure whereby the Weibull mean and variance are replaced each hour by a conditional mean and variance, with a correction that is theoretically exact for a Gaussian distribution. The program also has 2 subroutines, subroutine POLY and PARA, which compute the parameters k and c of Eqs. (4.2) and (4.3) numerically. This program is written to simulate a minimum of one year, and there is no upper duration limit. It is also capable of doing more than one set of simulations at a time.

The input for this program is on cards in the following order and format:

CARD NO.	COL. NO.	FORMAT	DATA
1	1 - 5	I5*	Number of years to be simulated
2	1 - 80	8A10	Title of the site (recommended)
3 - 7	1 - 10	F10.5	Coefficients for the polynomial approximation for the Gamma function. These coefficients are, respectively: -0.57486, +0.95124, -0.69986, +0.42455, -0.10107
8 - 19	1 - 10	F10.4	Monthly standard deviation (in m/s)
	11 - 20	F10.4	Lag one hourly autocorrelation by month
20 - 31	1 - 8	F8.4	Monthly mean wind speed (in m/s)

	9 - 80	24F3.2	Diurnal cycle effect (multiplier factor), 24 hours on one card.
32			Blank if end of data; a new card 1 for another simulation (i.e., repeat cards 1 - 32)

* Right justified

The line printer output of the program is a table of mean wind speeds and standard deviations (including the diurnal cycle effect) by month and hour of the day. The simulated hourly wind speed is written on tape and the format is

YYMMDDHHVVVVV

where	YY	Year, 1981	(Col. 1 - 2)
	MM	Month, 05 = May	(Col. 3 - 4)
	DD	Day	(Col. 5 - 6)
	HH	Hour, 01 - 24	(Col. 7 - 8)
	VVVVV	Wind speed, in integer centimeters per second	(Col. 9 - 13)

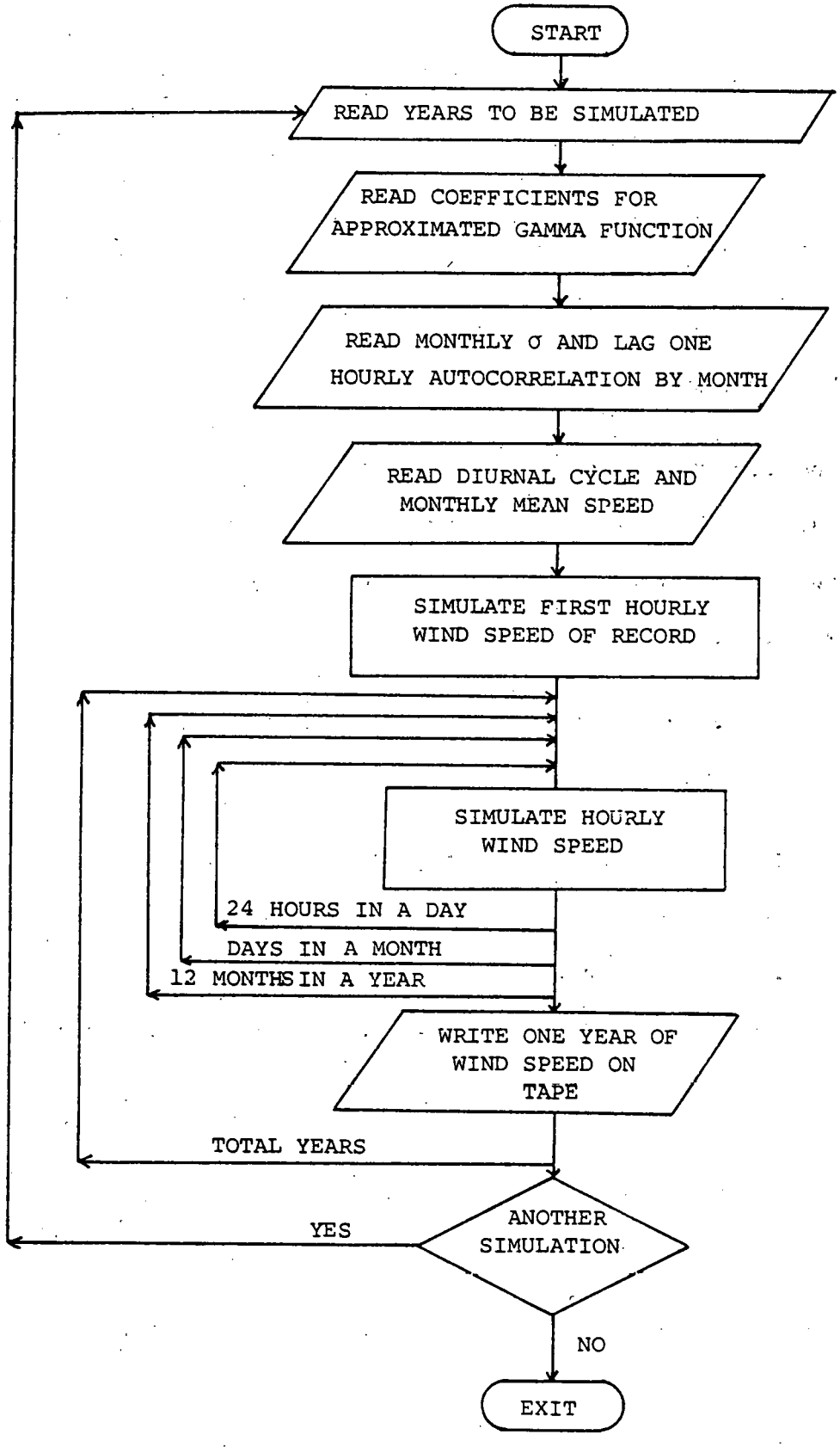

FIGURE. A.1 Computer Flow Chart for Program WEISIM

```
      PROGRAM WEISIM (INPUT,OUTPUT,TAPE5)
      DIMENSION DC(12,24),VM(12),VMEAN(12,24),SIGMA(12),STD(12,24),RHO(1
     12),CO(5),MOOM(24),MOMS(24),COV(24),P(24),C(24),NDAY(12),TITLE(8)>S
     1PD(12,31,24),VEL(24),MP(12,24),MS(12,24),ISPEED(12,31,24)
      REAL MOOM,MOMS,MC,MM
      DATA NDAY/31,28,31,30,31,30,31,31,30,31,30,31/
C THIS PROGRAM STMULATES HOURLY WIND SPEED AT ONE SITE.
C THE SIMULATION IS BASED ON WEIBUL DISTRIBUTION AND IT SIMULATES A
C MINIMUM OF ONE YEAR
C READ IN NUMBER OF YEARS TO BE SIMULATED
      1 READ 1001, NYEAR
C IN GENERAL INDICES ARE NY FOR YEARS, NM AND I FOR MONTHS, ND FOR DAYS
C AND NH AND J FOR HOURS
      IF (NYEAR)999,999,2
    2 READ 1002,(TITLE(K),K=1,8)
C READ IN THE COEFFICIENTS FOR COMPUTING THE PARAMETERS K AND C OF THE
C CDF OF WEIBUL DISTRIBUTION
      READ 1002,CO
C READ IN STANDARD DEVIATION AND LAG 1 HOUR AUTOCORRELATION FOR EACH
C MONTH
      DO 10 I=1,12
      READ 1003, SIGMA(I),RHO(I)
   10 CONTINUE
C READ IN MEAN WIND SPEED AND DIURNAL CYCLE FOR EACH MONTH. A BLANK
C FOR DIURNAL CYCLE MEANS NO CYCLE EFFECT
      DO 11 I=1,12
      READ 1004, VM(I),(DC(I,J),J=1,24)
      IF(DC(I,1).GE. 0.0001) GO TO 3
      DO 12 J=1,24
      VMEAN(I,J)=VM(I)
      STD(I,J)=SIGMA(I)
   12 CONTINUE
      GO TO 11
    3 DO 13 J=1,24
      VMEAN(I,J)=VM(I)*DC(I,J)
      STD(I,J)=SIGMA(I)*DC(I,J)
   13 CONTINUE
   11 CONTINUE
      PRINT 2001,(TITLE(K),K=1,8)
      PRINT 2002, NYEAR
      PRINT 2003
      PRINT 2004
      DO 14 J=1,24
      PRINT 2005, J, (VMEAN(I,J),I=1,12)
      PRINT 2006,(STD(I,J),I=1,12)
   14 CONTINUE
C SIMULATE THE FIRST HOURLY WIND SPEED OF THE RECORD
      L=1
      MOOM(L)=VMEAN(1,1)
      COV(L)=STD(1,1)/MOOM(L)
      CALL PARA (P,C,L,COV,MOOM,CO)
      SPD(L,1,1)=WEIBUL(P(L),C(L))
      VEL(L)=SPD(L,1,1)
      DO 19 NY=1,NYEAR
      NYR=1980+NY
C ADJUSTING FEBRUARY FOR A LEAP YEAR
      INY=NY/4
      FNY=INY
      YNY=NY
      YNY=YNY/4.
      ZNY=YNY-YNY
      IF(ZNY-0.001)32,32,33
   32 NDAY(2)=29
      GO TO 34
   33 NDAY(2)=28
   34 CONTINUE
      DO 20 IM=1,12
      NDY = NDAY(IM)
      DO 21 ID=1,NDY
      IF(NY.NE.1) GO TO 40
      IF(IM.NE.1) GO TO 40
      IF(ID.NE.1) GO TO 40
      II=3
      GO TO 41
   40 II=2
   41 DO 22 IJ=II,25
      IH=IJ-1
      IHP=IJ-2
      IF(IJ.NE.2)GO TO 71
```

```
      IF(ID.NE.1)GO TO 72
      JM=IM-1
      MODM(IH)=VMEAN(IM,IH)+RHO(IM)*(VEL(24)-VMEAN(JM,24))*STD(IM,IH)/
     1STD(JM,24)
      GO TO 73
   71 MODM(IH)=VMEAN(IM,TH)+RHO(IM)*(VEL(IHP)-VMEAN(IP,IHP))*STD(IM,IH)/
     1STD(IM,IHP)
      GO TO 73
   72 MODM(IH)=VMEAN(IM,TH)+RHO(IM)*(VEL(24)-VMEAN(IM,24))*STD(IM,IH)/
     1STD(IM,24)
   73 MODS(IH)=STD(IM,TH)*SQRT(1-RHO(IM)*RHO(IM))
      COV(IH)=MODS(IH)/MODM(IH)
      CALL PARA (P,C,IH,COV,MODM,CO)
      SPD(IM,ID,IH)=WEIBUL(P(IH),C(IH))
      VEL(IH)=SPD(IM,ID,TH)
      ISPEED(IM,ID,TH)=SPD(IM,ID,IH)*100
   22 CONTINUE
   21 CONTINUE
   20 CONTINUE
C  WRITE ONE YEAR OF HOURLY WIND SPEED ON TAPE 5
C  WIND SPEED IS IN CENTIMETERS PER SECOND
      NZ=NYR-1900
      DO 50 IM=1,12
      ND=NDAY(IM)
      DO 51 ID=1,ND
      DO 52 IH=1,24
      WRITE(5,3009)NZ,IM,ID,IH,ISPEED(IM,ID,IH)
   52 CONTINUE
   51 CONTINUE
   50 CONTINUE
   19 CONTINUE
      GO TO 1
 1001 FORMAT (I5)
 1002 FORMAT (8A10)
 1003 FORMAT (2F10.4)
 1004 FORMAT (F8.4,24F3.2)
 1005 FORMAT (F10.5)
 2001 FORMAT (1H1,/30X,8A10)
 2002 FORMAT(//25X,*THE PROGRAM HAS BEEN SET TO SIMULATE *,I5,* YEARS
     1OF DATA*,//)
 2003 FORMAT (10X,* MEAN WIND SPEEDS AND STANDARD DEVIATIONS (IN M/S) BY
     1 MONTH AND HOUR OF THE DAY*,//)
 2004 FORMAT(* HOUR    JANUARY   FEBURARY    MARCH     APRIL       M
     1AY        JUNE        JULY      AUGUST    SEPTEMBER   OCTOBER    NOVE
     1MBER   DECEMBER*,/)
 2005 FORMAT (1X,I2,2X,12F11.4)
 2006 FORMAT (5X,12F11.4)
 3009 FORMAT(4I2,I5)
  999 CONTINUE
      STOP
      END
```

CARD NR. SEVERITY DETAILS DIAGNOSIS OF PROBLEM

115 I 2SCO 115 FIELD WIDTH OF A CONVERSION DESCRIPTOR SHOULD BE AS LARGE AS THE MINIMUM SPECIFIED FOR THAT DESCRIPTOR.

SYMBOLIC REFERENCE MAP (R=2)

ENTRY POINTS DEF LINE REFERENCES

6211 WEISIM 1

VARIABLES	SN	TYPE	RELOCATION								
10764	C	REAL ARRAY	REFS	2	51	52	92	93			
10517	CO	REAL ARRAY	REFS	2	51	92	DEFINED	18			
10704	COV	REAL ARRAY	REFS	2	51	92	DEFINED	50	91		
7013	DC	REAL ARRAY	REFS	2	28	35	36	DEFINED	27		
6770	I	INTEGER	REFS	2*22	2*27	28	2*30	2*31	3*35	3*36	
				44	45	DEFINED	21	26	44	45	
7003	ID	INTEGER	REFS	72	80	93	94	2*95	2*106		
			DEFINED	69	104						
7006	IH	INTEGER	REFS	3*82	3*85	3*88	2*90	3*91	92	3*93	
				2*94	2*95	2*106	DEFINED	77	105		

```
      SUBROUTINE PARA(P,CK,K,VV,AVEV,CO)
      DIMENSION CO(10),P(24),CK(24),VV(24),AVEV(24)
      Q = 1.
      P(K) = 1.
      I = 1.
      P = 2.
      PP = 2.
      A = 1. + VV(K)**2
    5 C = (1. + CO(1) *(2./PP) + CO(2) *(2./PP)**2 + CO(3) *(2./PP)**3 +
     1 CO(4) *(2./PP)**4 + CO(5) *(2./PP) **5) * R
      D = (1. + CO(1) *(1./Q) + CO(2) *(1./Q)**2 + CO(3) *(1./Q)**3 +
     2CO(4) *(1./Q)**4 + CO(5) *(1./Q)**5 ) * T
      B = C / D**2
      E = B-A
      IF (E) 200,202,250
  200 P(K) = P(K) - 0.1
      Q = P(K)
      PP = P(K)
      T = 1.
 5000 IF (2./P(K) - 1.) 57,57,11
   11 CALL POLY (R,T,PP,O)
      GO TO 570
   57 R = 1.
  570 C = (1. + CO(1) *(2./PP) + CO(2) *(2./PP)**2 + CO(3) *(2./PP)**3 +
     1 CO(4) *(2./PP)**4 + CO(5) *(2./PP) **5) * R
      D = (1. + CO(1) *(1./Q) + CO(2) *(1./Q)**2 + CO(3) *(1./Q)**3 +
     2CO(4) *(1./Q)**4 + CO(5) *(1./Q)**5 ) * T
      B = C / D**2
      EM = B-A
      IF (EM*E) 30,202,35
   35 P(K) = P(K) - 0.1
      Q = P(K)
      PP = P(K)
      GO TO 5000
   30 P(K) = P(K) + 0.01
      T = 1.
 6000 IF (2./P(K) - 1.) 58,58,12
   12 CALL POLY (R,T,PP,O)
      GO TO 580
   58 R = 1.
  580 C = (1. + CO(1) *(2./PP) + CO(2) *(2./PP)**2 + CO(3) *(2./PP)**3 +
     1 CO(4) *(2./PP)**4 + CO(5) *(2./PP) **5) * R
      D = (1. + CO(1) *(1./Q) + CO(2) *(1./Q)**2 + CO(3) *(1./Q)**3 +
     2CO(4) *(1./Q)**4 + CO(5) *(1./Q)**5 ) * T
      B = C / D**2
      EEM = B-A
      IF (EM * EEM) 40,202,45
   45 GO TO 30
   40 P(K) = P(K) - 0.001
      Q = P(K)
      PP = P(K)
      T = 1.
 7000 IF (2./P(K) - 1.) 59,59,13
   13 CALL POLY (R,T,PP,O)
      GO TO 590
   59 R = 1.
  590 C = (1. + CO(1) *(2./PP) + CO(2) *(2./PP)**2 + CO(3) *(2./PP)**3 +
     1 CO(4) *(2./PP)**4 + CO(5) *(2./PP) **5) * R
      D = (1. + CO(1) *(1./Q) + CO(2) *(1./Q)**2 + CO(3) *(1./Q)**3 +
     2CO(4) *(1./Q)**4 + CO(5) *(1./Q)**5 ) * T
      B = C / D**2
      EEEM = B-A
      IF (EEM * EEEM) 50,202,55
   55 GO TO 40
   50 GO TO 150
  250 R = 1.
      T = 1.
  251 P(K) = P(K) + 1.
      Q = P(K)
      PP = P(K)
      IF (P(K) - 11.) 111,211,211
  111 C = (1. + CO(1) *(2./PP) + CO(2) *(2./PP)**2 + CO(3) *(2./PP)**3 +
     1 CO(4) *(2./PP)**4 + CO(5) *(2./PP) **5) * R
      D = (1. + CO(1) *(1./Q) + CO(2) *(1./Q)**2 + CO(3) *(1./Q)**3 +
     2CO(4) *(1./Q)**4 + CO(5) *(1./Q)**5 ) * T
      B = C / D**2
      EP = B-A
      IF (EP * E) 130,202,135
  135 GO TO 251
```

```
      130 P(K) = P(K) - 0.1
          Q = P(K)
          PP = P(K)
          T = 1.
          IF (2./P(K) - 1.) 61,61,16
       16 CALL POLY (R,T,PP,Q)
          GO TO 610
       61 R = 1.
      610 C = (1. + CO(1) *(2./PP) + CO(2) *(2./PP)**2 + CO(3) *(2./PP)**3 +
         1 CO(4) *(2./PP)**4 + CO(5) *(2./PP) **5) * R
          D = (1. + CO(1) *(1./Q) + CO(2) *(1./Q)**2 + CO(3) *(1./Q)**3 +
         2CO(4) *(1./Q)**4 + CO(5) *(1./Q)**5 ) * T
          B = C / D**2
          EEP = B-A
          IF (EP * EEP) 140,202,145
      145 GO TO 130
      140 P(K) = P(K) + 0.01
          Q = P(K)
          PP = P(K)
          T = 1.
          IF (2./P(K) - 1.) 62,62,17
       17 CALL POLY (R,T,PP,Q)
          GO TO 620
       62 R = 1.
      620 C = (1. + CO(1) *(2./PP) + CO(2) *(2./PP)**2 + CO(3) *(2./PP)**3 +
         1 CO(4) *(2./PP)**4 + CO(5) *(2./PP) **5) * R
          D = (1. + CO(1) *(1./Q) + CO(2) *(1./Q)**2 + CO(3) *(1./Q)**3 +
         2CO(4) *(1./Q)**4 + CO(5) *(1./Q)**5 ) * T
          B = C / D**2
          EEEP = B-A
          IF (EEEP * EEP) 160,202,165
      165 GO TO 140
      160 P(K) = P(K) - 0.001
          Q = P(K)
          PP = P(K)
          T = 1.
          IF (2./P(K) - 1.) 63,63,18
       18 CALL POLY (R,T,PP,Q)
          GO TO 630
       63 R = 1.
      630 C = (1. + CO(1) * (2./PP) + CO(2) * (2./PP)**2 + CO(3) * (2./PP)**3
         1+ CO(4) * (2./PP)**4 + CO(5) * (2./PP)**5) * R
          D = (1. + CO(1) *(1./Q) + CO(2) *(1./Q)**2 + CO(3) *(1./Q)**3 +
         2CO(4) *(1./Q)**4 + CO(5) *(1./Q)**5 ) * T
          B = C / D**2
          EEEEP = B-A
          IF (EEEEP * EEEP) 150,202,155
      155 GO TO 160
      202 CONTINUE
      150 CONTINUE
      211 CONTINUE
       66 CONTINUE
          CK(K) = AVEV(K)/D
          RETURN
          END
```

SYMBOLIC REFERENCE MAP (R=2)

ENTRY POINTS — DEF-LINE — REFERENCES

3 PARA 1 133

VARIABLES	SN	TYPE		RELOCATION								
467 A		REAL			REFS	14	29	46	62	77	93	109
						120	DEFINED	8				
0 AVEV		REAL	ARRAY	F.P.		2	132	DEFINED	1			
472 B		REAL				14	29	46	62	77	93	109
						122	DEFINED	13	28	45	61	76	92
470 C		REAL				124						
						126	13	28	45	61	76	92	108
						128	DEFINED	9	24	41	57	72	88
						130						
0 CK		REAL	ARRAY	F.P.		2		DEFINED	1	132		
0 CO		REAL	ARRAY	F.P.		2		S*9	S*11	S*24	S*26	S*41	S*43
					S*47	S*59		S*72	S*74	S*88	S*90	S*104	S*106
					S*120	S*122	DEFINED	S*1					

```
      1                SUBROUTINE POLY (P,T,P,Q)
                       DIMENSION S(100), U(100)
                       R = 2./P
                       I=1
      5                S(I) = 2./P - 1.
                     2 IF (S(I) - 1.) 15,15,3
                     3 R = R * S(I)
                       I = I + 1
                       S(I) = (S(I-1) - 1.)
     10                GO TO 2
                    15 J=1
                       U(J) = 1./Q
                       T = 1./Q
                       IF (T.LT. 1) T=1.
     15                6 IF (U(J) - 1.) 5,5,8
                     8 IF (J.EQ.1) GO TO 50
                     7 T = T + (U(J))
                       J = J+1
                       U(J) = (U(J-1) - 1.)
     20                GO TO 6
                     5 Q = 1./U(J)
                       P = 2./S(I)
                       GO TO 69
                    50 IF (T.GT.1) T=1.
     25                GO TO 7
                    69 RETURN
                       END
```

SYMBOLIC REFERENCE MAP (R=2)

ENTRY POINTS

3	POLY	1	26

VARIABLES

53	I	INTEGER			REFS	5	6	7	8	2*9	22	
					DEFINED	4	8					
54	J	INTEGER			REFS	12	15	16	17	18	2*19	21
					DEFINED	11	18					
0	P	REAL		F.P.	REFS	3	5	DEFINED	1	22		
0	Q	REAL		F.P.	REFS	12	13	DEFINED	1	21		
0	R	REAL		F.P.	REFS	7	DEFINED	1	3	7		
55	S	REAL	ARRAY		REFS	2	6	7	9	22		
					DEFINED	5	9					
0	T	REAL		F.P.	REFS	14	17	24	DEFINED	1	13	14
						17	24					
221	U	REAL	ARRAY		REFS	2	15	17	19	21		
					DEFINED	12	16					

STATEMENT LABELS

12	2		6	10
0	3	INACTIVE	7	4
37	5		21	2*15
31	6		15	20
34	7		17	25
0	8	INACTIVE	16	15
16	15		11	2*6
45	50		24	16
50	69		26	23

STATISTICS

PROGRAM LENGTH 369R 245

750008 CM USED

APPENDIX B

DETERMINATION OF CONSTANTS a AND b FOR THE EQUIVALENT LINEARIZED RELATIONSHIP BETWEEN WIND SPEED AND TURBINE POWER

Letting P be the power generated by a wind turbine and v be the wind speed, the equivalent linearized relationship is given by

$$P = a + bv \tag{B.1}$$

where $\hat{P}$ is equal to the linearized estimate of the generated power. The exact relationship between P and v, in general, can be written as follows,

$$\hat{P} = g(v) \tag{B.2}$$

where g is an arbitrary function (in reality, g is positive semi-definite, monatonically non-decreasing, and continuous with discontinuous derivatives at selected points).

The weighted integrated least-squared error of the linearization is:

$$e = \int_{-\infty}^{\infty} (\hat{P} - P)^2 w(v)\, dv \tag{B.3}$$

where w(v) is a weighting function for wind speed. An obvious function is the relative likelihood of occurrence of wind speed values. The probability density function of wind speed, f(v), provides this weighting as well as satisfies the weighting function prerequisite of integrating to unity. Equation (B.3) becomes

$$e = \int_{-\infty}^{\infty} (\hat{P} - P)^2 f(v)\, dv \tag{B.4}$$

One can minimize the error by setting the partial derivatives of Eq. (B.4) with respect to a and b equal to zero, then by solving the resulting pair of simultaneous equations for a and b as follows:

$$e = \int_{-\infty}^{\infty} (a + bv - g(v))^2 f(v)\, dv$$

$$= \int_{-\infty}^{\infty} (a^2 + b^2v^2 + g^2(v) + 2abv - 2ag(v) - 2bvg(v)) f(v)\, dv \tag{B.5}$$

$$\frac{\partial e}{\partial a} = 0 = a \int_{-\infty}^{\infty} f(v)\, dv + b \int_{-\infty}^{\infty} vf(v)\, dv - a \int_{-\infty}^{\infty} g(v)f(v)\, dv \tag{B.6}$$

$$\frac{\partial e}{\partial b} = 0 = b \int_{-\infty}^{\infty} v\ f(v)\, dv + a \int_{-\infty}^{\infty} vf(v)\, dv$$

$$- b \int_{-\infty}^{\infty} v\, g(v) f(v)\, dv \tag{B.7}$$

Applying the wind speed-turbine power relationship developed by Justus, Hargraves and Mikhail (1976), g(v) is given by

$$g(v) = \begin{cases} 0 & v \le v_i \\ A + Bv + Cv^2 & v_i < v \le v_r \\ R & v_r < v \le v_o \\ 0 & v > v_o \end{cases} \tag{B.8}$$

where $R = A + Bv_r + Cv_r^2$ is the related power; v_i, v_r and v_o are, respectively, cut-in, rated and cut-out wind speed. It should be noted that A, B, and C here are R times as large as those defined by Justus et al. The constants A, B and C are found by satisfying the continuity at v_i and v_r and the condition that the power at median wind speed ($v_m = (v_i + v_r)/2$) is equal to $R(v_m/v_r)^3$. This procedure has been shown by Justus et al. to adequately describe power output curves for wind turbines having a rated power from a few KW to 1500 KW. It appears to be adequate for higher rated power because the operating curves for the 2000 KW and 2500 KW do not vary significantly from the lower capacity turbines

(Thomas and Donovon, 1978). The resulting expressions for the constants are:

$$B = R \frac{(v_m^2 - v_i^2) - \left(\frac{v_m}{v_r}\right)^3 (v_r^2 - v_i^2)}{(v_r - v_i)(v_m - v_r)(v_m - v_i)} \tag{B.9}$$

$$C = \frac{R - B(v_r - v_i)}{(v_r^2 - v_i^2)} \tag{B.10}$$

$$A = -B\, v_i - C\, v_i^2 \tag{B.11}$$

Applying Eq. (B.8), Eqs. (B.6) and (B.7) become

$$0 = a\int_{-\infty}^{\infty} f(v)\, dv + b\int_{-\infty}^{\infty} vf(v)\, dv - a\int_{-\infty}^{v_i} 0f(v)\, dv - a\int_{v_i}^{v_r} (A+Bv+Cv^2) f(v)\, dv - a\int_{v_r}^{v_o} Rf(v)\, dv - a\int_{v_o}^{\infty} 0f(v)\, dv \tag{B.12}$$

$$0 = b\int_{-\infty}^{\infty} v\, f(v)\, dv + a\int_{-\infty}^{\infty} vf(v)\, dv - b\int_{-\infty}^{v_i} 0vf(v)\, dv - b\int_{v_i}^{v_r} (A+Bv+Cv^2)\, vf(v)\, dv - b\int_{v_r}^{v_o} Rvf(v)\, dv - b\int_{v_o}^{\infty} 0vf(v)\, dv \tag{B.13}$$

Adopting the Rayleigh distribution for wind speed for wind power conversion purpose (Wentink, 1976; Cliff,1977; Corotis, 1977; Justus, 1978), f(v) is then given by

$$f(v) = \frac{2v}{\phi^2} \exp\left[-\left(\frac{v}{\phi}\right)^2\right] \qquad \text{for } v \geq 0 \tag{B.14}$$

Tests were conducted to determine the range over which the equivalent linear relationship should be fitted to yield the best model. Ranges that were being considered are: 0 to ∞, 0 to v_o, 0 to v_r, v_i to v_o and v_i to v_r. Using the range (0, ∞) is not satisfactory because in

order to fit the actual curve over the full range, the agreement must be compromised in the important range near the mean wind speed, as can be seen from Fig. B.1. At the other extreme, using just the range (v_i, v_r) is not acceptable because it produces very large errors in the moderately important wind speed ranges below cut-in and between rated and cut-out. Another reason why the v_i to v_r range is not preferred is that the regional array average power curve exhibits smoothed transition regions of decreased slope (as compared to a single-site power curve) for wind speeds slightly above cut-in and below rated (Justus and Mikhail, 1978). The equivalent linear curve based on the range (v_i, v_r) is thus too steep over all but the center of the (v_i, v_r) range. The remaining three ranges all provide similar fits, and as shown by Fig. B.1 it is not obvious which range provides the best fit. The v_i to v_o range has been chosen for investigation since it is the total non-zero operating range of the turbine.

Adopting the integration limits of v_i and v_o, Eqs. (B.12) and (B.13) lead to the following expression for a and b:

$$b = A\left[\frac{F_1F_{25} - F_2F_{16}}{K}\right] + B\left[\frac{F_2F_{25} - F_3F_{16}}{K}\right] + C\left[\frac{F_3F_{25} - F_4F_{16}}{K}\right] + R\left[\frac{F_6F_{25} - F_5F_{16}}{K}\right] \qquad \text{(B.15)}$$

$$a = \frac{1}{F_{16}}\left(AF_1 + BF_2 + CF_3 + bF_{25}\right) \qquad \text{(B.16)}$$

where

$$F_{16} = F_1 + F_6 \qquad \text{(B.17a)}$$

$$F_{25} = F_2 + F_5 \qquad \text{(B.17b)}$$

$$K = (F_{25})^2 - F_{16}(F_3 + F_7) \qquad \text{(B.17c)}$$

in which

$$F_1 = E_i - E_r \tag{B.18a}$$

$$F_2 = v_i E_i - v_r E_r + \phi\sqrt{\pi}\left\{F_u(\sqrt{2}v_r/\phi) - F_u(\sqrt{2}v_i/\phi)\right\} \tag{B.18b}$$

$$F_3 = v_i^2 E_i - v_r^2 E_r + \phi^2 E_i - \phi^2 E_r \tag{B.18c}$$

$$F_4 = v_i^3 E_i - v_r^3 E_r + \frac{3\phi^2}{2}\left\{v_i E_i - v_r E_r\right\} + \frac{3\phi^3\sqrt{\pi}}{2}\left\{F_u(\sqrt{2}v_r/\phi) - F_u(\sqrt{2}v_i/\phi)\right\} \tag{B.18d}$$

$$F_5 = v_r E_r - v_o E_o + \phi\sqrt{\pi}\left\{F_u(\sqrt{2}\,v_o/\phi) - F_u(\sqrt{2}\,v_r/\phi)\right\} \tag{B.18e}$$

$$F_6 = E_r - E_o \tag{B.18f}$$

$$F_7 = v_r^2 E_r - v_o^2 E_o + \phi^2 (E_r - E_o) \tag{B.18g}$$

$$E_i = \exp[-(\frac{v_i}{\phi})^2] \tag{B.18h}$$

$$E_r = \exp[-(\frac{v_r}{\phi})^2] \tag{B.18i}$$

$$E_o = \exp[-(\frac{v_o}{\phi})^2] \tag{B.18j}$$

and $F_u(u)$ is the cumulative distribution function of the standardized Gaussian deviate.

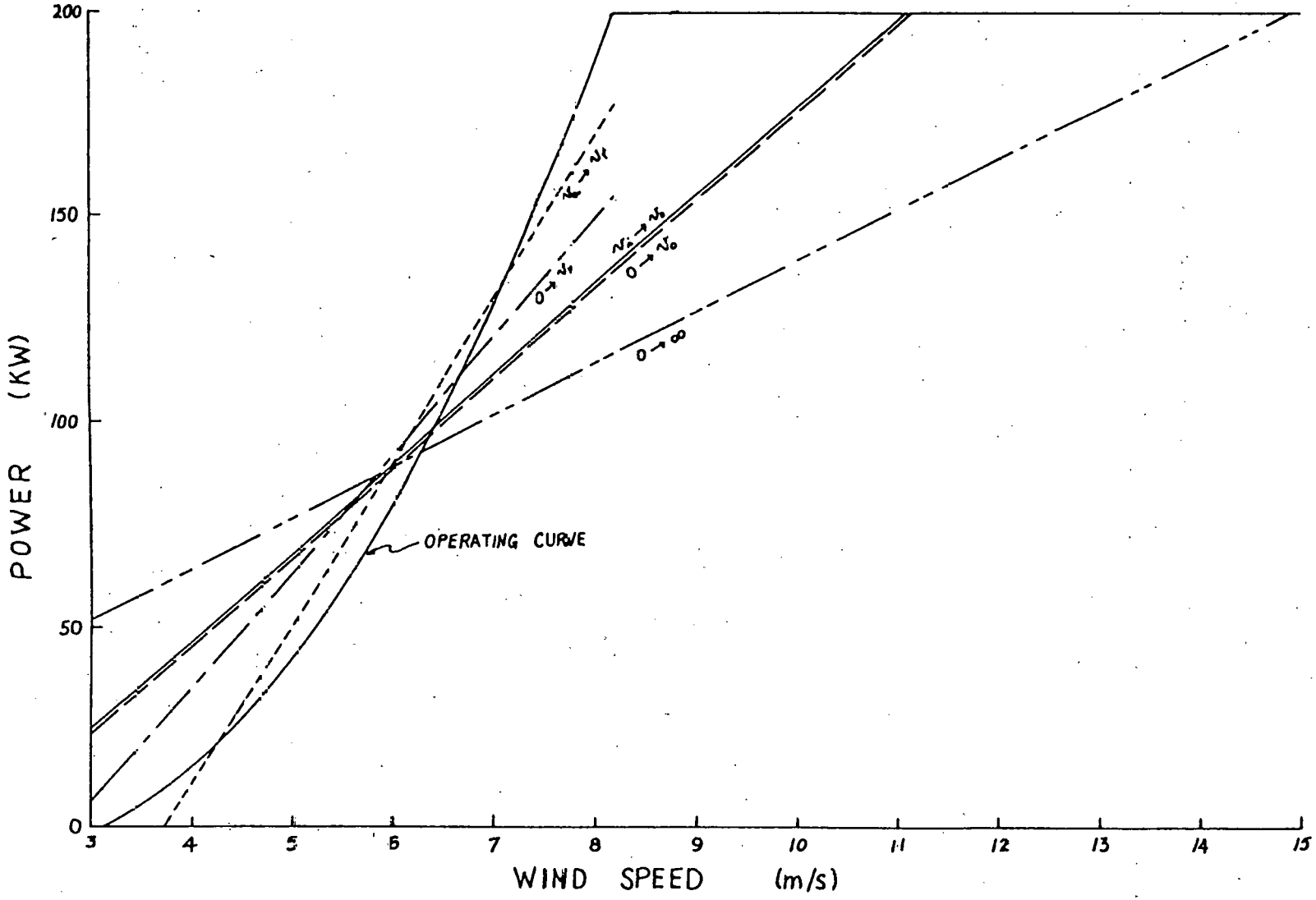

FIGURE. B.1 Comparison of Linear Power-Wind Speed Relation to the Operating Power Curve of a MOD 0A (200 KW) Wind Turbine in Wyoming Region at 11 a.m. in February.

APPENDIX C

DERIVATION OF AUTOCORRELATION FOR ARRAY SUMMED WIND SPEED

Let m_v and σ_v be the mean and standard deviation of wind speed for any particular site at a given point in time. Assume spatial homogeneity and temporal stationarity for all n sites in the array. The summed wind speed for hour i is given as

$$V_i = \sum_{k=1}^{n} v_{ik} \tag{C.1}$$

The autocorrelation between the summed speed at hour i and hour j is defined by

$$R(j-i) = \frac{E[V_i V_j] - E[V_i]\, E[V_j]}{\sqrt{Var[V_i]\, Var[V_j]}}$$

$$= \frac{E\left[\sum_{k=1}^{n} v_{ik} \sum_{\ell=1}^{n} v_{j\ell}\right] - (nm_v)\,(nm_v)}{\sum_{k=1}^{n} \sum_{\ell=1}^{n} cov\,[v_{ik}, v_{i\ell}]}$$

$$= \frac{nE[v_{ik}v_{jk}] + (n^2-n)\, E[v_{ik}v_{j\ell}] - n^2 m_v^{\,2}}{n\sigma_v^{\,2} + (n^2-n)\, \rho_s \sigma_v^{\,2}}$$

$$= \frac{n\left\{m^2_v + \rho(j-i)\, \sigma_v^2\right\} + (n^2-n)\left\{m_v^2 + \rho_s(j-i)\, \sigma_v^2\right\} - n^2 m^2_v}{n\sigma_v^2 \left\{1 + (n-1)\, \rho_s\right\}}$$

$$= \frac{\rho(j-i) + (n-1)\, \rho_s(j-i)}{1 + (n-1)\, \rho_s} \tag{C.2}$$

APPENDIX D

DERIVATION OF WIND SPEED AT WHICH NEGATIVE POWER IS COMPUTED

One can find the wind speed, v_{cr}, at which g(v) (Eq. (B.8)) is minimum by solving the equation

$$\frac{d[g(v)]}{dv} = B + 2C\,v = 0 \tag{D.1}$$

in which

$$v = v_{cr} = -\frac{B}{2\,C} \tag{D.2}$$

Substituting Eqs. (B.9) and (B.10) into Eq. (D.2) and letting

$$\beta = \frac{(v_m^2 - v_i^2) - (v_m/v_r)^3\,(v_r^2 - v_i^2)}{(v_r - v_i)\,(v_m - v_r)\,(v_m - v_i)} \tag{D.3}$$

$$\alpha = \frac{1 - \beta(v_r - v_i)}{(v_r^2 - v_i^2)} \tag{D.4}$$

Eq. (D.2) becomes

$$v_{cr} = -\frac{\beta}{2\alpha} \tag{D.5}$$

Expanding Eq. (D.5) and substituting $v_m = (v_i + v_r)/2$,

$$v_{cr} = \frac{-v_i^5 - 3v_i^4v_r - 2v_i^3v_r^2 - 8v_i^2v_r^3 - v_iv_r^4 - v_r^5}{-2v_i^4 - 4v_i^3v_r + 12v_iv_r^3 - 6v_r^4} = \frac{N}{D} \tag{D.6}$$

where v_{cr} is a function of v_i and v_r and independent of R.

Now, in order to ensure $g(v) \geq 0$ for $v_i \leq v \leq v_r$, then $v_{cr} \leq v_i$. Two conditions, $D < 0$ and $D > 0$, have to be considered separately for the inequality. First, consider the case where $D < 0$, which indicates

$$\frac{2v_i - v_r}{v_i + 2v_r} < \frac{v_f^3}{3v_r^3} \tag{D.7}$$

then $N \geq Dv_i$ has to be true, which implies

$$\left(\frac{v_i}{v_r}\right)^3 \leq \frac{4v_i - v_r}{v_i + 2v_r} \tag{D.8}$$

Since it would be easier to relate Eqs. (D.7) and (D.8) by the v_i , v_r ratio, letting $S = v_i / v_r$, Eqs. (D.7) and (D.8) become

$$\frac{2S - 1}{S + 2} < \frac{S^3}{3} \tag{D.9}$$

$$S^3 \leq \frac{4S - 1}{S + 2} \tag{D.10}$$

Similarly for the case $D > 0$ one obtains

$$\frac{2S - 1}{S + 2} > \frac{S^3}{3} \tag{D.11}$$

and

$$S^3 \geq \frac{4S - 1}{S + 2} \tag{D.12}$$

In summary, for $g(v) \geq 0$ when $v_i \leq v \leq v_r$, S has to satisfy either Eqs. (D.9) and (D.10) or Eqs. (D.11) and (D.12). It turns out that Eqs. (D.9) and (D.10) are never satisfied, and the values of S that satisfy Eqs. (D.11) and (D.12) are between 0.260 and 0,587, as can be seen in Figure D.1.

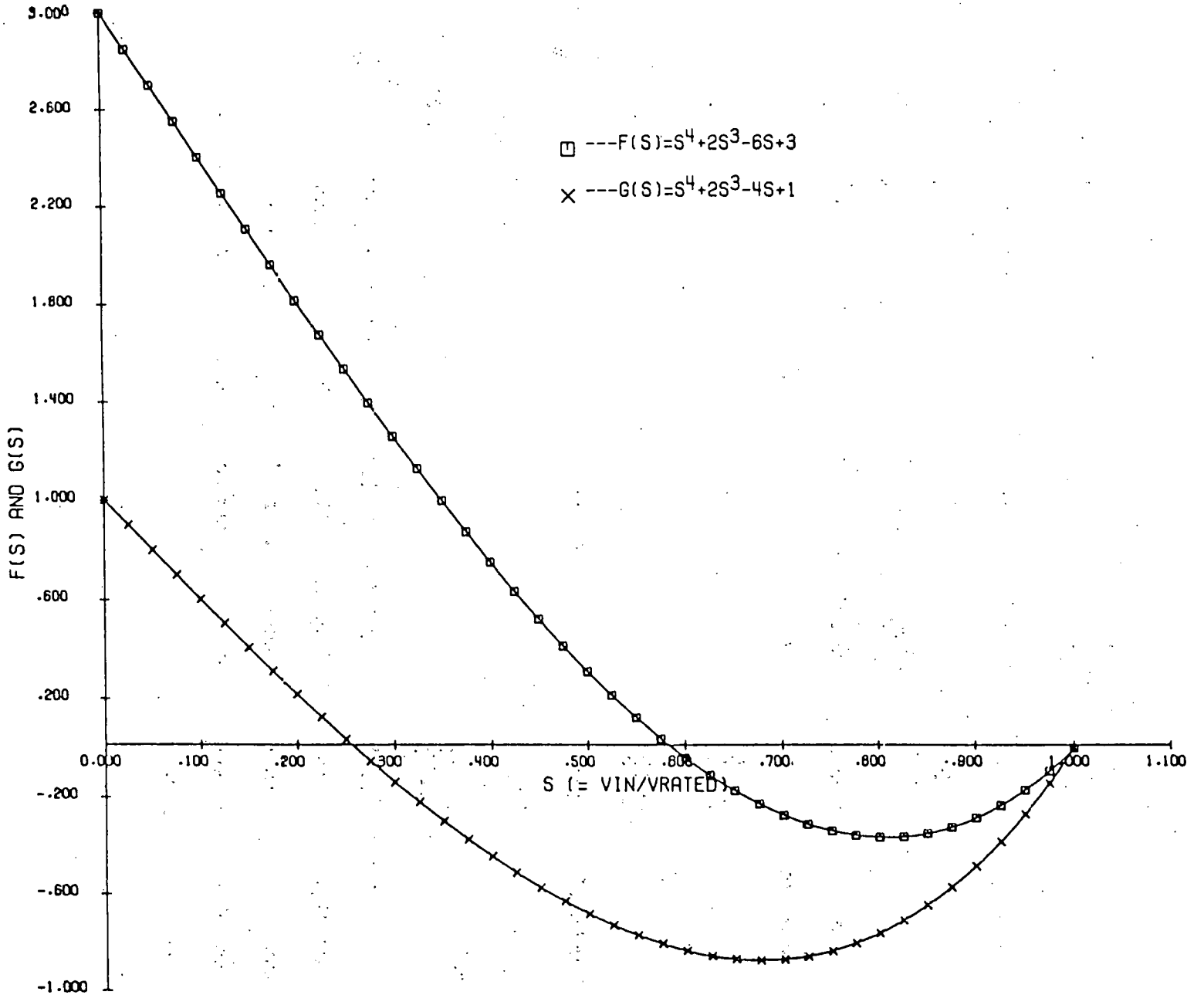

FIGURE D.1 Range of S Such That v_{cr} Is Less Than Or Equal To v_i

APPENDIX E

PROGRAM "ARASIM"

The ARASIM program simulates the hourly array power. The simulation adopts the Gauss-Markov process. This program is written to simulate at least one year of data. There is no upper limit to the time and number of sites in the region. The program is also written to do more than one set of simulations at a time.

The input for this program is on cards in the following order and format:

CARD NO.	COL. NO.	FORMAT	DATA
1	1 - 5	I5*	Number of years to be simulated
2	1 - 80	16A5	Title of the region (recommended)
3 - 14	1 - 8	F8.4	Monthly mean wind speed (in m/s)
	9 - 80	24F3.2	Diurnal cycle effect (multiplier factor), 24 hours on one card.
15	1 - 10	F10.3	Rated power in KW
	11 - 20	F10.3	Cut-in speed in m/s
	21 - 30	F10.3	Rated wind speed in m/s
	31 - 40	F10.3	Cut-out speed in m/s
16	1 - 5	I5*	Array size (i.e., number of sites in a region)
17 - 28	1 - 5	F5.3	Lag one hourly autocorrelation at a site
	6 - 10	F5.3	Zero lag spatial correlation between 2 sites

	11 - 15	F5.3	Lag one hourly spatial correlation between 2 sites
29			Blank if end of data; a new card 1 for another set of simulations (i.e., repeat cards 1 - 29)

* Right justified

The line printer output consists of mean wind speed (with the diurnal cycle effect) by month and hour of the day; the equivalent linearized wind turbine operating characteristics; the correlation coefficients; and the mean and standard deviation of array power in KW. The simulated hourly array power is written on magnetic tape in watts. The format is

YYMMDDHHPPPPPPPP

where	YY	Year, 1981	(Col. 1 - 2)
	MM	Month, 05 = May	(Col. 3 - 4)
	DD	Day	(Col. 5 - 6)
	HH	Hour, 01 - 24	(Col. 7 - 8)
	P...P	Array power in interger watts	(Col. 9 - 16)

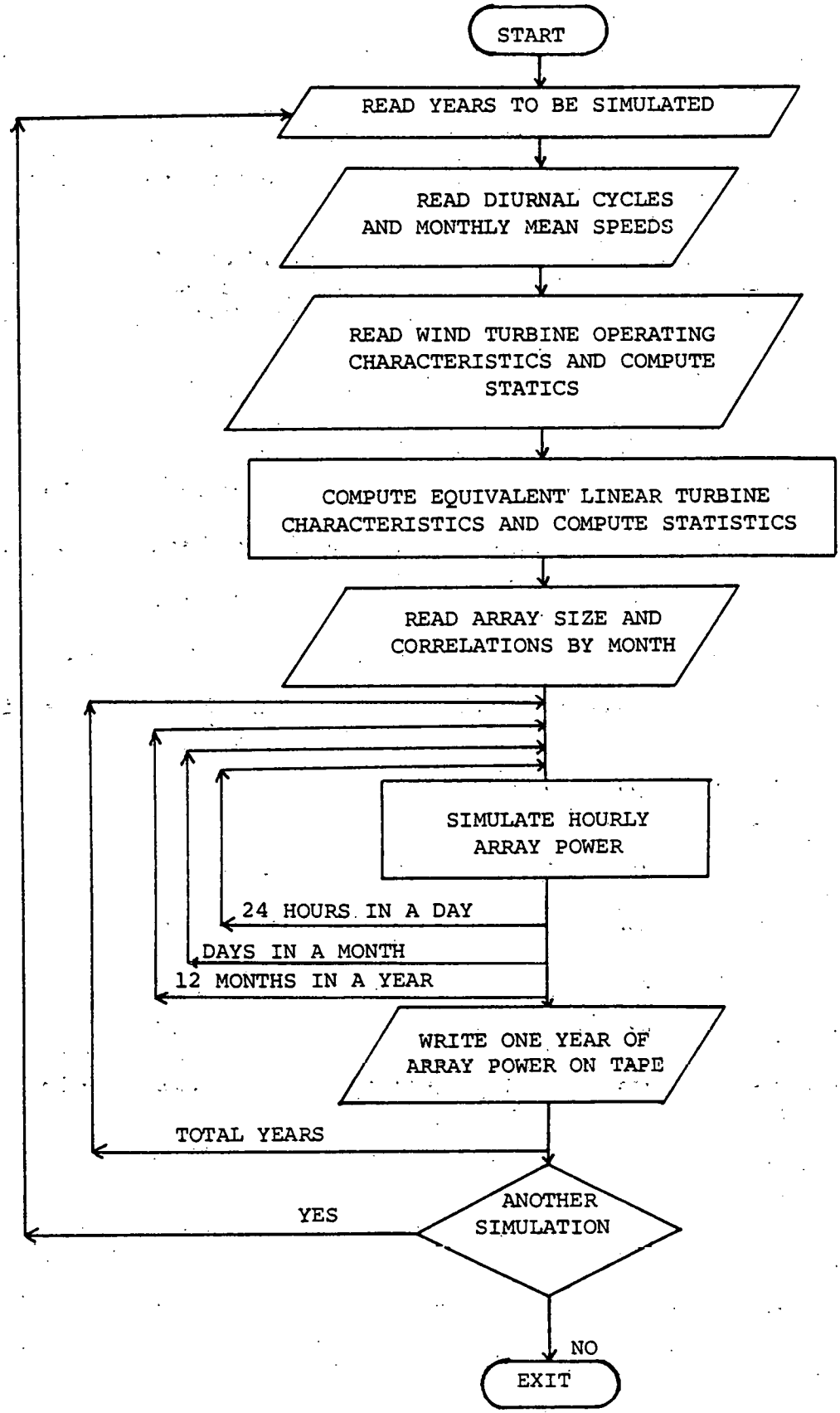

FIGURE E.1 Computer Flow Chart for Program ARASIM

```
      PROGRAM ARASIM (INPUT,OUTPUT,TAPE5)
      DIMENSION VM(12),DC(12,24),VMEAN(12,24),AA(12,24),BB(12,24),PI(12),
     2          STG2V(12,24),NDAY(12),CHAR(2),RHO(12),RHOS(12),
     3          RHOST(12),EXPP(12,24),STDP(12,24),P(12,31,24),TITLE(16)
      DIMENSION IPOW(12,31,24)
      DIMENSION STG(12,24)
      DATA CHAR /1HA,1HR/
      DATA NDAY /31,28,31,30,31,30,31,31,30,31,30,31/
      PI = ACOS(-1.0)
C
C READING NUMBER OF YEARS TO BE SIMULATED
C
    1 READ 1001, NYEAR
C
C IN GENERAL, INDICES ARE NY FOR YEARS, NM AND I FOR MONTHS, ND FOR DAYS,
C AND NH AND J FOR HOURS
C
      IF (NYEAR) 999,999,2
C
C
    2 READ 1002, (TITLE(K),K=1,16)
C READING MEAN WIND SPEED AND DIURNAL CYCLE FOR EACH MONTH.
C A BLANK FOR DIURNAL CYCLE MEANS NO CYCLE EFFECT
      DO 6 I = 1,12
      READ 1003,VM(I),(DC(I,J),J=1,24)
      IF (DC(I,1).GE.0.0001) GO TO 4
      DO 3 J = 1,24
    3 VMEAN(I,J) = VM(I)
      GO TO 6
    4 DO 5 J = 1,24
    5 VMEAN(I,J) = VM(I)*DC(I,J)
    6 CONTINUE
      PRINT 2001, (TITLE(K),K=1,16)
      PRINT 2002, NYEAR
      PRINT 2003
      PRINT 2004
      DO 7 J = 1,24
    7 PRINT 2005, J, (VMEAN(I,J),I = 1,12)
C
C READING OPERATING CHARACTERISTICS OF WINDMILL
C
      READ 1004, RATED,VIN,VRATED,VOUT
      IF (RATED .LE. 0.0001) GO TO 13
      VMED = (VIN+VRATED)/2.
C
C COMPUTING OPERATING CURVE
C
      B = (VMED**2-VIN**2)-((VRATED**2-VIN**2)*(VMED/VRATED)**3)
      B = RATED*B/((VRATED-VIN)*(VMED-VRATED)*(VMED-VIN))
      C = (RATED-B*(VRATED-VIN))/(VRATED**2-VIN**2)
      A = (-B*VIN)-(C*VIN**2)
      PRINT 2006, RATED,VRATED,VIN,VOUT
      PRINT 2007, A,B,C
C
C COMPUTING WIND SPEED AND EQUIVALENT LINEAR RESPONSE CHARACTERISTICS BY
C MONTH AND HOUR OF DAY
C
      SPPI = SQRT(PI)
      DO 11 I = 1,12
      J = 1
    9 PHI = 2.*VMEAN(I,J)/SPPI
      EVP = VRATED/PHI
      EVI = VIN/PHI
      EVO = VOUT/PHI
      EUP = 0.5+0.5*ERF(EVP)
      EUI = 0.5+0.5*ERF(EVI)
      EUO = 0.5+0.5*ERF(EVO)
      STG2V(I,J) = (VMEAN(I,J)**2)*((4./PI)-1.0)
      EI = EXP(-EVI**2)
      EP = EXP(-EVP**2)
      EO = EXP(-EVO**2)
      F1 = EI-EP
      F2 = VIN*EI-VRATED*EP+PHI*SPPI*(EUI-EUI)
      F3 = (VIN**2)*EI-(VRATED**2)*EP+(PHI**2)*(EI-EP)
      F4 = (VIN**3)*EI-(VRATED**3)*EP+1.5*(PHI**2)*(VIN*EI-VRATED*EP)+1.
     25*SPPI*(PHI**3)*(EUP-EUI)
      F5 = VRATED*EP-VOUT*EO+PHI*SPPI*(EUO-EUP)
      F6 = EP-EO
      F7 = VRATED**2*EP-VOUT**2*EO+PHI**2*(EP-EO)
```

```
      SIG(I,J) = (F2+F9)**2-(F3+F7)*(F1+F6)
      F25 = F2+F5
      F16 = F1+F6
      RR(I,J) = A*(F1*F25-F2*F16)+B*(F2*F25-F3*F16)+C*(F3*F25-F4*F16)+RA
     2TED*(F6*F25-F5*F16)
      BB(I,J) = RR(I,J)/SIG(I,J)
      AA(I,J) = (A*F1+B*F2+C*F3+RATED*F6-BB(I,J)*F25)/F16
      IF (DC(I,1) .LE. 0.0001) GO TO 9
      J = J+1
      IF (J-24) 8,9,11
    9 DO 10 K = 2,24
      SIG2V(I,K) = SIG2VET,1)
      RR(I,K) = BB(I,1)
   10 AA(I,K) = AA(I,1)
   11 CONTINUE
      PRINT 2008
      PRINT 2009
      DO 12 J = 1,24
      PRINT 2010, J, CHAR(1),(AA(I,J),I=1,12)
   12 PRINT 2011, CHAR(21,(RR(I,J),I=1,12)
      GO TO 16
   13 DO 15 I = 1,12
      DO 14 J = 1,24
      AA(I,J) = 0.0
   14 RR(I,J) = 1.0
   15 CONTINUE
   16 CONTINUE
C
C READING CORRELATIONS AND ARRAY SIZE
C
      READ 1005, N
      XN = N
      PRINT 2012, N
      IPOW = XN*RATED
      DO 17 I = 1,12
      READ 1006, RHO(I),RHOS(I),RHOST(I)
      R(I) = (RHO(I)+(XN-1.)*RHOST(I))/(1.+(XN-1.)*RHOS(I))
   17 PRINT 2013,I,RHO(I),RHOS(I),RHOST(I),R(I)
C
C RHO(I)    IS LAG ONE AUTOCORRELATION,
C RHOS(I)   IS ZERO-LAG SPATIAL CORRELATION, AND
C RHOST(I)  IS LAG ONE SPATIAL CORRELATION
C R(I)      IS ARRAY POWER LAG ONE AUTOCORRELATION
C
C
C EXPP AND VARP ARE UNCONDITIONED MEAN AND VARIANCE OF TOTAL ARRAY POWER
C
      DO 19 I = 1,12
      DO 18 J = 1,24
      EXPP(I,J) = XN*(AA(I,J)+BB(I,J)*VMEAN(I,J))
      VARP = XN*BB(I,J)**2*SIG2V(I,J)*(1.+(XN-1.)*RHOS(I))
   18 STDP(I,J) = SQRT(VARP)
   19 CONTINUE
C
C SETTING UP STATISTICS PRIOR TO 1 AM ON 1/1/81 TO INITIATE SERIES
C
      PP = 1.
      EPP = 1.
      SDP = 1.
      SPP = SQRT(1.0-R(1)**2)
      PRINT 2014
      PRINT 2015
      PRINT 2009
      DO 20 J = 1,24
   20 PRINT 2016, J,(EXPP(I,J),I=1,12)
      PRINT 2017
      PRINT 2015
      PRINT 2009
      DO 21 J = 1,24
   21 PRINT 2016, J,(STDP(I,J),I=1,12)
      PRINT 2018
      DO 31 NY = 1,NYEAR
      NYR = 1980+NY
C
C ADJUSTING FEBRUARY FOR A LEAP YEAR
C
      INY = NY/4
      XNY = INY
      YNY = NY
```

```
      YNY = YNY/4.
      XNY = YNY-XNY
      IF (XNY-0.001) 22,22,23
   22 NDAY(2) = 29
      GO TO 24
   23 NDAY(2) = 28
   24 CONTINUE
      DO 27 NM = 1,12
      NDY = NDAY(NM)
      DO 26 ND = 1,NDY
      DO 25 NH = 1,24
      EP = EXPP(NM,NH)+R(NM)*(PP-EPP)*STDP(NM,NH)/SDP
      SP = STDP(NM,NH)*SQRT(1.0-R(NM)**2)/SPP
      P(NM,ND,NH) = ONORAL(EP,SP)
      EPP = EXPP(NM,NH)
      SDP = STDP(NM,NH)
      PP = P(NM,ND,NH)
      IF (P(NM,ND,NH) .EQ. TPOW) GO TO 41
      IF (P(NM,ND,NH) .LE. 0.0) GO TO 42
      IPOW(NM,ND,NH) = P(NM,ND,NH)*1000
      GO TO 25
   41 IPOW(NM,ND,NH) = TPOW*1000
      GO TO 25
   42 IPOW(NM,ND,NH) = 0
   25 SPP = 1.0
   26 CONTINUE
   27 CONTINUE
      NZ = NYR-1900
      DO 30 NM = 1,12
      NDY = NDAY(NM)
      DO 29 ND = 1,NDY
      DO 28 NH = 1,24
      WRITE (5,2019) NZ,NM,ND,NH,IPOW(NM,ND,NH)
   28 CONTINUE
   29 CONTINUE
   30 CONTINUE
   31 CONTINUE
      GO TO 1
  999 CONTINUE
 1001 FORMAT (I5)
 1002 FORMAT (16A5)
 1003 FORMAT (F8.4,24F3.2)
 1004 FORMAT (4F10.3)
 1005 FORMAT (I5)
 1006 FORMAT (3F5.2)
 2001 FORMAT (1H1,2X,16A5)
 2002 FORMAT (///,* THE PROGRAM HAS BEEN SET TO SIMULATE*,I3,
     2       * YEARS OF DATA*,///)
 2003 FORMAT (7X,*MEAN WIND SPEEDS (IN M/S) BY MONTH AND HOUR OF THE*,
     2       * DAY*,//)
 2004 FORMAT (10X,*JANUARY  FEBRUARY  MARCH  APRIL  MAY  JUNE*,
     2       *  JULY  AUGUST  SEPTEMBER  OCTOBER  NOVEMBER*,
     3       * DECEMBER*,/,* HOUR*,/)
 2005 FORMAT (1X,I3,4X,12F9.4)
 2006 FORMAT (////,* THE WIND TURBINE BEING CONSIDERED HAS A RATED *,
     2       *POWER OF *,F9.3,* KW AT A WIND SPEED OF *,F6.2,* M/S.*,
     3       /,* THE CUT IN SPEED IS *,F6.2,* M/S. AND THE CUT OUT *,
     4       *SPEED IS *,F6.2,* M/S.*,//)
 2007 FORMAT (* THE OPERATING CURVE IS CHARACTERIZED BY A = *,F12.4,
     2       *, B = *,F12.4,*, AND C = *,F12.4,//)
 2008 FORMAT (1H1,29X,*EQUIVALENT LINEARIZED WIND TURBINE OPERATING *,
     2       *CHARACTERISTICS*,//)
 2009 FORMAT (* HOUR  JANUARY  FEBRUARY  MARCH  APRIL  *,
     2       *  MAY  JUNE  JULY  AUGUST  SEPTEMBER  *,
     3       *OCTOBER  NOVEMBER  DECEMBER*,/)
 2010 FORMAT (1X,I2,1X,F7.3,12F11.4)
 2011 FORMAT (4X,A1,12E11.4)
 2012 FORMAT (1H1,* THERE ARE*,I3,* WIND TURBINES IN THE ARRAY*,//)
 2013 FORMAT (* FOR MONTH*,I3,* THE LAG ONE AUTOCORRELATION =*,F5.3,
     2       *, THE SPATIAL CORRELATION =*,F5.3,*,*,/14X,*AND THE LAG*,
     3       * ONE CROSS CORRELATION =*,F5.3,*.  THE LAG ONE*,
     4       *AUTOCORRELATION FOR THE TOTAL ARRAY POWER =*,F5.3,*.*,/)
 2014 FORMAT (1H1,*DY,*MEAN ARRAY POWER*,/)
 2015 FORMAT (66X,*MONTH*)
 2016 FORMAT (1X,I2,2X,12F11.4)
 2017 FORMAT (///,53X,*STANDARD DEVIATION OF ARRAY POWER*,/)
 2018 FORMAT (1H1)
 2019 FORMAT (4I2,I8)
      ENDFILE5
```

```
      STOP
      END
```

CARD NR. SEVERITY DETAILS DIAGNOSIS OF PROBLEM

200 I 25CD 200 FIELD WIDTH OF A CONVERSION DESCRIPTOR SHOULD BE AS LARGE AS THE MINIMUM SPECIFIED FOR THAT DESCRIPTOR.

SYMBOLIC REFERENCE MAP (R=?)

ENTRY POINTS DEF LINE REFERENCES
6211 ARASIM 1

VARIABLES SN TYPE RELOCATION

```
 7647 A          REAL
11035 AA         REAL          ARRAY
 7645 B          REAL
11475 BA         REAL          ARRAY
 7646 C          REAL
12625 CHAR       REAL          ARRAY
 7735 DC         REAL          ARRAY
 7660 EI         REAL
 7662 EO         REAL
 7716 EP         REAL
 7701 EPP        REAL
 7661 ER         REAL
12673 EXPP       REAL          ARRAY
 7656 FUI        REAL
 7657 FUO        REAL
 7655 FUR        REAL
 7653 FVI        REAL
 7654 FVO        REAL
 7652 FVR        REAL
 7663 F1         REAL
 7673 F16        REAL
 7664 F2         REAL
 7672 F25        REAL
 7665 F3         REAL
 7666 F4         REAL
 7667 F5         REAL
 7670 F6         REAL
 7671 F7         REAL
 7636 I          INTEGER
 7706 INY        INTEGER
35353 IPOW       INTEGER       ARRAY
 7637 J          INTEGER
 7635 K          INTEGER
 7674 N          INTEGER
 7714 ND         INTEGER
12611 NDAY       INTEGER       ARRAY
 7713 NDY        INTEGER
 7715 NH         INTEGER
 7712 NM         INTEGER
 7704 NY         INTEGER
 7634 NYEAR      INTEGER
 7705 NYR        INTEGER
```

```
REFS   53   83   86  DEFINED   91
REF     2   93   98      129  DEFINED    86    93
REFS   49   50   51       53       83    86
DEFINED 48   49
REFS    2   85   86       92       99   129   130
DEFINED 83   85   92      104
REFS   51   53   83       85  DEFINED    50
REFS    2   98   99  DEFINED
REFS    2   86   31       87  DEFINED    25
REFS   72   73  2*74  2*75  DEFINED    69
REFS   77   78  2*79  DEFINED    71
REFS  172  DEFINED  170
REFS  173  DEFINED  137      173
REFS   72   73  2*74  2*75       77       78   2*79
DEFINED 70
REFS    2  144  170      173  DEFINED   129
REFS   75   76  DEFINED    66
REFS   77  DEFINED    67
REFS   73   76       77  DEFINED    65
REFS   66   69  DEFINED    63
REFS   67   71  DEFINED    64
REFS   65   74  DEFINED    62
REFS   80   82       83       86  DEFINED    72
REFS  4*83   86  DEFINED    82
REFS   86   81  2*83       86  DEFINED    73
REFS  4*83   86  DEFINED    81
REFS   80  2*83       86  DEFINED    74
REFS   83  DEFINED    75
REFS   80   81       83  DEFINED    77
REFS   80   82       83       96  DEFINED    78
REFS   80  DEFINED    79
REF   2*25   26  2*28  3*31       38       61   2*68
      2*80   83  3*85  2*86       87  2*91  2*92  2*93
      2*98   99  103       104  3*115  4*117  5*117  4*129
      3*130  131  144       149  DEFINED    24       38       59
        98   99  101       114       127      144      149
REFS  157  DEFINED       166
REFS    5  101  DEFINED      178       196      182
REF     2   28  2*31  2*38       61  2*68       80
       83  2*86       88       89  2*90       99      103
      104  4*129  2*130      131  2*144  2*145
DEFINED 25   27   30   37   60   88   97
      102  124  143  148
REFS   21   33   91       92       93
DEFINED 21   33   90
REFS  111  112  DEFINED      119
REFS  172  175  176      177  2*178      190      182
 2*101  DEFINED  168  199       DEFINED    8      162      164
REFS    2  187  195
REFS  168  189  DEFINED      167      198
REFS  2*170  171  172      173      174      175      176
REFS  2*178  169  182  2*191  DEFINED  169  190
REFS  187  3*170  2*171      172      173      174      175
      176  177  2*178      180      182      188  2*191
DEFINED 164
REFS  182  184       185  DEFINED    181
REFS   18   34      151  DEFINED     13
REFS  186  DEFINED      152
```

APPENDIX F

BRIEF SUMMARY OF MODIFIED STATISTICAL ANALYSIS PROGRAMS

Computer programs WINDATR, PERIR and RUTOCOR were modified, respectively, from WINDATB, PERSIST and AUTOCOR (Corotis, 1976, 1977). The modification basically consists of reducing the computation time by deleting the velocity-cubed analyses and adjusting the data (in value) by a conversion factor in order to use the original programs efficiently. A power unit, PUN, is introduced which is defined in every analysis from the input data. It is recommended that PUN should be greater than or equal to one-thirtieth of the total array power.

WINDATR

Program WINDATR computes the hourly, monthly, seasonal and annual average and variance for array power. Through these statistics the relative importance of diurnal, monthly, seasonal or annual pattern can be evaluated with respect to either means or variances. The basic input to this program is a sequence of hourly array power in integer watts. These are read through a COMPASS* program This program reads one month of array power at a time. The program is written to analyze a minimum of one month of data and a maximum record length of 25 years.

PERIR

Program PERIR analyzes array power data for duration of runs. An array power histogram based on every two PUNs is computed for each season. Run levels based on every two PUNs are also used for

seasonal duration of runs. The input for this program is basically a record of hourly array power read by a COMPASS* program from a magnetic tape. This program is written to analyze a minimum record length of one season and there is no upper limit in the record length.

RUTOCOR

The RUTOCOR program computes a series of seasonal autocorrelation function for the array power. The autocorrelation function is computed for a maximum time lag of 336 hours (2 weeks). The normalized correlation function

$$\rho(\tau) = \frac{R(\tau)}{R(0)} \tag{F.1}$$

where $R(\tau)$ and $R(0)$ are, respectively, the autocorrelation at time lag of τ and zero is presented on the output. The basic input of this program is the hourly array power read by a COMPASS* program from a magnetic tape. One season of array power is read from the input tape at a time. The program is written to analyze at least one season of data and a maximum of 25 years.

* The COMPASS program is unique to the Northwestern University CDC system, and would normally be replaced by a FORTRAN read statement if used on another computer system.

APPENDIX G

SUMMARY OF NEW NATIONAL WEATHER SERVICE SITES

Dunkirk (WBAN #14747) is located in New York at latitude 42°30', longitude 79°17'. The data were recorded each hour for the period 1/1/49 - 12/31/53. The field elevation is about 200 m, and the anemometer height was 9 m.

Livingston (WBAN #24150) is located in Montana at latitude 45°40', longitude 110°32'. The data were recorded each hour for the period 1/1/48 - 12/31/54. The field elevation is about 1400 m, and the anemometer height was 7.6 m.

Cape Hatteras (WBAN #93729) is located in North Carolina at latitude 35°16', longitude 75°33'. The data were recorded each hour for the period 3/1/57 - 12/31/64. The field elevation is about 2.4 m, and the anemometer height was 9.75 m.

Dalhart, Texas (WBAN #93042) is located at latitude 36°01', longitude 102°33'. The data were recorded each hour for the period 1/1/49 - 12/31/54. The field elevation is about 1215 m, and the anemometer height was 19.2 until 9/15/54, at which time it was changed to 7 m.

Laguardia (WBAN #14732) is located in New York at latitude 40°46', longitude 73°54'. The data were recorded each hour for the period 7/1/48 - 6/30/61. The field elevation is about 12 m, and the anemometer height was 25.3 m.

North Platte (WBAN #24023) is located in Nebraska at latitude 41°08', longitude 100°42' between 1/4/40 and 1/15/52, and at latitude 41°08', longitude 100°41' between 1/15/52 and the present. The data were

recorded each hour for the period 1/1/48 - 6/30/64. The field elevation was 850 m from 1933 to 1952, and 848 m from 1952 to 1976, and the anemometer height was 14.6 m from 1/4/40 to 1/15/52 and 9.75 m from 1/15/52 to 8/12/64.

Mount Shasta (WBAN #24215) is located in California at latitude 41°19', longitude 122°19'. The data were recorded each hour for the period 1/1/50 - 12/31/51. The field elevation is about 1090 m and the anemometer height was 39.6 m.

Blue Canyon (WBAN #23225) is located in California at latitude 39°17', longitude 120°42'. The data were recorded each hour for the period 1/1/48 - 12/31/51. The field elevation is about 1610 m, and the anemometer height was 9.1 m.

Concord (WBAN #14745) is located in New Hampshire at latitude 43°12', longitude 71°31' between 5/1/41 and 8/8/62, and at latitude 43°12', longitude 71°30' between 8/8/62 and the present. The data were recorded each hour for the period 1/1/48 - 12/31/64. The field elevation is about 100 m, and the anemometer height was 14.3 m from 5/1/41 to 8/8/62 and 6.1 m from 8/8/62 to present.

Manchester (WBAN #14710) is located in New Hampshire at latitude 42°56', longitude 71°26'. The data were recorded each hour for the period 4/1/51 - 3/31/67. The field elevation is about 76 m, and the anemometer height was unknown between 1949 and 4/53, 19.8 m between 4/53 and 5/55, 18.3 m from 5/55 to 4/66, and 3 m from 4/66 to 1968.

Portsmouth (WBAN #04743) is located in New Hampshire at latitude 43°05', longitude 70°49'. The data were recorded each hour for the period 4/1/56 - 12/31/74. The field elevation is about 39 m, and the anemometer height was 4.6 m from 1956 to 3/57, 4 m from 3/57 to 1/31/58, 32 m from 1/31/58 to 4/59, and 4 m from 4/59 to 1976.

Lebanon (WBAN #94765) is located in New Hampshire at latitude 43°38', longitude 72°19'. The data were recorded each hour for the period 1/1/59 - 12/31/64. The field elevation is about 172 m, and the anemometer height was 11.9 m.

West Lebanon (WBAN #14776) is located in New Hampshire at latitude 43°38', longitude 72°19'. The data were recorded each hour for the period 1/1/49 - 12/31/58. The field elevation is about 172 m, and the anemometer height was 14 m from 1947 to 10/29/53, and 11.9 m from 10/29/53 to 1958.

APPENDIX H

VIEW OF SITE USED

FOR CHAPTER 3 STUDY

FIGURE H.1 View Looking Northeast to Lake Michigan from Anemometer Location

FIGURE H.2 View Looking Northeast toward Anemometer on Roof from Ground

☆U.S. GOVERNMENT PRINTING OFFICE: 1981-740-145/1265